COMMITTEE CERTIFICATION OF APPROVED VERSION

The committee for Zhifang Zhao certifies that this is the approved version of the following dissertation:

DISTRIBUTION AND TARGETING OF CLC-3

Committee:

Steven A. Weinman, M.D., Ph.D., Supervisor

Lisa A. Elferink, Ph.D.

Cornelis Elferink, Ph.D.

Guillermo Altenberg, M.D., Ph.D.

Roger G. O'Neil, Ph.D.

Dean, Graduate School

DISTRIBUTION AND TARGETING OF CLC-3

by

Zhifang Zhao

Dissertation
Presented to the Faculty of The University of Texas Graduate School of
Biomedical Sciences at Galveston
in Partial Fulfillment of the Requirements
for the Degree of

Doctor of Philosophy

Approved by the Supervisory Committee

Steven A. Weinman, M.D., Ph.D.
Lisa A. Elferink, Ph.D.
Cornelis Elferink, Ph.D.
Guillermo Altenberg, M.D., Ph.D.
Roger G. O'Neil, Ph.D.

November 2006
Galveston, Texas

Key words: Endocytosis, ClC-3

Dedicated to my dearest parents!

ACKNOWLEDGEMENTS

First of all, I will give the best acknowledgement to Dr. Steven A. Weinman, my mentor. He always inspires and challenges me and gives me the advice whenever I needed it. This dissertation could not be completed without his help.

I would like to acknowledge my committee members, who generously provided me guidance on the project.

I would like to acknowledge Xinhua Li and Junfang Hao, who cooperate with me on this project.

I would like to acknowledge Ting Wang and Yanchun Li in our lab for their team support.

I would like to acknowledge Ning Li, Xiaofei Zhang, Yafei Huang and Xuan Zhang who give me kind help in these years during my study.

I would like to acknowledge the faculties and staffs in the department who support my study and research.

Finally, I would like to acknowledge Sheng Yan, my dearest husband. We share life experiences, in tears or in joys. I would like to acknowledge Estelle Sophia Yan, my dearest daughter. Because of you, my life is different.

DISTRIBUTION AND TARGETING OF CLC-3

Publication No._____

Zhifang Zhao, Ph.D.
The University of Texas Graduate School of Biomedical Sciences at Galveston, 2006

Supervisor: Dr. Steven A. Weinman

ClC-3 is a ubiquitously expressed chloride channel that is present in synaptic vesicles and endosome/lysosome compartments. The channel is largely intracellular, but has been observed at the plasma membrane as well. The aim of this study was to identify the trafficking pathway for delivery of ClC-3 to intracellular sites. When transiently transfected into COS-7 cells, approximately 6% of ClC-3 localized to the plasma membrane as assessed by surface biotinylation. Plasma membrane ClC-3 was rapidly endocytosed with $t_{1/2}$ of approximately 9min. Biotinylation experiment detected a portion of ClC-3 recycled back to the cell surface. Antibody binding to an external HA epitope demonstrated that the plasma membrane is an intermediate trafficking site for ClC-3 destined for intracellular compartments. ClC-3 was associated with clathrin at the plasma membrane and in early endocytic vesicles. It also colocalized with transferrin-labelled endosomes. It dissociated from clathrin at later times to localize in large vesicles. GST pull-down assays demonstrated that the N-terminal of ClC-3 binds to both clathrin and AP-2. Deletion of dileucine cluster within the cytosolic N terminal (amino acids 13-19) resulted in a molecule that had decreased endocytosis and increased surface expression. This deletion also abolished interaction with clathrin in GST pull down experiments. We conclude that ClC-3 is primarily an intracellular channel but it is transiently inserted into the plasma membrane from where it is rapidly endocytosed. Internalization of ClC-3 depends on the interaction between an N-terminal dileucine cluster and clathrin.

TABLE OF CONTENTS

LIST OF FIGURES

LIST OF TABLES

LIST OF ABBREVIATIONS

VDAC…… Voltage-Dependent Anion Channel (mitochondrial porin)
CFTR……. Cystic Fibrosis Transmembrane conductance Regulator
ClC …… Chloride Channel of the CLC Gene Family
CBS ……Cystathionine β Synthase
ClC-ec …… *Escherichia coli* CLC
EBP50……. ERM-binding phosphoprotein 50
CCV……Clathrin Coated Vesicles
TfnR……Transferrin Receptor
AP…….....Adaptor Protein
CHC……....Clathrin Heavy Chain
CLC……Clathrin Light Chain
Il-2……Interleukin-2
LMWPs……Low-Molecular-Weight Proteins
MesNa……. sodium 2-mercaptoethanesulfonate
COS-7……..African green monkey kidney cells
Y2H……..yeast two hybrid
TGN……..Trans-Golgi Network
RISC……. RNA-induced Silencing Complex
GST……..Glutathione S-transferase
PNGase F……..Peptide: N-glycosidase F
PDZ……..postsynaptic density-95, Disc-large, and Zonulin-1
WT …….. Wild type
MPRs…… mannose 6-phosphate receptors
MVB……. multivesicular body
Arf……. ADP-ribosylation factor
Eps15……..epidermal growth factor receptor substrate 15
Hrs……. hepatocyte growth factor-regulated tyrosine kinase substrate
PTC ……proximal tubular cells

CHAPTER 1 INTRODUCTION

CHLORIDE CHANNELS

Six classes of chloride channels

Chloride is essential for the function of all eukaryotic cells and its movement across cell membranes is dependent on the function of a group of transport proteins called "chloride channels". The past decade has brought great progress in the understanding of these molecules. Six classes of chloride channels have been identified. They are the ClC family, the CLCA family, the CLIC family, the mitochondrial voltage-dependent anion channel (VDAC), the neuronal ligand-gated chloride channels, and the cystic fibrosis transmembrane conductance regulator (CFTR) (1). Among these, the ClC chloride channel/transport protein family is the most ubiquitously expressed and highly conserved. ClC family members are found in cells from prokaryotes to mammals and are functional in plasma membranes as well as intracellular vesicles. They participate in housekeeping process such as pH regulation, trans-epithelial transport, and regulation of electrical excitability. Genetic abnormalities of these proteins lead to a number of severe inherited diseases. Mutations in human ClC channels are known to cause a variety of diseases such as myotonia (ClC-1) (2, 3), Bartter's syndrome (ClC-K) (4, 5), Dent's disease (ClC-5)(6) , congenital osteopetrosis and neurodegeneration (ClC-7) (7, 8) and possibly epilepsy. Mouse models have revealed that ClC gene disruptions cause blindness and infertility as well (9).

ClC family

A bacterial ClC protein from *E. coli* (ClC-ec) has served as a prototype for determining aspects of the structure-function relationship for the entire ClC family. This is valuable because the core transmembrane domain structure of the ClC proteins is highly conserved from bacteria to mammals. However, the mammalian channels have

additional N and C terminal cytosolic domains. The X-ray crystallographic high-resolution structure of the bacterial ClC protein was determined by McKinnon and colleagues (10). The protein exists as dimer of two identical subunits in which each monomer has one pore (10). Within each pore, there are three Cl^- binding sites. The pore is conductive when the chloride-binding site nearest the extracellular solution is occupied by a chloride ion. When it is occupied by a glutamate carboxyl group, the pore is closed.

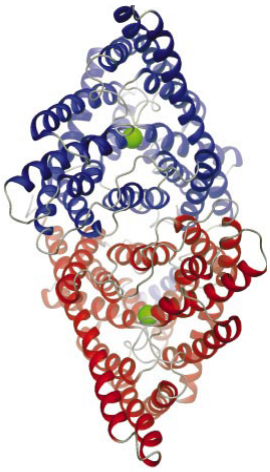

Fig 1.1 ClC structure. Stereo view of a ribbon representation of the ClC dimer from the extracellular side. The two subunits are blue and red. The green sphere represents a Cl^- ion in the selectivity filter. The ClC chloride channel contains multiple transmembrane domains. It is a dimeric structure with two-fold symmetry of each monomer. (Adapted from Ref 10).

Nine mammalian ClC family members have been identified (11).They are localized either at the plasma membrane or in intracellular membrane sites and can have a ubiquitous or a more restricted tissue distribution. ClC-3, ClC-4, and ClC-5 represent one branch of this family that functions primarily intracellularly. They share about 80% sequence identity with each other. These channels are located mainly in membranes of intracellular vesicles, mostly in the endocytic pathway (9).They have similar channel

properties; can form heterodimers with other family members, and contribute to endosomal acidification and trafficking (12, 13).

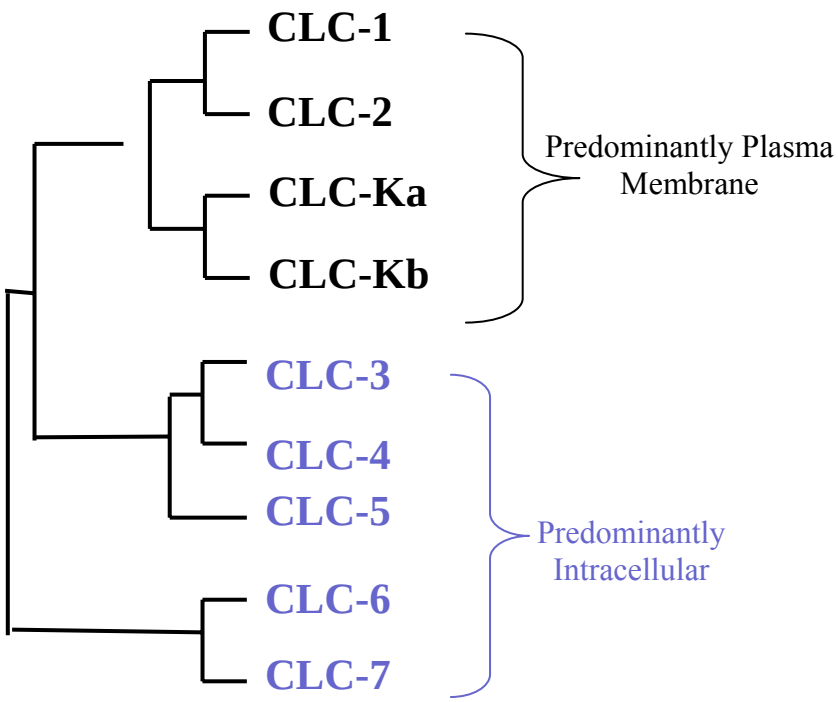

Fig 1.2 Mammalian ClC-3 transport proteins. The chloride channels/transporters can be divided into different subfamilies. ClC-3, ClC-4, and ClC-5 represent one branch of this family that functions primarily intracellularly.

Function of intracellular ClC channels-acidification of intracellular compartments

Chloride channels/transporters are present in the plasma membrane and in membranes of intracellular organelles. They are involved in stabilization of membrane potential, synaptic inhibition, cell volume regulation, transepithelial transport, and extracellular and vesicular acidification. ClC-3, 4, 5, 6, 7 each localize primarily intracellularly. A wealth of information using knock-out mouse models has shown that ClC channels play important roles in the acidification of intracellular vesicles.

The disruption of ClC-3 partially inhibited the acidification of synaptic vesicles in vitro (14), and the luminal pH of a vesicle fraction mainly representing endosomes was elevated (15). Over-expression of the ClC-3 chloride channel also promotes acidification of endosomes and lysosomes (16, 17). ClC-5 is also clearly necessary for efficient acidification in the endosomal pathway. Impaired endosomal acidification in the proximal tubule is observed in ClC-5 deficient mice and in human patients with ClC-5 mutations. This causes the proteinuria, hypercalciuria, and nephrolithiasis (Dent's disease) seen in ClC-5 deficiency (17). ClC-6 protein is abundant in the nervous system. Native ClC-6 resides in late endosomes. Disruption of ClC-6 results in a lysosomal storage phenotype that is most likely related to changes in endosomal H^+ or Cl^- concentrations (18). ClC-7 is present at the membrane of late endosomes and lysosomes (8). It co-localizes with the H^+-ATPase in the ruffled border of osteoclasts. Loss of the ClC-7 chloride channel leads to osteopetrosis because osteoclasts become unable to acidify the resorption lacuna (8). Therefore, the ClC proteins play critical roles in multiple intracellular acidification processes.

VESICULAR ACIDIFICATION IS FUNDAMENTAL FOR VESICLE IDENTITY

Subcellular organelles have their own characteristic luminal pH which is important in their physiological function. Organelles along the secretory pathway, from endoplasmic reticulum to Golgi complex to sorting endosomes and lysosomes, become more and more acidic. In the endocytic pathway, the early endosomes are generally thought to have a pH value of 5.5 to 6.3, the late endosome is typically lower than 5.5, and the pH value of lysosomes in most cells can be about 4.6 (19).

Intravesicular pH plays a major role in regulating the stability of ligand-receptor interactions. There are three types of ligand-receptor interactions. Some ligands bind to receptors that internalize and recycle rapidly to the plasma membrane. These ligands dissociate in the early endosome, where the pH value is relatively neutral. Low-density

lipoprotein and α2-macroglobulin fall into this category. Receptors that don't rapidly recycle back to the plasma membrane but are trafficked between endosomes and the Golgi complex, dissociate their ligands at late endosomes, where the lumen is more acidic. Mannose 6-phosphate receptors that involve in the delivery of lysosomal enzymes fall into this category. Finally, receptors that do not dissociate from their ligands at all are typically degraded in lysosomes, together with their bound ligands. In these cases the ligand-receptor interaction is not pH dependent. This is a mechanism to down-regulate the receptors at the plasma membrane such as the Fc receptor for IgG (20).

Many pathogens infect their target cells by opportunistically making use of the endocytic and secretory pathways within the cells. Since the activity of acid hydolases is increased as the pH decreases, pathogens can be killed by this acidification process. Alternatively, many pathogens have evolved resistance to the effects of acid hydrolases and thus can evade this defense mechanism to establish persistent intracellular infections. Therefore, maintaining proper pH value in the lumen of intracellular compartments is required for ligand dissociation, activation of proteases and sometimes killing of pathogens.

ACIDIFICATION ROLE OF CLC PROTEINS: TWO MODELS

The acidification of intracellular compartments definitely requires the ClC chloride channels/transporters. However, the precise mechanism of how the ClC proteins are required remains a matter of debate. Two possible models have been proposed.

Shunting of proton pump generated voltage gradients

The acidification process appears to require two major proteins, the vacuolar proton pump (V-ATPase) which actively transports H^+ from the cytosol into the vesicle lumen and a ClC channel. One hypothesis is that the steady-state pH of the lumen depends on the balance of proton pumping and chloride influx from chloride channel

(21). This is because the pumping of protons is an electrogenic process that transfers positive charge into the vesicle lumen and requires parallel movement of a negatively charged ion, chloride. ClC channels are thought to provide an electric shunt for the electrogenic H^+-ATPase, thereby facilitating the acidification of compartments in the endosomal/lysosomal pathway.

A new model: Cl^-/H^+ exchange

Until recently, the above model has been the accepted explanation for the role of chloride channels in vesicular acidification. However, it may oversimplify the roles of chloride transport proteins. In this regard, new insight has been obtained once again from the prokaryotic ClC structure that has productively guided understanding of the eukaryotic ClC channels. The ClC-ec1 protein in E. coli was recently shown to be a Cl^-/ H+ antiporter, instead of an ion channel (22). ClC-4 and ClC-5, two of the three mainly endosomal ClC proteins have also been proven to function as electrogenic Cl^-/H+ exchangers, resembling the transporter activity of the bacterial protein ClC-ec1 (23, 24). Cl^-/H^+ exchangers will directly couple Cl^- gradients to vesicular pH gradients, but in this case, Cl^- will enter the vesicle in exchange for H^+. This process is also electrogenic, will dissipate the positive intravesicular potential, and will add Cl^- to the vesicular lumen, but all at the expense of the H^+ gradient generated by the v-ATPase.

There are several possible explanations for this unexpected finding. First, extracellular Cl^- is generally many fold greater than intracellular Cl^-. In this case, immediately upon budding, the endocytic vesicle has a cytosolic directed Cl^- gradient and a lumen that is slightly more alkaline than cytosol. This would drive the activity of a Cl^-/H^+ exchanger in the direction of Cl^- exit and H^+ entry to the vesicle and would give the newly endocytosed vesicle a head start on acidification. This means ClC-4 and ClC-5 might directly acidify endosomes shortly after they pinch off from the plasma membrane because H^+ in the cytoplasm may exchange for luminal Cl^-, since Cl^- is present at the higher extracellular concentration than the intracellular side. However, after the pinch

from the plasma membrane, acidification would be driven by the v-ATPase. At this point the Cl^-/H^+ exchanger will shunt protons from the H^+ pump but would consequently use the proton gradient to drive the concentrative uptake of Cl^- into the vesicle lumen. This would provide the necessary osmotic driving force for vesicle expansion as well as provide higher concentrations of Cl^- that may be required for processes such as ligand dissociation, enzymatic activities and protein folding (7). The highly electrogenic Cl^-/H^+ exchange of ClC-4 and ClC-5 remains compatible with the previous concept that vesicular ClCs will shunt the positive current that arises from the H^+-ATPases in endosomal/lysosomal compartments, however in this model it is more of a mechanism for the energy from the protein pump to allow the concentrative uptake of Cl^-. The discovery of ClC-4/ClC-5 as antiporters further suggests a physiological role both in facilitating endosomal acidification and in regulating the Cl^- concentration in endosomal compartments. Due to the extreme similarity of function and conductance characteristics (Li et al 2000) it is reasonable to anticipate a similar function for ClC-3.

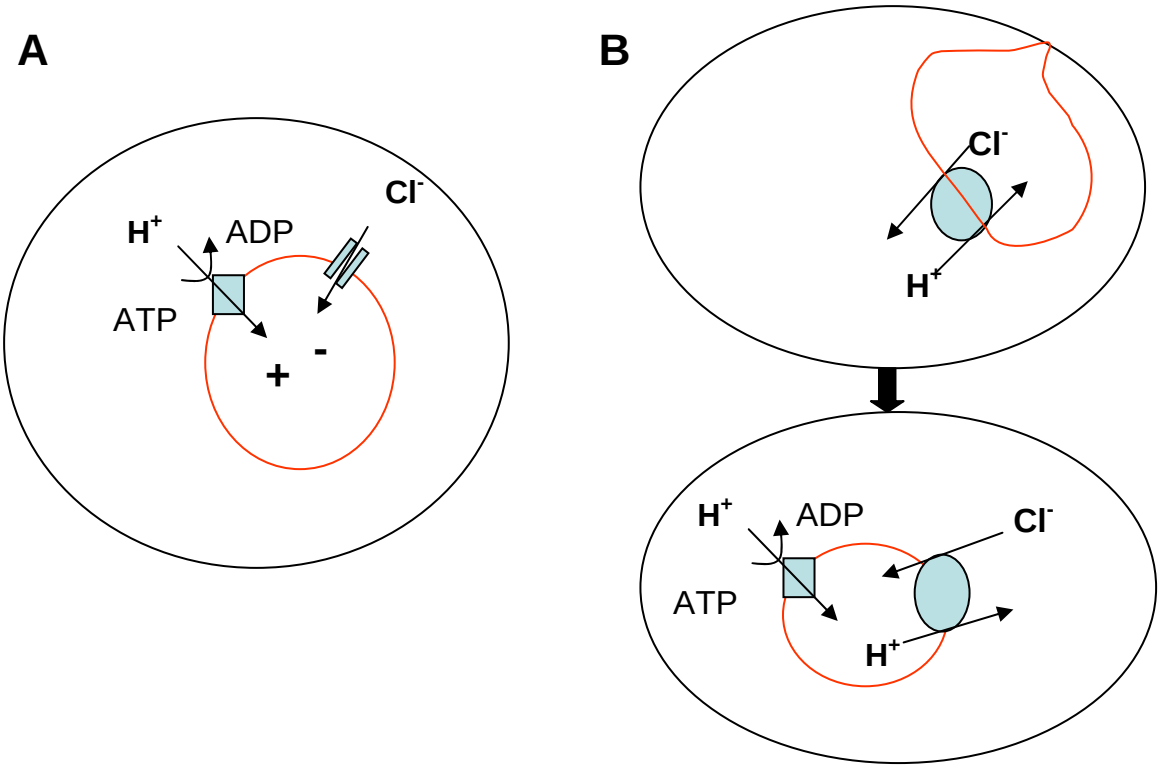

Fig 1.3 Chloride channels play roles in the acidification of the vesicular lumen. Both proton pump and chloride channel/transporter exist at the vesicular membrane. **A.** the chloride channel model shows the direct shunting of the electrogenic transport potential of H^+ **B.** The antiporter model shows that the Cl^-/H^+ exchangers may initiate the acidification of the endocytic vesicles. After the vesicles have pinched from the plasma membrane, they bring Cl^- into the vesicle at the expense of the electrochemical protein gradient. The estimated stoichiometry is 2 Cl^- for 1 H^+.

As discussed above, intracellular ClC proteins are important in facilitating luminal acidification. They are located mainly in membranes of intracellular vesicles, mostly in the endocytic pathway. In order to understand how they function in cells, we have to determine how they traffic along the intracellular compartments and what the factors that control their trafficking are.

TRAFFICKING PATHS TO ENDOSOME/LYSOSOME

Lysosome biogenesis

The lysosome is an intracellular degradative compartment for removal of materials from the cells. It is the terminal destination for many endocytic, autophagic, and secretory materials targeted for destruction. Identification of lysosomes is aided by the presence of highly glycosylated integral membrane proteins, many acid-dependent hydrolases and the lack of both the cation-dependent (CD) and cation-independent (CI) mannose 6-phosphate receptors (MPRs). This latter property distinguishes lysosomes from late endosomal compartments. There are two models for lysosome biogenesis: the "Maturation" model and the "Vesicle- transport" model. In the "Maturation" model, early endosomes are formed by coalescence of vesicles from the plasma membrane, removal of recycling vesicles, and addition of trans-Golgi network (TGN)-derived vesicles. Then they will mature to late endosomes, and eventually to lysosomes. However, in the "vesicle-transport" model, early endosomes, late endosomes and lysosomes are postulated to be stable compartments. Here transport proceeds from early endosomes through a multivesicular body (MVB) to late endosomes which mature into lysosomes or possibly to mature lysosomes directly (25). These two models are not mutually exclusive and it is possible that cells use both for lysosome biogenesis.

Two pathways to lysosomes

Lysosomal hydrolases are transported to their destination by an MPR-dependent pathway and an MRP-independent pathway. Most newly synthesized enzymes are modified with mannose 6-phosphate and bind mannose 6-phosphate receptors (MPRs) at the TGN. They traffic in vesicles to either early or late endosomes, where the hydrolases dissociate from the MPRs and are delivered to lysosomes, while the MPRs retrograde transport back to the TGN. An MPR-independent pathway also exists, yet has not been well characterized. Like MPRs, lysosomal integral membrane proteins (e.g., lamp-1) can

travel from the TGN to endosomes and lysosomes directly. However, these proteins can also travel from the TGN and insert to plasma membrane and subsequently become internalized and reach the lysosomes indirectly via the endocytic pathway as previously. Different lysosomal membrane proteins seem to use each pathway to varying extents (26).

Coat proteins are important in the sorting of membrane proteins to lysosomes

Eukaryotic cells have evolved to contain multiple different intracellular membrane bound domains. Vesicles continuously bud from one membrane, travel within the cell and fuse with a different membrane. Sorting of transmembrane proteins to endosomes/lysosomes is mediated by vesicle transport. Protein coats, the supramolecular assemblies that are deposited on the membranes, play key roles in the formation of vesicular transport carriers and in the selection of cargo proteins for transportation. Many coats have scaffold components such as clathrin. Furthermore, the ADP-ribosylation factor (Arf) and phosphoinositides initiate coat assembly by functioning as docking sites for adaptor proteins. The adaptors can bind to the scaffolding proteins such as clathrin that polymerize to form the outer layer of the coats, or bind to regulatory proteins that affect various aspects of coat function. They also bind to sorting signals in cargo proteins that mediate their concentration in the coated membrane domains (27, 28).

In general, intracellular targeting of membrane proteins is accomplished by the presence of specific short cytoplasmic motifs, which bind to adaptor proteins specific for individual compartments. Most sorting motifs characterized to date exist within the cytosolic part of the transmembrane protein. In general, the sorting signals consist of short, linear arrays of amino acid residues, in which two or three are critical for function. One of the best described motifs which produce intracellular retention of proteins is the tyrosine-based tetra-peptide motif, YXXϕ. Where ϕ is a hydrophobic amino acid (29). Tyrosine motifs can mediate internalization from plasma membrane (30), lysosomal targeting (20), basolateral targeting or TGN-to-endosome sorting (31). Another well

defined motif is the dileucine motif (32). The consensus sequence of the canonical dileucine motif is EXXXLL, where E may be replaced with D and L with I or V. Dileucine motifs have as broad a range of functions as that of tyrosine based sorting signals. They may be important in interacting with AP complexes and lysosomal targeting.

Rab proteins are monomeric small GTPases that mediate the tethering of membrane vesicles to the cytoskeleton and to acceptor organelles. SNARE proteins, soluble *N*-ethyl-maleimide-sensitive attachment protein receptors, are highly α-helical proteins that mediate the specific fusion of vesicles with target membranes. There are two classes, vesicle-membrane SNAREs (v-SNAREs) and target-membrane SNAREs (t-SNAREs) (33).

Clathrin and its adaptor proteins play roles in both direct and indirect pathway to lysosomses.

Clathrin is a structural protein that contains three heavy chains and three light chains. It binds to adaptor proteins through its "terminal domain". Clathrin polymerizes into polyhedral lattices and serves as the scaffold of membrane coats. Clathrin coated vesicles contain either of two hetero-tetrameric adaptor protein (AP) complexes, AP1 or AP2, which are derived from the TGN or the plasma membrane, respectively. The two AP proteins have similar composition. Each of them contains four subunits: (i) a small σ subunit, (ii) a medium μ subunit, (iii) two large subunits: a β subunit and a more divergent subunit, either γ or α. The β subunit is particularly important for clathrin binding. The μ and the β subunits play important roles in cargo selection. YXXϕ and dileucine motifs bind to μ subunits of AP proteins (34). The AP proteins play roles in the recruitment of clathrin to specific organelle membranes, the selection of cargo proteins for incorporation into clathrin coated vesicles, and interaction with accessory factors that regulate coat assembly and disassembly. They thus participate in vesicle formation, targeting and interactions with the cytoskeleton. Arf proteins are small GTP-binding

proteins of the Ras superfamily. Arf1 and Arf3 play roles in recruiting AP-1 to the TGN and endosomes. Arf proteins are binary switches for coat formation. They are active in the GTP-bound state and mediate the assembly of the coats. When they are in GDP-bound state, they are inactive and coats are dissembled (35). AP-3 is another adaptor protein. It is also a tetramer. It is found on clathrin coats associated with endosomes. However, it may function in the absence of clathrin (36). Another family of monomeric adaptors known as the GGAs (Golgi-localized, γ-ear-containing ADP-ribosylation factor-binding proteins) also belongs to components of TGN clathrin coats and serve the same functions as the AP complexes (33). In addition, epsins, epidermal growth factor receptor substrate 15 (Eps15), Eps15 related sequence (Eps15R), and hepatocyte growth factor-regulated tyrosine kinase substrate (Hrs) are all clathrin associated proteins that are involved in the recruitment of ubiquitylated transmembrane proteins to clathrin-coated areas of the plasma membrane and endosomes (35). In Table 1.1, I summarize the important properties of clathrin coats.

Clathrin-based systems play important roles in a large portion of the vesicular traffic originating from the plasma membrane and the trans-Golgi network that reaches the endosomal/lysosomal compartment. Clathrin-mediated endocytosis (CME) regulates the cell-surface expression and function of receptors, channels, transporters and other integral membrane proteins by facilitating fast and selective internalization of these proteins. Due to its ability to self-assemble into cages and curved lattices, clathrin serves as 'brawn' that drives membrane invagination and vesicle formation. The adaptor protein complexes are the 'brains'. They direct clathrin assembly into curved lattices and couple it to cargo recruitment (37, 38).

Table 1.1 The Properties of Clathrin Coats

Coat	Sorting signals	Localization	Functions
Clathrin-AP1	YXXØ, [DE]XXXL[LI]	TGN, endosomes	Sorting between TGN and endosomes, basolateral sorting
Clathrin-AP2	YXXØ, [DE]XXXL[LI], FXNPXY	Plasma membrane	Endocytosis
Clathrin-GGAs	DXXLL	TGN, endosomes	Sorting from TGN to endosomes
Clathrin-Hrs	Ubiquitin	Endosomes	Sorting from early to late endosomes

Through clathrin-dependent endocytosis, some transmembrane proteins can internalize and travel to lysosomes through the indirect pathway. Clathrin-dependent endocytosis consists of two categories: constitutive endocytosis and regulated endocytosis. Transferrin receptor (TfnR), for example, can constitutively internalize and recycle back to the plasma membrane. In contrast to constitutive internalization, regulated endocytosis depends on ligand binding and resulting phosphorylation and ubiquitin-mediated interactions for the endocytosis to occur. Endocytosis of different cargo molecules through the clathrin pathway is controlled by specific molecular interactions. Although EGFR and TfnR are both internalized through clathrin mediated pathways, there are different limiting steps of internalization of these two proteins. The independence of these internalization pathways is demonstrated by the fact that activated EGFR continues to be internalized at a constant rate even when the pathway of

endocytosis for TfnR is saturated (39). This suggests that different interactions among the endocytic components or posttranslational modifications occur in this process. In Fig. 1.4, I show the critical components of clathrin mediated endocytosis.

A great advance in recent years has been the discovery of ubiquitin as a conserved signal for cargo proteins internalization and sorting to the lysosomes. Receptors and other cargo proteins, either from the plasma membrane or TGN, are first ubiquinated or then delivered to the endosomes where the ubiquitinated membrane proteins are recognized by the Hrs/STAM/Eps 15 complex. Hrs, a clathrin adaptor, can recognize cargo and recruit clathrin to stabilize a micro-domain in the endosomes in which the cargo proteins are retained. The cargo proteins trapped in the Hrs complex are then passed to the ESCRT (endosomal sorting complex required for transport) complex and finally trafficked to and degraded in lysosomes. Growth factor receptors become ubiquitinated upon ligand association and are thus routed to lysosomes via this Hrs pathway (40).

Rabs and SNAREs involved in lysosome sorting

Rabs are small GTPases that play switching roles in vesicle formation, motility, tethering and docking. More than 60 different Rab proteins are present in mammals. They are active in the GTP bound state in which they bind to membranes and recruit accessory molecules and effectors of vesicle docking/fusion. Although the roles of the majority of Rabs are not well identified, the functions of several members are understood in some details. Rab7 and Rab9 are localized to the surface of the late endocytic compartments. Rab7 appears to be important for antegrade transport to the lysosome while Rab9 mediates retrograde transport from late endosomes to the TGN (26). Rab4 is localized to early/recycling endosomes. It plays roles in sorting/recycling in early endosomes(41). The function of Rab5 involves ligand sequestration at the plasma membrane, CCV-EE and EE-EE fusion. The direct effectors of Rab5 include EEA1, a tethering factor for endosome fusion (42). Rab11 participates in the recycling through perinuclear recycling endosomes and trafficking from plasma membrane to the Golgi complex (43).

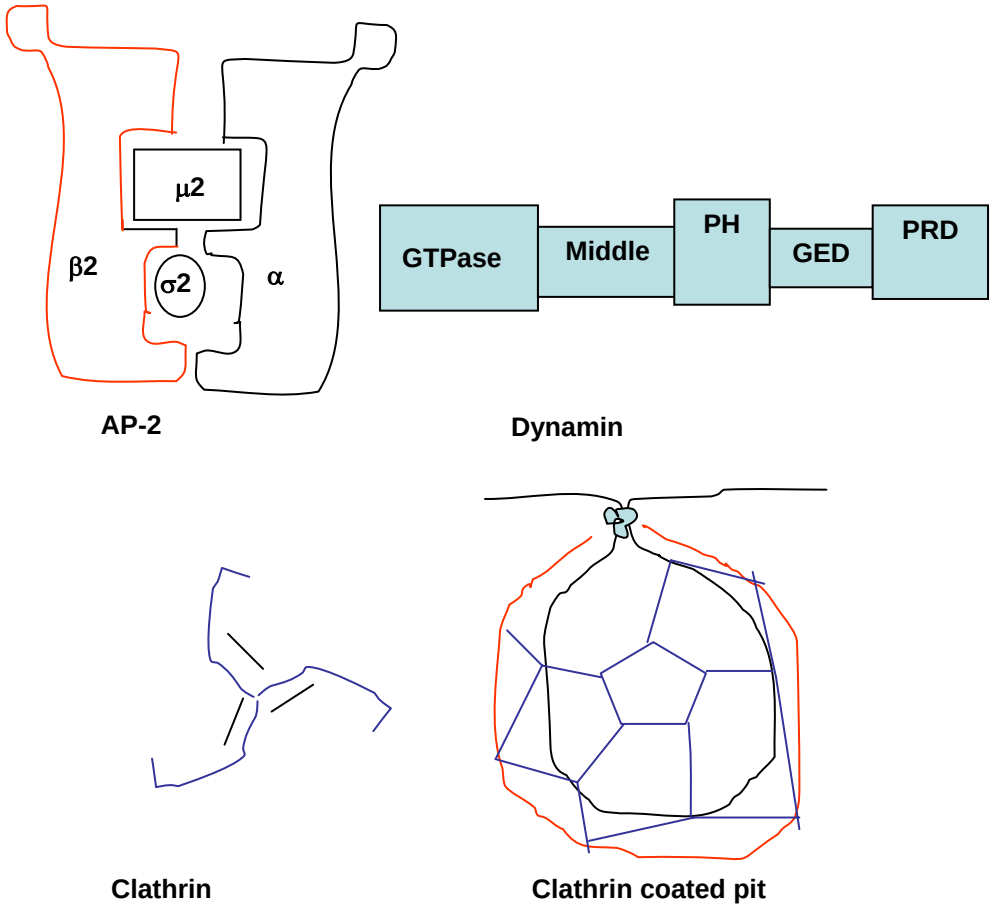

Fig 1.4 Clathrin Mediated Endocytosis. Clathrin triskelions contain three clathrin heavy chains (CHC) and three tightly associated light chains (CLC). AP-2 complexes are tetramers. They are targeted to the plasma membrane by the α-adaptin subunits, where they mediate clathrin assembly through the β2-subunit. AP-2 interacts directly with targeting signals on cargo proteins through its μ2 subunit. Dynamin is a multidomain GTPase that plays a role in the fission and the release of CCVs.

Targeting and membrane fusion also require another family of proteins called SNAREs. These are present on both vesicles (v-SNAREs) and target membranes (t-SNAREs). Among them, Syntaxin 7 and VAMP-7, play roles in heterotypic and

homotypic fusions involving lysosomes. Syntaxin 8 resides in endosomes, lysosomes and possibly the TGN. It may play a role in sorting from early to late endosomes. Rab effectors and modified lipids interact with SNAREs and are essential to sorting specificity (26) .

In summary, extensive catalogs of proteins are involved in lysosomal sorting. The following figure showed the major players which have been well studied in the lysosome sorting process.

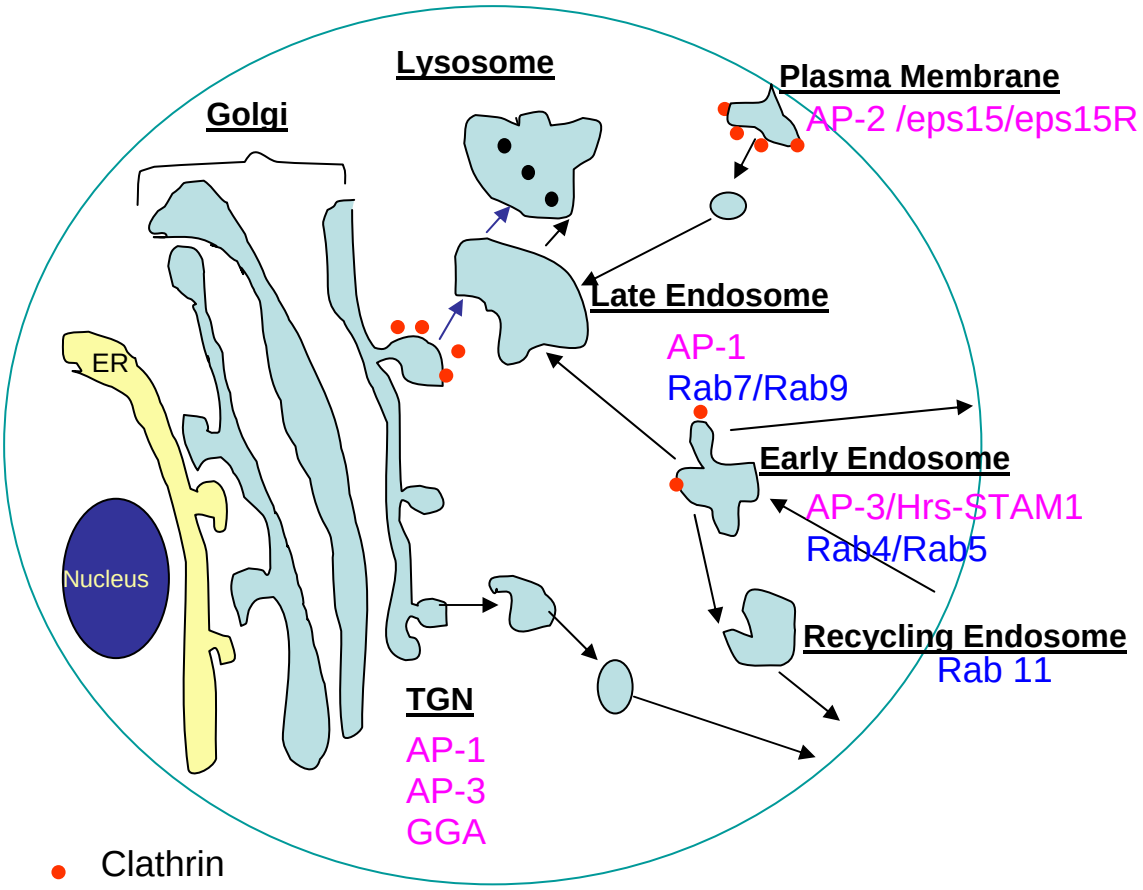

Fig 1.5 Sorting pathways leading to lysosomes. In the biosynthetic-secretory pathway protein molecules are synthesized at the ER and then transported to the Golgi network,

the late endosomes and finally to lysosomes. In the endocytic pathway, molecules are internalized in vesicles derived from the plasma membrane and transported to early endosomes and then via late endosomes to lysosomes. Clathrin, adaptor proteins, Rabs and other accessory proteins play roles in the two pathways to lysosomes as indicated.

OVERVIEW OF CHLORIDE CHANNEL TRAFFICKING

CFTR

Great progress has been made in the molecular identification of chloride channels. Among the six classes of chloride channels, the cystic fibrosis transmembrane conductance regulator (CFTR) has been most thoroughly investigated. CFTR is a chloride channel that is responsible for the cAMP-activated anion conductance of epithelial cell apical membranes. CF disease arises due to a decreased number and/or activity of CFTR in the apical membranes of secretory epithelial cells, such as those in the airways, exocrine pancreas, and intestines. The distribution and trafficking of CFTR has been thoroughly investigated and a model has been developed as follows:

Properly folded, newly-synthesized CFTR leaves the rough endoplasmic reticulum and travels through the Golgi, where it undergoes glycosylation to form the mature protein. Mature CFTR molecule leaves the Golgi in vesicles that can move directly to the apical plasma membrane or to the recycling endosome. CFTR-containing vesicles continually traffic between recycling endosomes and plasma membrane. However, the rates of trafficking and protein distribution are determined by cell type, differentiation, and phosphorylation state. CFTR eventually reaches the late endosome-to-lysosome pathway for degradation. Misfolded CFTR mutants and significant wild-type immature CFTRs are degraded by the proteosome. Therefore, as an integral membrane protein, CFTR may be transiently located at all subcellular compartments in the protein secretion pathway. Although there is no doubt that CFTR functions as chloride channel at the apical membrane of the epithelial cells, many studies also show that a significant

amount of mature CFTR is located in intracellular compartments. These intracellular CFTR molecules are functional and cAMP stimulation can regulate the distribution of CFTR between the apical membrane and intracellular compartments. Different studies show that the C terminal of CFTR can bind to the plasma membrane endocytic adaptor AP-2, which may guide it into the clathrin-dependent endocytic pathway (44). The most common mutation in Caucasian CF patients is CFTRΔF508. While wild type CFTR can recycle back to the plasma membrane, mutant CFTR is ubiquitylated and diverted to degradation in the lysosome (45).

ClC-5

ClC-3, -4 and -5 constitute a branch of endosomal/lysosomal chloride proteins with diverse functions. Among them, trafficking has been best studied for ClC-5. It is highly expressed in early and recycling endosomes in subapical compartments of the renal proximal tubule. It is known that low-molecular-weight proteins (LMWPs) are reabsorbed by endocytosis via megalin and/or cubilin, the multiligand tandem receptors abundantly expressed at the brush border of kidney proximal tubular cells (PTC). In ClC-5 KO mice, intracellular trafficking of these receptors is affected by a slower apical internalization and a more severe slowing down of the recycling of megalin and cubilin to the brush border. This explains the preferential retention of these receptors in endosomes. Therefore, disruption of ClC-5 impairs receptor-mediated endocytosis by defective trafficking of megalin and cubilin in kidney proximal tubules (46). A PY motif exists between the two CBS domains in the C terminal of ClC-5. This motif can interact with WW-domains of the ubiquitin ligase WWPII, a Nedd4 family member, thus stimulating the endocytosis of ClC-5 (47) A mutant disrupting the second CBS domain of ClC-5 is unable to traffic normally to acidic endosomes but is present in a perinuclear compartment, colocalizing with the Golgi complex (48). Expression of an R648X mutant leads to a significant increase in surface expression when compared to wild type ClC-5 (49). ClC-5 is thus a channel that is present at the plasma membrane and the endosome

and its ability to be retained in these compartments requires targeting motifs in its C-terminal cytosolic domain.

ClC-3

An examination of the structure of ClC-3 identifies three distinct domains: a transmembrane channel core and N and C terminal cytosolic domains. Several putative signal motifs are included in the cytosolic domains. Three different splice variant isoforms have been identified that differ only in the cytosolic domains. The 3 splice variants are: ClC-3 short form, ClC-3 long form (50), which contains an additional 58 amino acid segment at the N terminal and ClC-3B, which contains an alternate C terminal sequence (51). Note that the transmembrane channel cores are the same in all three.

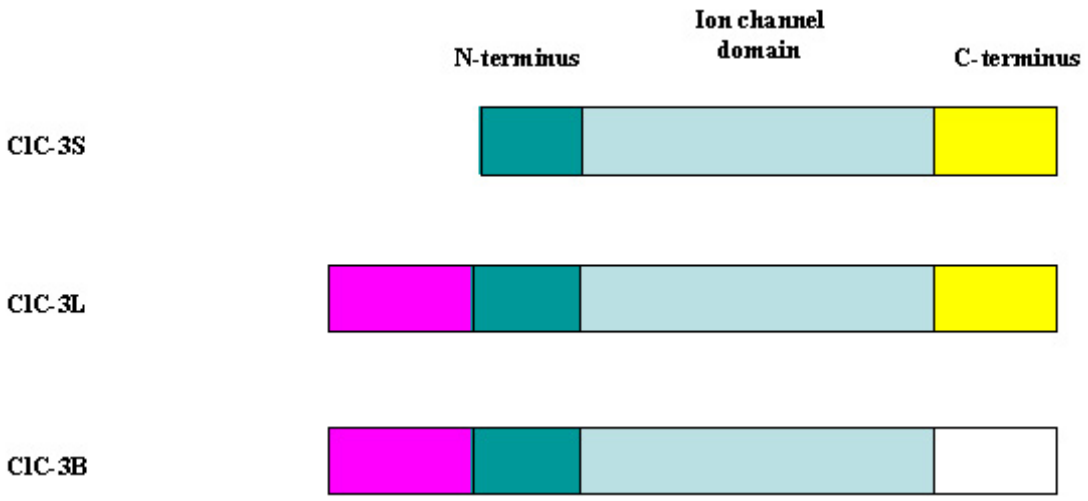

Fig 1.6 Domain Organization of the ClC-3 isoforms. ClC-3 short form (ClC-3S) contains N and C cytosolic domains and a transmembrane channel core. ClC-3 long form (ClC-3L) contains an additional 58 amino acid segment at the N terminal and ClC-3B is a variant of the ClC-3 long form that contains an alternate C terminal sequence.

The trafficking path of ClC-3 and the mechanisms regulating its trafficking are poorly understood. Although the transmembrane channel cores are the same in all three

ClC-3 splicing variants, the distribution pattern of the three varies. The ClC-3 short form was predominantly present in the endosomal/lysosomal compartment. The vesicle formation pattern seen with ClC-3 over-expression was specific to the short form of ClC-3 and was not seen with ClC-3 long form (16). ClC-3B contains a PDZ-binding domain at its C terminal. It resides in the Golgi where it co-localizes with a small amount of CFTR, another known PDZ-binding chloride channel. Furthermore, certain physiological conditions such as hypo-osmollality (52) and intracellular Ca2+ (53) may induce the translocation of ClC-3 from intracellular sites to the plasma membrane.

The experiments described in this dissertation focuses exclusively on the ClC-3 short form. This isoform was chosen for investigation because it expresses well in different mammalian cell lines, and previous work from our lab has determined its biophysical properties and demonstrated its functional activity. In addition, there has been controversy regarding the precise cellular localization of this protein. Therefore, a careful investigation of the localization and trafficking of ClC-3 short form was required to advance knowledge in this field. All the data in this dissertation will show results obtained from ClC-3 short form.

CENTRAL HYPOTHESIS AND OVERVIEW OF THE RESULTS

The function of ClC-3 has been studied with knock out mice by Jentsch and colleagues. These studies showed that disruption of ClC-3 in mice leads to degeneration of the hippocampus (14). In spite of the establishment of this knockout mice model, there is still a critical gap in the knowledge base that centers on the distribution and trafficking of ClC-3. Little is known about the definitive distribution and trafficking pattern of ClC-3 and the factors controlling the specific distribution of intracellular ClC-3. Our Central Hypothesis is: ClC-3 is an intracellular chloride channel. It traffics from plasma membrane to the late endosome/lysosome through clathrin-coated vesicles. Intracellular targeting of ClC-3 is accomplished by specific motifs in the cytosolic part of the

molecule which bind to adaptor proteins. The investigations, that are described in the following chapters have identified the distribution of ClC-3, determined its trafficking pathways, and identified the targeting motifs and adaptor proteins, which play important roles in controlling the distribution.

Subsequent chapters will focus on my studies of the ClC-3 chloride channel. In the first experimental chapter, I describe the development of the experimental methods to perform the study and their use as tools to evaluate the distribution and trafficking of the wild type ClC-3. In the second experimental chapter, I describe studies to identify the critical motif which controls the movement of ClC-3. In the third experimental chapter, I describe an investigation of the interaction between ClC-3 and adaptor proteins in the trafficking process. Together, this work unveils the mechanism of the ClC-3 transport.

SIGNIFICANCE

My study provides a fundamental understanding of ClC-3 trafficking and the factors controlling its distribution. This work enhances our understanding of protein-protein interactions of this channel family and gives insight into how intracellular chloride channels are controlled. Further understanding of the trafficking path and physiological role of chloride channels can lead to novel therapeutic approaches for diseases in which chloride channel trafficking is impaired such as cystic fibrosis. Furthermore, understanding the roles of ClC channels in endocytosis and regulation of intracellular pH will potentially allow new methods to alter endocytosis pathways that are used by pathogens such as viruses for entry into cells.

CHAPTER 2
STEADY STATE DISTRIBUTION AND TRAFFICKING OF CLC-3

INTRODUCTION

The function of ClC-3 has been best defined in brain where it is required for acidification of hippocampal synaptic vesicles (14). However, it is also present in most non-neuronal cells as well (50) and there is still uncertainty about its localization and function in these cells. Several groups have detected ClC-3 at the plasma membrane (53, 54), but others have found it primarily to be in endosomal or lysosomal compartments (15, 16, 55). There is controversy whether it resides at the plasma membrane and functions as a swelling -activated channel (56) or an intracellular channel functioning as a pH regulator (16). Furthermore, the trafficking path of ClC-3 is unknown and whether it shuttles between different compartments has not been determined. The objective of the experiments reported in this chapter is to identify the distribution and trafficking path of ClC-3 when expressing in heterologous cell lines. In this chapter, we use different strategies to elaborate this issue. A methods section will follow the presentation and discussion of the results.

Many of the trafficking process in cells are temperature dependent. Lower temperature can slow trafficking steps differentially in several cell types. Incubation at 18°C will subject cells to an 18°C blockade, which is permissive for internalization from the cell surface but significantly attenuates exit from early endosome as well as the trans-Golgi network (57). Incubation of the cells at 4°C is a condition not permissive to trafficking, which blocks all vesicle movement (58). The studies presented in this chapter will use multiple different constructs and fusion proteins derived from the ClC-3 short form and assess their trafficking properties. In the following figure, I illustrate the four wild type ClC-3 constructs used in this chapter.

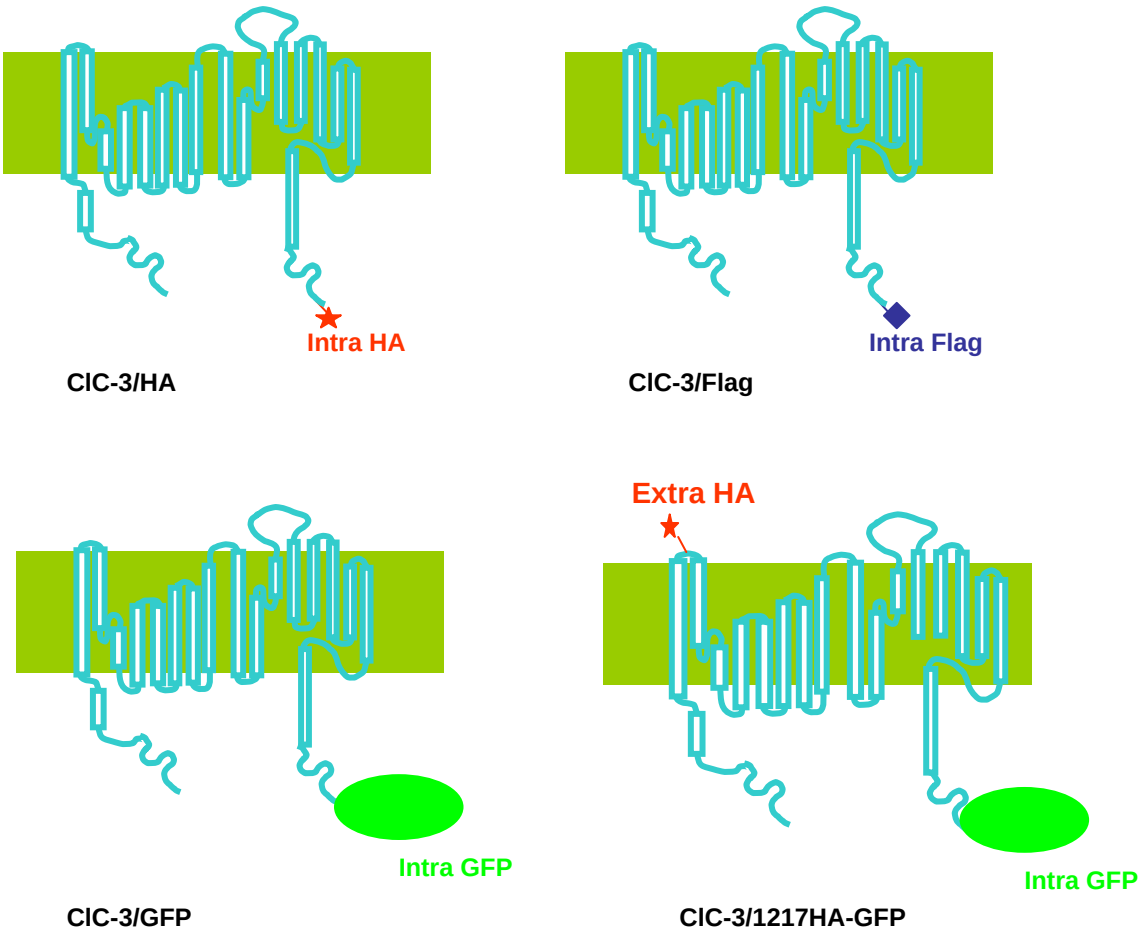

Fig 2.1 Wild type ClC-3 constructs used in this chapter. ClC-3/HA has an intracellular HA tag at its cytosolic C terminal. This construct has been used in the biotinylation assays. **ClC-3/GFP** has an intracellular GFP moiety fused at its cytosolic C terminal. This construct has been used in imaging studies, cell fractionation, and biotinylation studies. **ClC-3/Flag** has an intracellular Flag tag at its cytosolic C terminal. This construct has been used in the co-localization study between ClC-3 and ClC-5. **ClC-3/1217HA-GFP** has an extra-cellular HA epitope between the B and C loop of ClC-3 as well as an intracellular GFP tag at its cytosolic C terminal. This construct has been used in the imaging studies on the trafficking path of ClC-3.

RESULTS

ClC-3 primarily localizes in large vesicular structures.

Use of a ClC-3/GFP fusion protein for the study of localization

At the time my studies began in 2001, work in our lab had already shown that a fusion protein in which GFP was fused to the C terminus of ClC-3 produced measurable plasma membrane currents when expressed in CHO cells (59). This result proved that the ClC-3/GFP fusion protein is functional. Furthermore, it indicated that at least a fraction of ClC-3 is localized at the plasma membrane. My work was thus initiated based on this simple finding.

ClC-3 expression results in the formation of acidic vesicles

Expression of ClC-3 in CHO cells uniformly results in the formation of large intracellular vesicular structures with ClC-3 itself localizing to the membrane of these vesicles. Figure 2.2 demonstrates the appearance of the ClC-3/GFP fusion protein transiently expressed in four different cell types. It is notable that in each case ClC-3 localizes to large intracellular vesicular structures that appear identical to those previously reported in CHO cells (16). This phenotype is therefore independent of the cell type used.

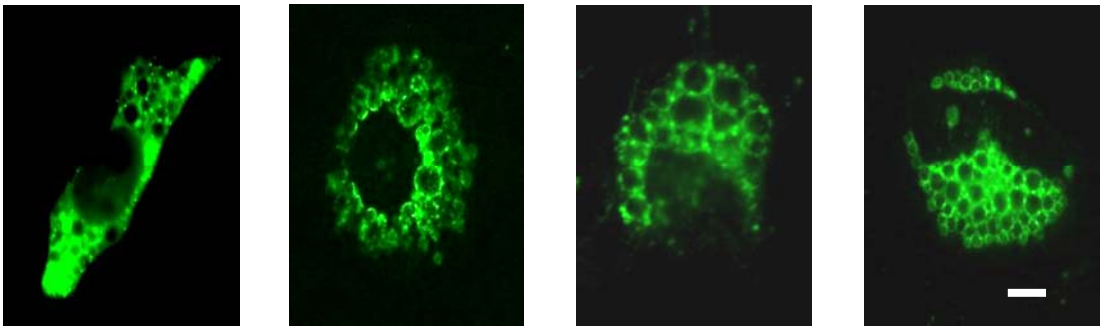

CHO-K1 **COS-7** **HeLa** **Huh-7**

Fig 2.2 Pattern of ClC-3 localization in different cell lines: Cells were transfected with ClC-3/GFP, fixed, and observed by epi-fluorescence microscopy. ClC-3/GFP fluorescence is represented in green. Note the appearance of large vesicular structures in each of the four different cell lines tested. Bar, 10 μm applies to all images.

The vesicular structures formed specifically with ClC-3 and were not induced by ClC-5 expression (Fig 2.3 A). However, when we co-expressed ClC-3 and ClC-5 in Hela cells, large intracellular vesicular structures formed again. In addition, both ClC-3 and ClC-5 co-localized to these structures (Fig 2.3B).

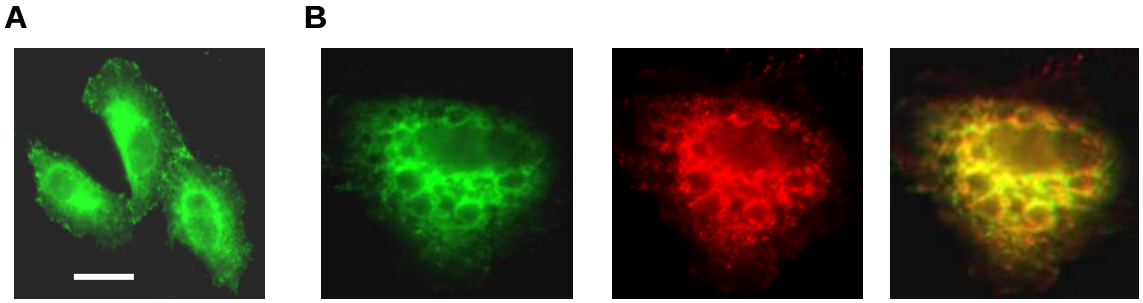

Fig 2.3. Expression of ClC-5 in Hela cells. A. Hela cells were transfected with ClC-5/GFP, fixed and observed by epi-fluorescence microscopy. ClC-5/GFP fluorescence is

represented in green. Note there are no large vesicles formed. **B.** Hela cells were co-transfected with ClC-3/Flag and ClC-5/GFP, fixed, and immunolabelled with anti-Flag primary antibodies. Alexa-594 goat anti-mouse IgG was the secondary antibody. The fluorescent images of ClC-5/GFP (green) or ClC-3 (red) are displayed along with each other. Bar, 10 μm. When ClC-5 and ClC-3 were coexpressed in Hela cells, large vesicles again formed in the cells and the image of ClC-5 overlapped with that of ClC-3.

Large vesicles are late endosome/lysosome.

To determine the characteristics of these vesicles, we examined the internal pH of ClC-3 containing vesicles in living cells. This was accomplished by exposing transfected cells to LysoSensor blue, a membrane-permeable weak base with acid-dependent fluorescence (pKa 5.1). This molecule is useful for identification of acidic compartments because it is selectively concentrated in acidic spaces where its fluorescence quantum yield is dramatically increased. In practice, its blue fluorescence can only be observed in highly acidic spaces (60). After LysoSensor was incubated with ClC-3/GFP-transfected cells for 30min, the lumen of the vesicles exhibited very strong blue fluorescence (Fig. 2.4). Non-transfected cells generally demonstrated small blue fluorescent spots, but these were dramatically smaller and less intense than in the transfected cells and were not visible under the imaging conditions used in Fig. 2.4. This demonstrates that the ClC-3-associated vesicles have a strongly acidic interior, whereas untransfected cells lack such large acidic compartments.

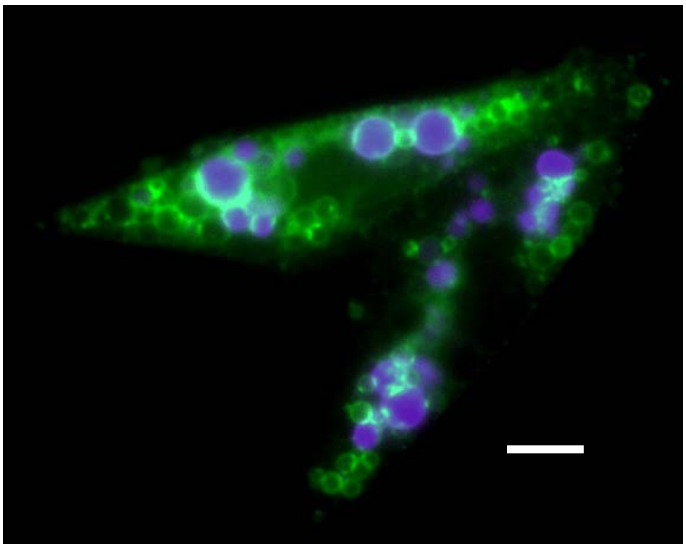

Fig 2.4 Acidic lumen in ClC-3-associated vesicles. Chinese hamster ovary (CHO-K1) cells were transfected with ClC-3/GFP. Transfected cells were incubated with LysoSensor blue for 30 min and then observed without fixation. Images displayed are composites of LysoSensor fluorescence and ClC-3/GFP fluorescence. Bar, 10 μm.

The most commonly used method of separating suspensions of mixed populations of biological particles is centrifugation on density gradients. Cell fractionation experiments showed that ClC-3 has a broad distribution pattern and it is primarily in fractions 5-9, which corresponds to 6-12% gradient. Lamp-2, the lissome membrane protein, is primarily in fractions 4-6, which demonstrates a great overlap with ClC-3 (Fig 2.5).

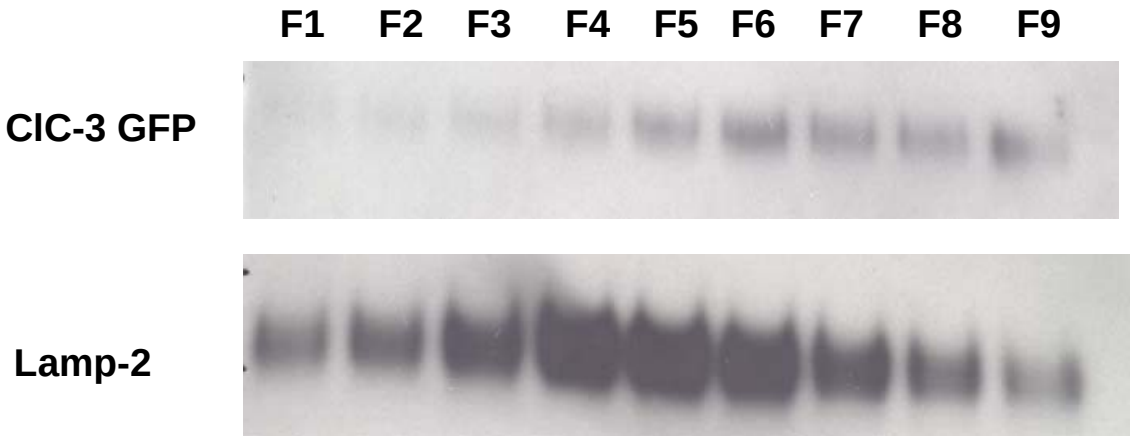

Fig 2.5 Subcellular fractionation of ClC-3/GFP in transected COS-7 cells. COS-7 cells were transiently transfected with ClC-3/GFP. Cell homogenates were loaded on pre-formed 5-25% Optiprep (Iodixanol) linear gradients. After ultracentrifugation, 9 fractions were collected. For immunoblotting, fractions were pelleted and the pellets were dissolved in SDS-PAGE sample buffer and subjected to electrophoresis and immunoblotting. Blots were probed with antibodies for GFP and Lamp-2. Note that the distribution of ClC-3 overlaps with that of Lamp-2.

Because both ClC-3 and Lamp-2 have broad distribution patterns, we performed immunofluorescent microscopy in order to better visualize the colocalization between ClC-3 and Lysosomal markers. In Fig 2.6, I showed that both lysosome associated membrane proteins lamp-1 and lamp-2 colocalize with ClC-3. Cathepsin D, a known lysosomal enzyme, is present in the lumen of some but not all ClC-3 containing vesicles. The lack of cathepsin D staining in all vesicles could either be due to heterogeneity of the vesicles or could reflect loss of this soluble protein as a result of the fixation and permeabilization steps. These data thus demonstrate that the ClC-3 vesicles have characteristics of late endosomal/lysosomal structures (Fig 2.6).

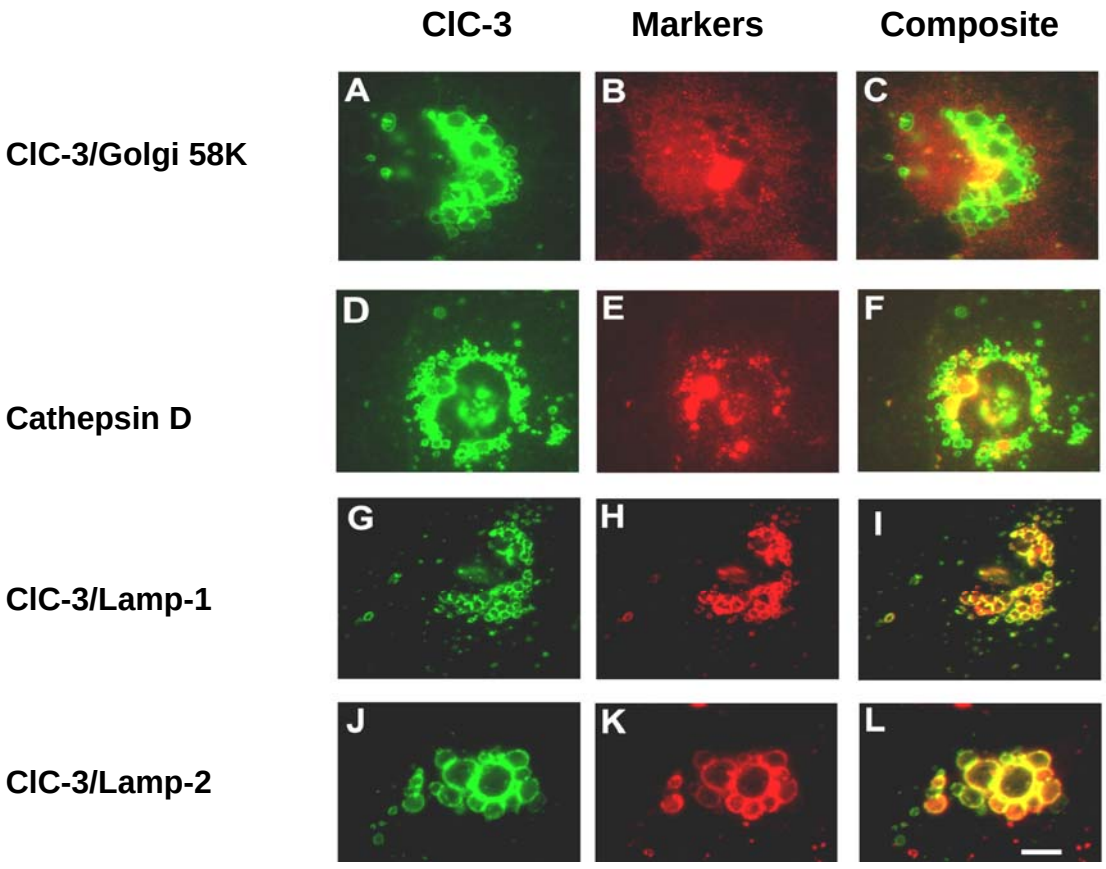

Fig 2.6 Colocalization of ClC-3 with marker proteins. Huh-7 cells were transfected with ClC-3/GFP, fixed, and immunolabelled with anti-Golgi 58K (A-C), anticathepsin D (D-F), anti-lamp-1 (G-I), or anti-lamp-2 (J-L) primary antibodies. Alexa-594 goat anti-mouse IgG was the secondary antibody. The fluorescent images of ClC-3/GFP (green, A, D, G, and J) or marker protein (red; B, E, H, and K) are displayed along with the respective composite images (C, F, I, and L). Areas of colocalization appear yellow in the composite images. Bar 10 μm.

A small portion of ClC-3 is at plasma membrane

Previous patch clamp studies from our lab demonstrated the presence of characteristic chloride currents when wt ClC-3 was transiently expressed in CHO-K1 cells (61). This result shows the functional existence of ClC-3 at the plasma membrane. In order to confirm the surface expression of ClC-3, we performed biotinylation studies. EZ-Link Sulfo-NHS-SS-Biotin Labeling Reagent enables simple and efficient biotin labeling of amine-containing biomolecules in solution. Specific labeling of cell surface proteins and evaluation of their recycling and internalization process are common applications for this water-soluble, membrane impermeable and cleavable biotinylation reagent. Therefore, it has become an important tool for studying the expression and regulation of receptors and transporters. It allows differentiation of plasma membrane proteins from those localized to intracellular organelle membranes and by using membrane impermeant cleavage reagents it allows an assessment of internalization and recycling of cell surface proteins. Once the cell surface proteins have been biotinylated, the labeled proteins can be specifically precipitated using streptavidin conjugated resin beads. Subsequently the target protein can be detected with specific antibodies.

A schematic representation of a typical experimental protocol to detect plasma membrane proteins is shown in Fig 2.7.

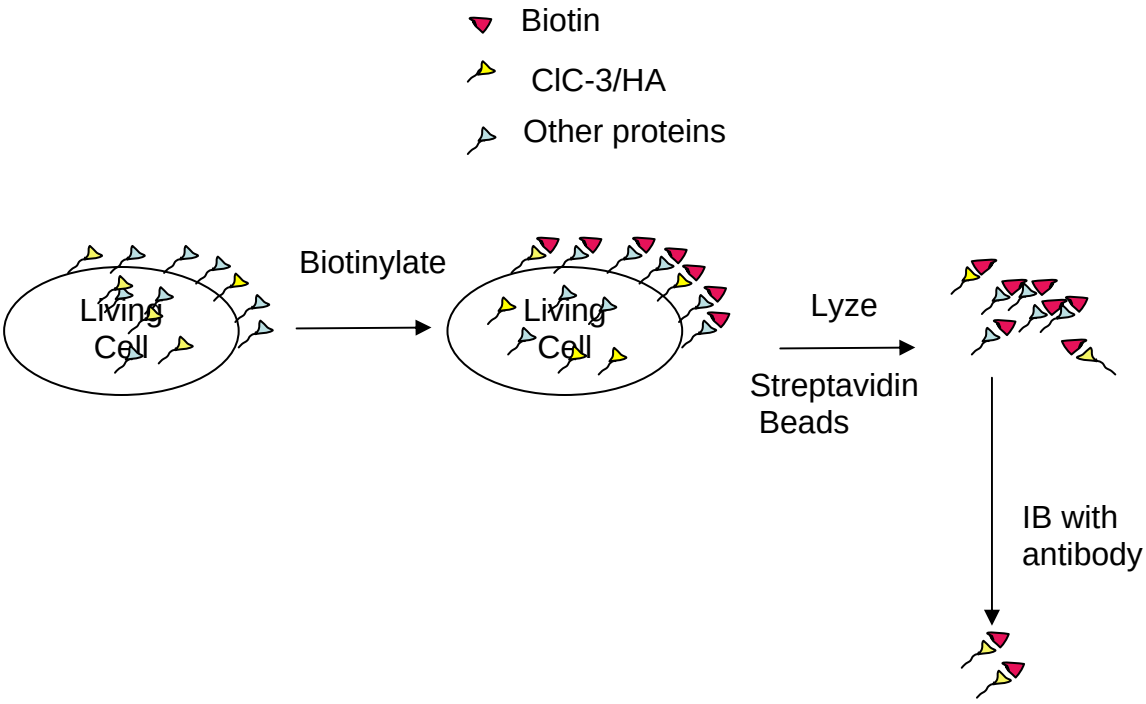

Fig 2.7 Strategy to Identify Plasma Membrane Proteins with Biotinylation. COS-7 cells were transfected with ClC-3. After 48 h, the transfected cells were incubated with biotinylation reagent at 4 °C. The cells were then lysed and the lysates were precipitated with streptavidin-agrose beads. The streptavidin pellets were subjected to SDS-polyacrylamide gel electrophoresis and western blotting. ClC-3 was detected by specific antibody.

We transiently transected COS-7 cells with GFP tagged ClC-3 and determined the extent of its presence at the plasma membrane. GluR6/GFP, a known plasma membrane receptor, was used as a reference (62). Fluorescent microscopy showed a predominant plasma membrane distribution of GluR6/GFP, but not ClC-3 /GFP (Fig 2.8A).

To further determine whether ClC-3 was present at the plasma membrane, we used surface biotinylation. Recombinant ClC-3/GFP was transiently expressed and cell surface proteins were labeled at 4°C with sulfo-NHS-SS-biotin. Cells were then lysed, biotinylated proteins were precipitated with streptavidin coated beads and analyzed by

SDS-PAGE and immunoblotting. GluR6 showed a strong band both in total lysate (T) and in the streptavidin pellet (P). Biotinylated ClC-3 was also present, however, unlike GluR6, it accounted for only approximately 6% of the total protein (Fig 2.8B). These data confirm that ClC-3 is present on the cell membrane but unlike the case for GluR6, the plasma membrane is a relatively minor site for ClC-3 at steady-state.

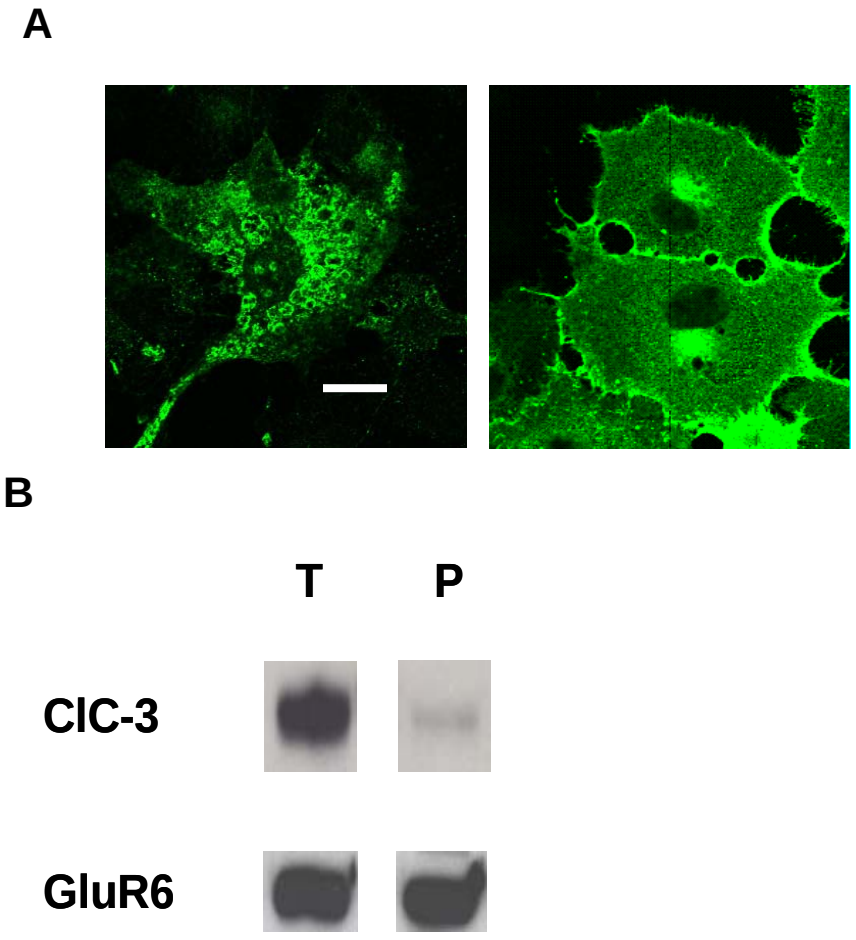

Fig 2.8 Presence of ClC-3 at the plasma membrane. COS-7 cells were transiently transfected with either ClC-3/GFP or the plasma membrane receptor GluR6/GFP. **A.** Confocal microscopy images of ClC-3 (left) or GluR6 (right) demonstrating strong membrane localization of GluR6 and primarily intracellular distribution of ClC-3. **B**.

Transfected cells were surface biotinylated as described, and subjected to lysis, and immunoblotting of lysates and streptavidin precipitates. T- Total lysate (25 μg protein), P-streptavidin precipitate derived from 200 μg of input lysate protein.

Trafficking of ClC-3

Plasma membrane ClC-3 undergoes rapid internalization.

In order to test whether plasma membrane ClC-3 undergoes endocytosis, we assessed biotin internalization by a variation of the experimental protocol previously described (63). Sulfo-NHS-SS-Biotin is a thiol-cleavable amine-reactive biotinylation reagent that can be cleaved with sodium 2-mercaptoethanesulfonate (MesNa). The advantage of MesNa over other thiols is that it dissolves readily in polar solutions and is charged by the sodium sulfoxide group on the succinimidyl ring. It therefore cannot penetrate the cell membrane by itself. The procedure to detect endocytosis of ClC-3 is shown in Figure 2.8.

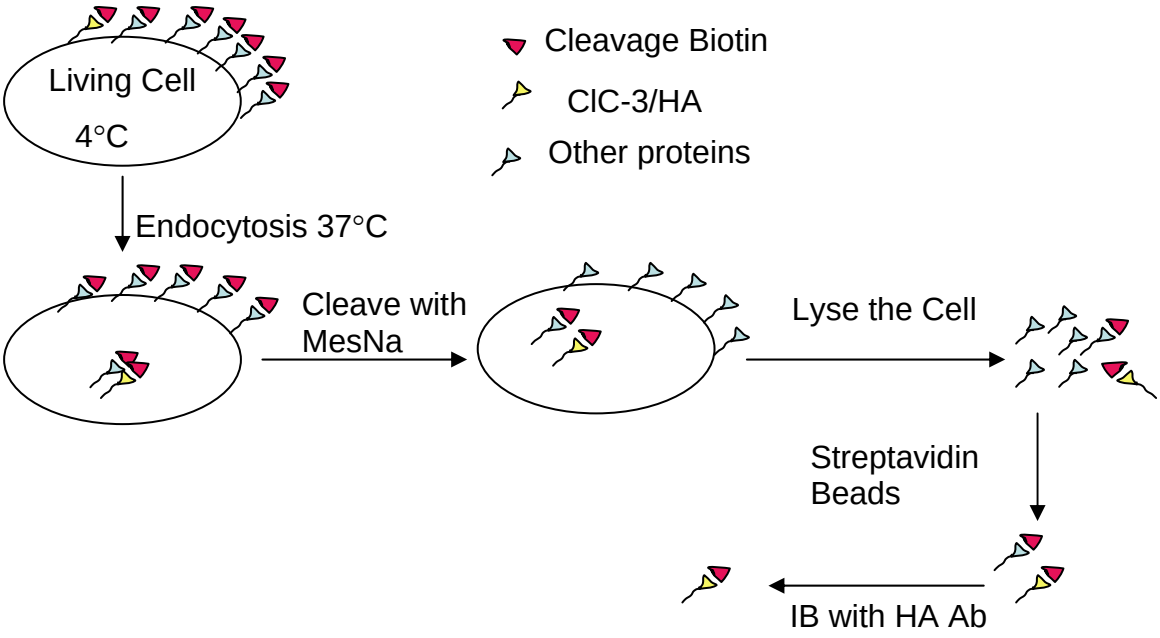

Fig 2.9 Strategies to Detect Endocytosis of ClC-3/HA. COS-7 cells were transfected with ClC-3/HA. The transfected cells were cultured for 48 h and then incubated with the biotinylation reagent at 4°C. The cells were than shifted to 37 °C for a variable period of time. Biotinylated proteins that do not undergo internalization during the 37° incubation period are susceptible to cleavage by MesNa. Only those proteins that undergo endocytosis are protected from cleavage and thus able to be precipitated with streptavidin beads. ClC-3 was detected by HA antibody.

Using this cleavage biotin experiment, we demonstrated that surface expressed ClC-3 undergoes endocytosis. Cell surface proteins were biotinylated with sulfo-NHS-SS-Biotin (Fig. 2.10A, lane 1), and cleaved with MesNa either immediately after biotinylation (Fig. 2.10A, lane 2) or after a 15min incubation at 37°C (Fig. 2.10A, lane 3). ClC-3 demonstrated substantial retention of biotinylation after the 15 min incubation, representing endocytosis during the incubation period.

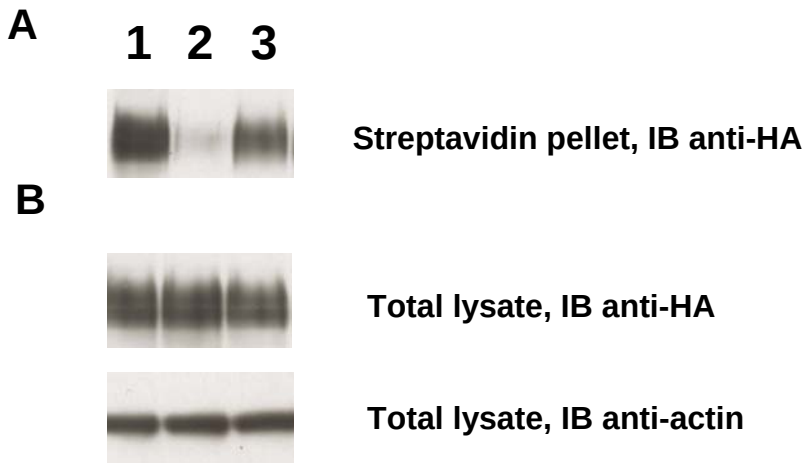

Fig 2.10 Internalization of plasma membrane ClC-3. **A.** ClC-3/HA transfected COS-7 cells were surface biotinylated with sulfo-NHS-SS-biotin, which was subsequently cleaved with MesNa, prior to streptavidin precipitation. HA immunoblot of streptavidin pellets was shown. Lane 1, streptavidin pellets before cleavage; lane 2, streptavidin pellets after immediate cleavage; lane 3, streptavidin pellets after biotinylated cells were first incubated for 15 min at 37°C prior to cleavage. **B.** Loading control of A. Upper panel, HA immunoblot of total lysates; lower panel, actin immunoblot of total lysate. This showed that the expression level of ClC-3 in the total lysates is the same in three groups.

We next measured the time course of ClC-3 internalization. After biotinylation at 4°C with sulfo-NHS-SS-biotin, the cells were incubated at 37°C for different times prior to cleavage and then subjected to streptavidin pulldown and western blot for ClC-3. Fig 2.11 demonstrates results from 3 similar experiments. These data showed that the endocytosis of ClC-3 molecule reached its plateau at about 15 minutes.

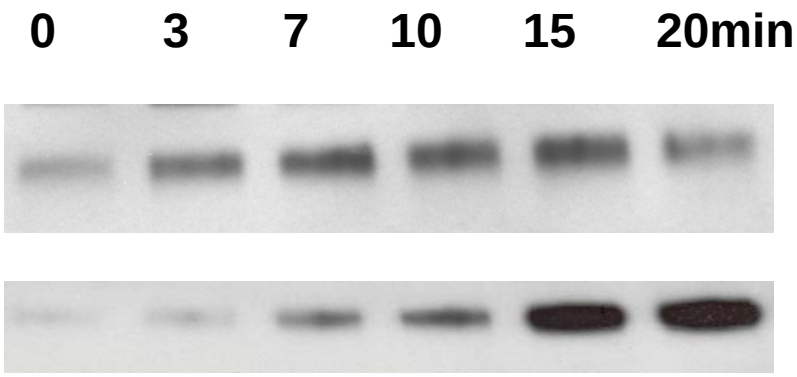

Fig 2.11 Time course of internalized ClC-3 The cleavage biotin experiment was performed as in Fig 2.10 but the time of incubation between biotinylation and cleavage varied as indicated. The blots shown are from a single representative experiment that was repeated 3 times with similar results.

Plasma membrane ClC-3 moves to large internal vesicles.

In order to follow the trafficking of ClC-3, we inserted an extracellular epitope on the ClC-3 molecule. We used a specific antibody to bind the epitope and chased the movement of the ClC-3 molecule. The assumptions of this experiment are: Only external epitope can bind to the specific antibody; antibody doesn't dissociate from ClC-3 after internalization; binding of the antibody will not alter the trafficking of ClC-3.

We generated an additional ClC-3 construct, ClC-3 1217HA/GFP, with an extracellular HA epitope between the B and C loop (Fig 2.1). This is in contrast to the ClC-3/HA, which has an internal HA epitope that was used for the biotinylation experiments.

To test the validity of the assumptions necessary to use this external epitope construct for the study of endocytosis, we transfected COS-7 cells with two ClC-3 HA variants and observed HA labeling by immunofluorescence microscopy with and without cell permeabilization. The HA antibody specifically recognized the extracellular HA tag in non-permeabilized cells.

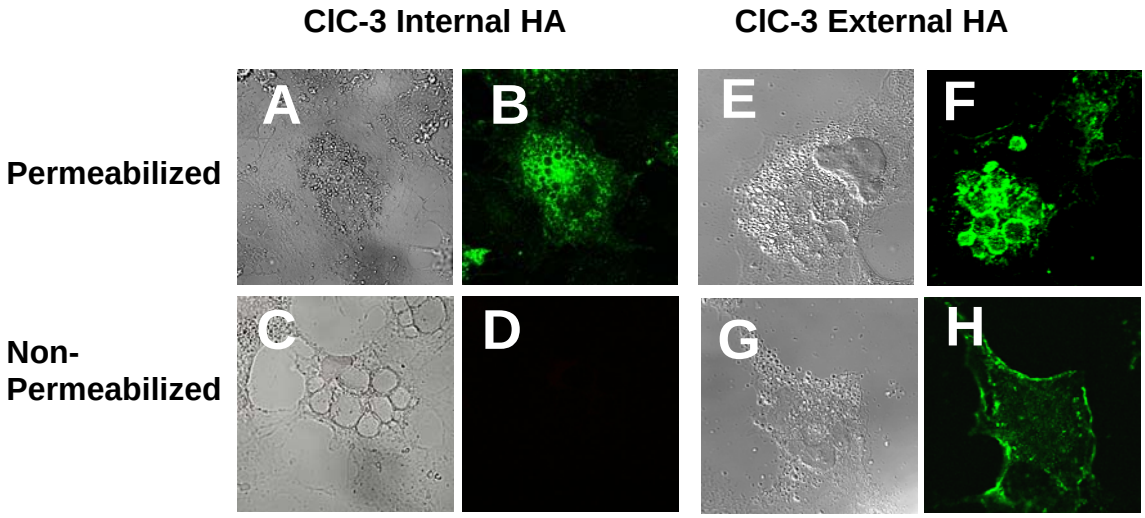

Fig 2.12 HA antibody specifically labeled the extracellular epitope of HA. A-D. COS-7 cells were transfected with ClC-3 internal HA, fixed, and immunolabelled with anti-HA either with (A, B) or without (C, D) membrane permeabilization by saponin. Transmission images (A, C) and HA immunofluorescence (B, D) are shown. **E-H** shows the same protocol for COS-7 cells transfected with the ClC-3 external HA construct either with (E, F) or without (G, H) membrane permeabilization. Transmission images (E, G) and HA immunofluorescence (F, H) are shown.

To follow trafficking, COS-7 cells were transfected with a ClC-3 construct containing the external HA epitope and fused to GFP at the internal C-terminal end of the protein. The cells were then incubated for 45 minutes at 37°C with anti-HA antibody. The cells were rinsed in PBS to wash away the extra antibody and then chased in DMEM medium at 37°C for different times. Finally, cells were fixed, permeabilized, and incubated with fluorescent secondary antibodies. Before the chase, HA staining was clearly defined at the plasma membrane (Fig 2.13A, red). The green GFP fluorescence was however, only seen intracellularly. This may have resulted because the majority of ClC-3 was intracellular and adjusting image sensitivity did not allow visualization of the

much dimmer plasma membrane fluorescence. To see if there was GFP present on the plasma membrane, we amplified the green channel (Fig. 2.13D), confirming that there is also a plasma membrane distribution and it corresponds to the site of HA labeling (Fig 2.13E). We next observed the effect of different chase times. After a 30 min chase, plasma membrane resident ClC-3 moved to small endocytic vesicles (Fig. 2.13B) but by 2 h it had accumulated into the large central vesicles (2.13E) that are the major site of the total cellular ClC-3 at the steady state (16).

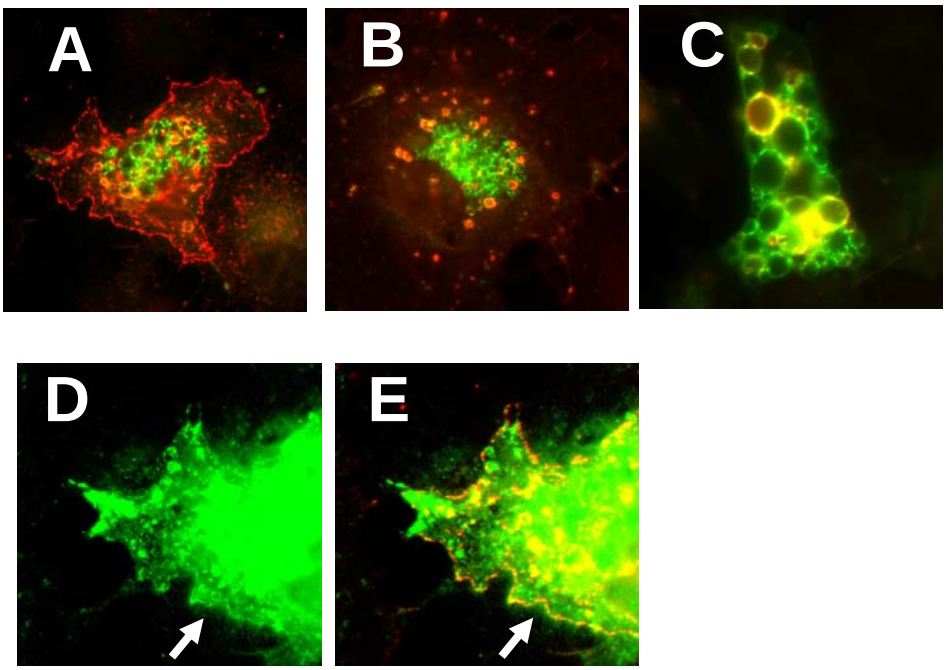

Fig 2.13 Trafficking path of ClC-3. A-C COS-7 cells were transfected with ClC-3/1217HA-GFP, labeled with HA antibody for 45min (panel A) and chased at 37°C for 30 min (panel B) and 2 h (panel C). In **D** and **E** intensity in the green channel was amplified.

Recycling of ClC-3 HA

To measure recycling of ClC-3 from the cell surface, COS-7 cells were treated with cycloheximide to inhibit the de novo protein synthesis and incubated under trafficking permissive conditions (37 °C) in the presence of the biotinylation reagent. The alteration of the amount of biotinylated protein over time was monitored. Under these conditions, the membrane-impermeant biotinylating reagent will label ClC-3 molecules that cycle through the plasma membrane. We compared the time course of ClC-3 biotinylation using this protocol with that of two control proteins, transferrin receptor which is known to participate in membrane recycling (58) and the α-subunit of the Na-K ATPase which recycles only to a minimal extent (57). As shown in Fig. 2.14A (upper panel) and Fig 2.14B (closed circles), transferrin receptor is only partially biotinylated at time zero and its biotinylation increases over two fold until reaching a maximum by approximately 30 min. Biotinylation of Na-K ATPase (Fig. 2.14A, lower panel; Fig 2.14B, triangles) is much more stable and increases only minimally over this period. ClC-3 (Fig. 2.14A, middle panel; Fig 2.14B, open circles) behaves nearly identically to transferrin receptor and is unlike Na-K ATPase. Therefore, like transferrin receptor, it appears to undergo recycling.

We further used another variant of the cleavage biotin experiment to confirm the recycling of ClC-3. To measure the recycling of ClC-3, we biotinylated the cell surface pool, allowed it to internalize, striped off remaining surface biotin, then incubated at 37°C for 30 minutes to allow recycling. At the end of this protocol any biotinylated ClC-3 recycled to the surface was then cleaved by a second treatment with MesNa (Fig 2.14 C). The first three lanes are the same as the three lanes of Fig 2.10A. They are used to show whether surface expression and endocytosis occurred. ClC-3 and transferrin receptor both demonstrated retention of biotinylation after the 15 min incubation at 37 °C, which demonstrated that endocytosis occurred during this period. On the contrary, Na-K ATPase demonstrated no internalization. Lanes 4 and 5 (Fig 2.14C) show the results of this specific test for recycling. In lane 4, after allowing endocytosis and

performing a first round of cleavage, the cells were incubated for an additional 30 min at 0° and then subjected to cleavage a second time. In lane 5, the additional incubation occurred at 37° before the second round of cleavage. When comparing the band intensity of Lane 4 and lane 5, we found that as long as cells were kept at 4°, a second round of cleavage did not appreciably change the amount of biotinylated ClC-3. However, 30 min incubation at 37° rendered an additional fraction of both ClC-3 and transferring receptor sensitive to cleavage. The average decrease was 53.9% for transferrin receptors and 64.7% for ClC-3. Therefore, both proteins recycle to similar degrees. ClC-3 behaves similarly to transferrin receptors, the positive control known for its recycling from the intracellular compartment to the plasma membrane.

Assessment of the quantitative proportions of direct and indirect pathways

In order to test whether the trafficking to the plasma membrane is a major pathway for ClC-3's traveling, we designed an experiment combining pulse-chase labeling, surface biotinylation and immunoprecipitation to directly determine the fraction of newly synthesized ClC-3 that is, even transiently, inserted into the plasma membrane ClC-3/HA transfected cells were pulse labeled for 20 min with ^{35}S methionine and chased in PBS in the presence of the biotinylation reagent. Streptavidin precipitation was next used to separate the ClC-3 molecules which had been inserted into the plasma membrane from those that had remained intracellularly. We then separately immunoprecipitated ClC-3 from each of these 2 fractions and used autoradiography to detect the protein bands. The ratio between the surface pool of ClC-3 and the intracellular pool of ClC-3 was then quantitated by the densitometry analysis. It appeared that about 25% of newly synthesized ClC-3 traffics through the plasma membrane (Fig 2.15 A, upper panel).

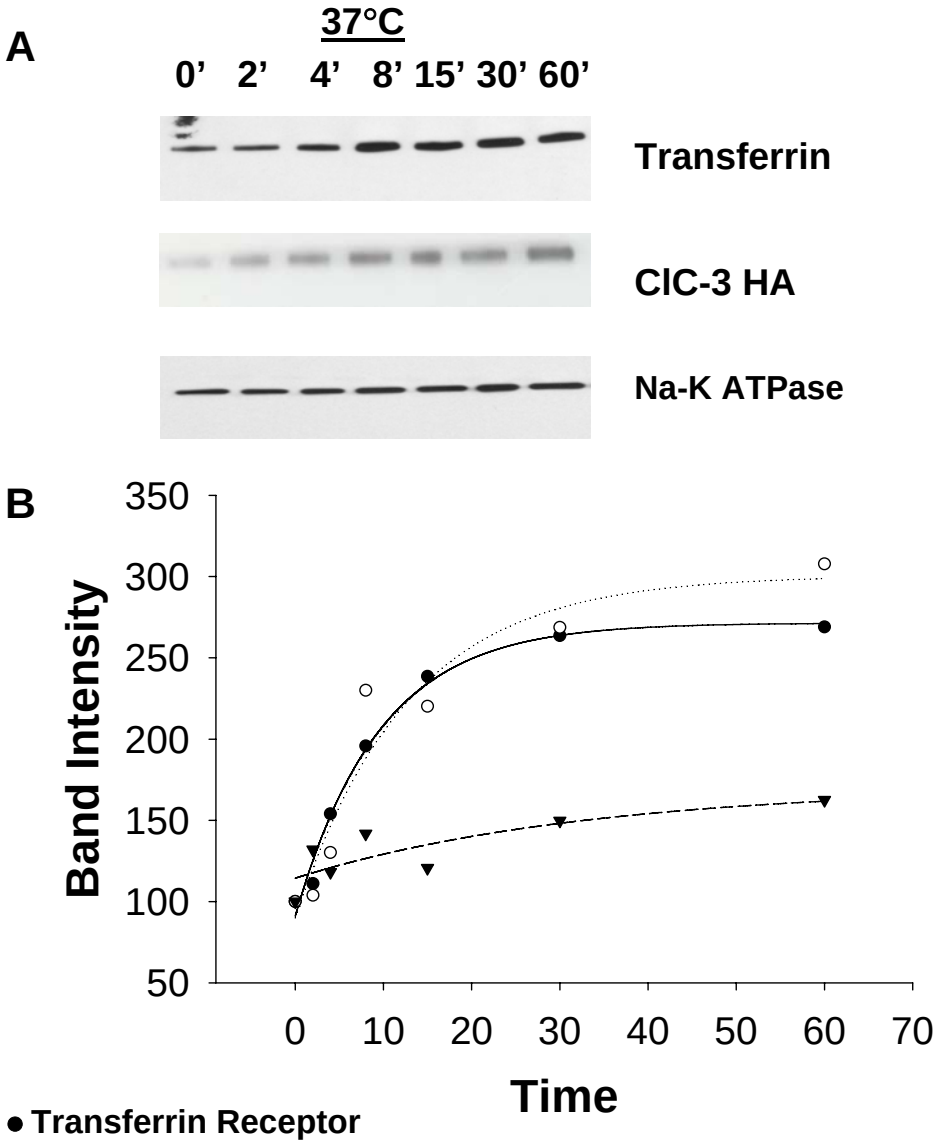
A
37°C
0’ 2’ 4’ 8’ 15’ 30’ 60’
Transferrin
ClC-3 HA
Na-K ATPase
B
Band Intensity
350
300
250
200
150
100
50
0 10 20 30 40 50 60 70
Time
● Transferrin Receptor
○ClC-3
▼Na-K-ATPase

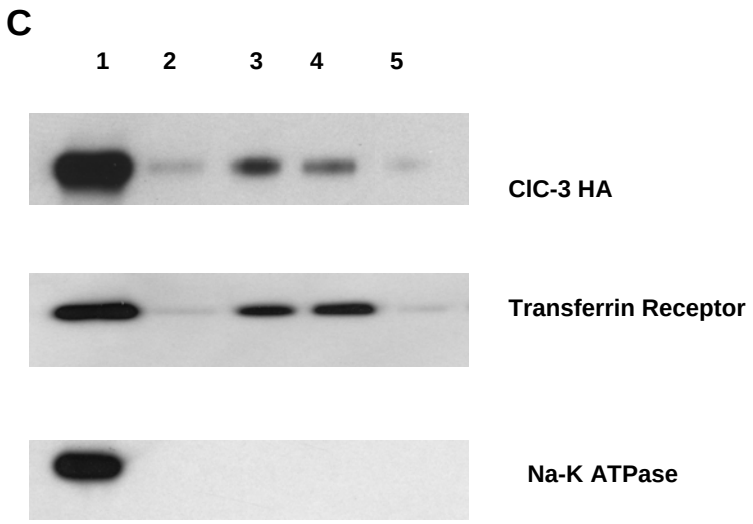

Fig 2.14 ClC-3 recycles from plasma membrane. A, After treatment of COS-7 cells with cycloheximide for 2h, biotinylation of surface expressed proteins was carried out 4°C and then continued at 37°C for different times. Representative blot is shown. **B**, Average percentage of biotinylation is determined by densitometry analysis of 4 experiments. Data were fitted to a single exponential equation $y=y_0+ a (1-e^{-bx})$ % with Sigmaplot. Biotinylation=100× (surface expressed ClC-3 at 37°C/ surface expressed ClC-3 at 4°C). n=5 **C.** Representative blot of a two-step cleavage of biotinylated ClC-3. Upper panel, HA immunoblot of streptavidin pellets; ClC-3/HA transfected COS-7 cells were surface biotinylated with sulfo-NHS-SS-biotin, which was subsequently cleaved with MesNa, and then incubated in DMEM at 4°C or 37°C for 30 minutes to promote recycling, followed by cleavage with MesNa again. The cells were then lysed and subjected to streptavidin precipitation. Lane 1, streptavidin pellet before cleavage; lane 2, streptavidin pellet after immediate cleavage; lane 3, streptavidin pellet after biotinylated cells were first incubated for 15 min at 37°C prior to cleavage. Lane 4, streptavidin pellet after biotinylated cells were first incubated for 15 min at 37°C, subjected to the first MesNa cleavage, then incubated in DMEM at 4°C for 30 min and cleaved a second time

with MesNa. Lane 5, streptavidin pellet after biotinylated cells were first incubated for 15 min at 37°C, subjected to MesNa cleavage, then incubated in DMEM at 37 °C for 30 min and then cleaved for a second time with MesNa. Middle panel, identical treatments as the upper panel, but the streptavidin pellets were blotted with antibody against the transferrin receptor. Lower panel, same protocol, blotted with antibody against the α subunit of Na-K ATPase. n=6.

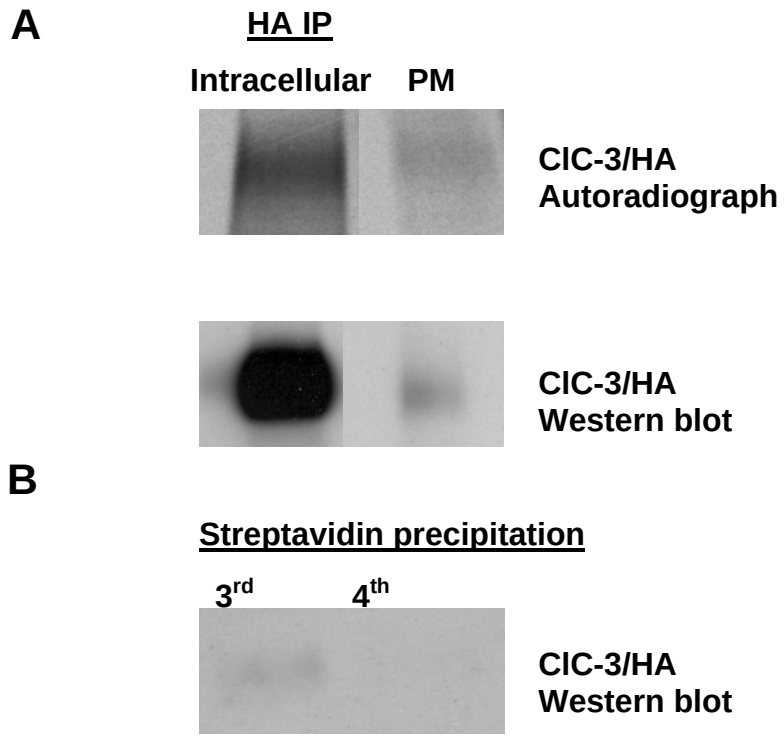

Fig 2.15 Intracellular and surface appearance of newly synthesized ClC-3/HA in transfected COS-7 cells. A. Cells were pulse labeled for 20 min with ^{35}S methionine and chased in PBS with biotinylation reagent. For each experiment, a second dish of cells was treated identically except that no ^{35}S methionine was added. This dish of cells served as control to evaluate the efficiency of streptavidin precipitation and immunoprecipitation. Biotinylated cells were lysed, subjected to streptavidin precipitation and the plasma

membrane (PM) pool and intracellular pool of proteins was immunoprecipitated separately with HA antibody and subjected to electrophoresis. Newly synthesized ClC-3 was detected with autoradiography (upper panel) and total ClC-3 by western blot for the non-radioactive sample (lower panel). **B** Evaluation of the efficiency of the streptavidin pull down step. Note that after 3 rounds of streptavidin precipitation, all biotinylated ClC-3 has been pulled down and there is no more left on the beads.

DISCUSSION

There is a long-standing controversy regarding the localization of ClC-3. Several groups have detected ClC-3 at the plasma membrane (53, 54) and have even suggested that its primary function is as a plasma membrane chloride channel. Others have found it primarily in intracellular compartments of the endosomal/lysosomal pathway (15, 16, 55). The results in this dissertation used immunofluorescence and biotinylation to show that ClC-3 is primarily in intracellular compartments, and it reaches this location by a combination of direct and indirect pathways. At steady-state, small portion of ClC-3 is present at the plasma membrane and in a recycling vesicle pool. The plasma membrane serves as an intermediate site of ClC-3 trafficking from where it is destined for intracellular sites. The disparate results regarding ClC-3 localization might thus be explained by changes in trafficking where conditions such as hyposmotic cell swelling (52) and intracellular Ca^{2+} increases (53) could alter the distribution of ClC-3 between intracellular sites and the plasma membrane.

Multiple mechanisms are involved in targeting intracellular membrane proteins. They may traffic directly from ER to Golgi and then to a sorting trans-Golgi pool before reaching other intracellular destinations. Alternatively, many proteins are first inserted into the plasma membrane and then reach intracellular sites via endocytosis. This latter "indirect" trafficking process can involve clathrin-mediated endocytosis, caveolae-mediated endocytosis, or clathrin- and caveolae-independent endocytosis (64). Our

experiments with pulse-chase, biotinylation and a ClC-3 derivative with an extracellular HA epitope were able to demonstrate three characteristics of ClC-3 trafficking. First, ClC-3 seemed to have a complicated trafficking pattern. It undergoes both direct and indirect trafficking to lysosomes, the final destination. The direct pathway appears to be the major trafficking pathway taken by the ClC-3 molecule. However, A significant amount of ClC-3 traffics via the indirect pathway whereby it moves from the plasma membrane to small endocytic vesicles and finally to large, acidic late endosomal/ lysosomal vesicles.

A second characteristic of ClC-3 is that its overexpression in different cell types results in the formation of abnormal vesicles in the cells. These vesicles varied in their size and pH since LysoSensor blue can preferentially labels the largest of the vesicles (Fig. 2.4) and cathepsin D also resides in some, but not all, of the vesicles (Fig 2.6). It is possible that this apparent heterogeneity results from the technical artifacts because Lysosensor blue might preferentially photo bleach in the smaller vesicles and we may not have been able to label all the cathepsin D in the lysosomes in the immuno-staining process. However, an alternative explanation for the heterogeneity is that ClC-3 vesicles consist of different subpopulations that have different origins and morphological appearances. It is important to note that expression of ClC-5 (Fig. 2.3) or ClC-4 (65) did not produce large vesicles. However, when we co-transfected ClC-3 and ClC-5 into Hela cells, large vesicles were produced. This was identical to the typical distribution pattern of ClC-3 at steady state. In this circumstance, ClC-3 and ClC-5 cocloalzed with each other, leaving open the possibility that ClC-3 and ClC-5 form heterodimers and when they do it is the ClC-3 moiety that determines distribution. This interpretation is consistent with the demonstration of heterodimer formation by Suzuki and his colleagues (12).

The third novel finding of these experiments is that ClC-3 is present in a recycling pool. To detect the recycling of ClC-3, the ClC-3 transfected cells were incubated at 37°C with biotin and the amount of biotinylated protein was monitored as a function of

incubation time. Since newly synthesized ClC-3 was inhibited by cycloheximide, the increase in the amount of biotinylated ClC-3 over time cannot be attributed to synthesis of new molecules but rather to the appearance of a previously unlabeled pool of ClC-3 on the plasma membrane. Therefore, recycling occurs. With our two-step cleavage biotinylation experiment, we further demonstrated that the surface pool of ClC-3 which has been biotinylated traveled back to the surface after incubation for 30 minutes at 37°C, where the bound biotin could once again be cleaved with the extracellular cleavage reagent.

It is important to note that the lack of a specific antibody to ClC-3 made it necessary for us to perform our experiments with several different epitope tagged ClC-3 constructs. It can thus be asked whether the presence of the epitope tags altered trafficking in our studies. In our studies, the ClC-3 molecule tolerated the insertion of C-terminal GFP, C-terminal HA or an external loop HA without any change in its ability to form large intracellular vesicles or its steady-state distribution. We therefore conclude that in our system, these epitope additions do not alter trafficking of the molecule. Rossow and colleagues, however, recently reported that the addition of a GFP tag to the short form of the ClC-3 channel altered its steady state distribution in NIH/3T3 cells (66), This result was clearly in contradiction to our direct observations and may result from differences in the precise constructs or cell systems used.

METHODS

Reagents and antibodies

General reagents were obtained from Sigma-Aldrich or Fisher Scientific. PfuTurbo® DNA Polymerase was from Stratagene (La Jolla, CA); FuGENE 6 from Roche (Indianapolis, IN); EZ-link sulfo-NHS-SS-biotin and ImmunoPure Immobilized Streptavidin Gel were from Pierce Biotechnology (Rockford, IL); Cycloheximide (Cat # 01810) was from Sigma-Aldrich (St. Louis, MO); Endo H was from Roche (cat # 1 088

726). OptiPrep™ was from Axis-Shield. Antibodies were purchased as indicated: mouse monoclonal anti GFP antibody (cat# 632381) was from Clontech (Mountain View, CA); mouse monoclonal anti HA antibody (cat# MMS-101R) from Covance (Princeton, NJ); rabbit polyclonal anti HA antibody (cat# H6908) from Sigma-Aldrich (St. Louis, MO) ; mouse monoclonal anti transferrin receptor antibody (cat# 13-6800) was from Zymed Laboratories (San Francisco, CA); mouse monoclonal anti sodium potassium ATPase antibody (cat# ab7671) and antibodies against Golgi marker 58k protein were from Abcam, antibody against human cathepsin D was from Upstate Biotechnology, anti-lamp-1 monoclonal antibody H4A3, and anti-lamp-2 monoclonal antibody H4B4 (each at 1:200, Developmental Studies Hybridoma Bank, University of Iowa), goat polyclonal anti actin antibody was from Santa Cruz (cat# sc-1616, Santa Cruz, CA). LysoSensor blue was from Molecular Probes. Alexa Fluor® 488 goat anti-mouse IgG (H+L), Alexa Fluor® 594 goat anti-mouse IgG (H+L) and Alexa Fluor® 594 chicken anti-goat IgG (H+L) were from Molecular Probes. Donkey anti-rabbit IgG HRP-linked whole antibody (cat# NA934V) and sheep anti-mouse IgG HRP-linked whole antibody (cat# NA 931V) were from Amersham Biosciences.

Constructs and cell lines

ClC-3/GFP and ClC-3/HA , constructs with cytosolically localized GFP or HA epitopes, were constructed in pEGFP-N1 as described previously (16, 65). ClC-3/1217HA-GFP, a ClC-3 construct with an extracellular/lumen side HA epitope between the B and C helix (10), was generated from the parent constructs using the QuikChange® site-directed mutagenesis kit (Stratagene). All constructs were confirmed by sequencing in the Protein Chemistry Laboratory of the University of Texas Medical Branch. COS-7 cells were grown in Dulbecco's modified Eagle's medium supplemented with 10% fetal bovine serum. COS-7 cells were transiently transfected with the different cDNAs using FuGENE 6 or Lipofectamine™ 2000.

Immunostaining and Microscopy

Transfected cells were grown on glass coverslips. They were fixed with methanol at -20 °C for 10 min, washed in PBS, and incubated with primary antibodies against Golgi marker 58k protein 1:100, Abcam), human cathepsin D (1:100, Upstate Biotechnology), anti-lamp-1 monoclonal antibody H4A3, and antilamp-2 monoclonal antibody H4B4 (each at 1:200, Developmental Studies Hybridoma Bank, University of Iowa). Secondary antibodies were Alexa Fluor 594-conjugated goat anti-mouse IgG or Alexa Fluor 594 goat anti-rabbit IgG (1:500, Molecular Probes).

To follow endocytosis of ClC-3, COS-7 cells expressing the external HA construct were grown on 18-mm coverslips, and incubated with HA antibody (1:400) at 37°C in PBS for 45minutes as indicated. After incubation and washing, the cells were rinsed, fixed with 3% paraformaldehyde in phosphate-buffered saline, permeabilized with 0.25% saponin, then labeled with secondary antibody.

Cells were observed in a Nikon Eclipse 800 (Melville, NY) epifluorescence microscope with the FITC-filter set (excitation 465–495 nm, dichroic mirror 505 nm, emission 515–555 nm) for Alexa Fluor 488 conjugates, Texas red filter set (excitation 540–580 nm, dichroic mirror 595 nm, emission 600–660 nm) for Alexa Fluor 594 conjugates. Images were acquired by using a Dage-MTI (Michigan City, IN) camera for later processing by Adobe Photoshop software.

Biotinylation Assays

COS-7 cells were grown in 6 cm dishes and transfected with different constructs. At 48 h after transfection, cells were washed twice in ice-cold PBS and incubated with 1ml of sulfo-NHS-SS-biotin diluted in PBS (pH 8) for 30min at 4°C. Un-reacted biotinylation reagent was quenched with 50 mM glycine. After three washes at 4°C in PBS, cells were immediately lysed or incubated in DMEM for various times at either 4°C or 37°C prior to incubation with cleavage solution (150mM NaCl, 20mM Tris, 50mM MesNa, pH 8.6) and subsequent cell lysis in ice-cold lysis buffer (50mM Tris-HCl,

150mM NaCl, 0.5% IGEPAL CA-630 with protease inhibitor cocktail (Sigma P8340). The biotinylated proteins were incubated with streptavidin-agrose beads and precipitated at 3000g for 2 minutes. Lysates and pellets were subjected to SDS-polyacrylamide gel electrophoresis. The proteins were electrophoretically transferred to polyvinylidene difluoride membranes (Bio Rad), blocked overnight at 4°C with 5% nonfat dried milk, 0.1% Tween 20 in tris-buffered saline (TBS) and subsequently incubated with anti-HA antibody (1:1000) or anti-GFP antibody (1:1000). The membranes were then washed and incubated with appropriate secondary antibodies, and detected with the ECLplus chemiluminescence system. Immunoreactive bands were quantified by densitometry using TotalLab software (UltraLum Inc., Claremont, CA). Statistical significance was tested using paired t test.

Percent of surface expression was calculated by comparing total lysate ClC-3 with the biotinylated fraction as $100*P/ (T*F)$ where P is the density of the ClC-3 band in the streptavidin pellet, T is the density of the ClC-3 band in the total lysate aliquot, and F is the ratio of total lysate used for streptavidin precipitation compared to the quantity applied directly to the gel, i.e. (lysate volume used for streptavidin precipitation/ lysate volume applied to gel). Percent endocytosis was calculated from experiments in which cells were biotinylated, incubated at 37 °C, and then exposed to biotin cleavage reagent. Numerically it was represented as $100*(D_t-D_0)/S$ where D_t is the quantity of biotinylated ClC-3 remaining after cleavage at any given time, D_0 is the quantity of biotinylated ClC-3 after cleavage at time 0, and S is the total surface ClC-3 determined by biotinylation without cleavage at time 0. The assumption here is that the pellet precipitated 100% of the biotinylated ClC-3 and the non-biotinylated ClC-3 remained in the supernatant.

For the recycling experiment, two variant biotinylation experiments were performed. The first one was carried out as follows. ClC-3/HA transfected COS-7 cells were rinsed twice with PBS and treated with cycloheximide (20μg/ml) for 2h. The cells were then incubated at 4°C for 30min with biotinylation solution. After that the cells were further incubated with biotinylation solution at 37°C for different periods of time.

After rinsing cells into ice-cold PBS solution containing glycine to quench the excess biotin, biotinylated proteins were extracted and were subject to streptavidin bead precipitation and western blot.

For the two-step cleavage experiments, COS-7 cells transfected with ClC-3/HA for 2 days. Cells were then washed twice in ice-cold PBS and incubated with 1ml of sulfo-NHS-SS-biotin diluted in PBS (pH 8) for 30min at 4°C. Un-reacted biotinylation reagent was quenched with 50 mM glycine. After three washes at 4°C in PBS, cells were incubated in DMEM for 15 min at 37°C followed by the first round of incubation with cleavage solution at 4 °C. Cells were then incubated in DMEM either at 4 °C or 37 °C for 30min, after which the second round of incubation with cleavage solution at 4 °C was performed. The cells were then lysed and subjected to streptavidin beads precipitation and western blot.

Subcellular Fractionation

COS-7 cells were plated on 100-mm dishes and transiently transfected with ClC-3 GFP. After 48 h, plates were rinsed twice with Buffer A (0.25 M sucrose, 10 mM triethanolamine, 1 mM EDTA, pH 7.4) and harvested by gentle scraping into 5 ml of homogenization buffer (85% Buffer A (v/v) and 15% of Buffer B (10 mM Tris, pH 7.4, 5 mM KCl, 1 mM EDTA, 128 mM NaCl)). Cells were spun at 300 × *g* and resuspended in 0.3 ml of homogenization buffer plus protease inhibitors, followed by homogenization at 4 °C by 12 passages through a 25-gauge needle attached to a 1-ml syringe. Post-nuclear supernatants were prepared by two consecutive centrifugations at 1000 × *g*. Supernatants were loaded on pre-formed 5-25% Optiprep (Iodixanol), linear gradients that had been pre-cooled to 4 °C. Continuous gradients were formed by diffusion of discontinuous gradient (5%, 10%, 15%, 20% and 25%) at 4 °C overnight. Gradients were spun for 5h at 40,000 rpm at 4 °C in a SW41 rotor in a Beckman ultracentrifuge. 9 fractions (1ml each) were collected. For immunoblotting, fractions were pelleted in a Beckman High Speed Micro-centrifuge at 4 °C in a TLA45 rotor at

125,000 × *g* for 60 min. Pellets dissolved in SDS-PAGE sample buffer were subject to electrophoresis and immunoblotting (67, 68).

Metabolic labeling, surface biotinylation, and immunoprecipitation

ClC-3/HA transfected COS-7 cells were grown in 10 cm dishes to a confluence of 90%. They were then metabolically labeled by incubation for 20 min with 0.8 mCi/ml of ^{35}S-methionine (Amersham Biosciences AG1094) in methionine-free DMEM medium. Monolayers were washed 3 times with PBS before adding sulfo-NHS-SS-biotin at a concentration of 0.5mg/ml for 4h at 37 ° C. After quenching with 50 mM glycine in PBS, the cells were lysed with ice-cold lysis buffer (50mM Tris-HCl, 150mM NaCl, 0.5% IGEPAL CA-630 with protease inhibitor cocktail (Sigma P8340). Postnuclear supernatants were obtained after centrifugation at 10,000g for 15 min. Streptavidin precipitation was then sequentially performed 4 times until all the biotinylated ClC-3/HA has been pulled down. The streptavidin pellets were combined and biotinylated proteins were cleaved off the beads by incubation in the cleavage solution (150mM NaCl, 20mM Tris, and 50mM MesNa, pH 8.6) at 4 °C twice for 12 h. The final streptavidin supernatant and cleavage product of the streptavidin pellets were both immunoprecipitated with polyclonal HA antibody (Sigma H6908 1:200) and protein A/G beads (Pierce 20421). First, samples were precleared of proteins with nonspecific binding. A 50% slurry of protein A/G-agarose beads (Pierce, cat# 20421) in a volume of 200 µl was added. After 6 h incubation at 4 °C, the beads were removed by centrifuged for 2 min at 3,000 x *g*. The beads were saved in 25 µl 2×sample buffer (Invitrogen, cat# LC2676). The precleared supernatant was subsequently incubated at 4 °C overnight on a rotator with the specific HA antibody. Fresh protein A/G-agarose beads (200 µl of 50% slurry) were added and then incubated 6 h at 4 °C. After centrifugation at 3,000g for 2 min, the supernatant was aspirated. The beads were washed and antibody-antigen complexes were dissociated with 2×sample buffer (Invitrogen LC2676. Electrophoresis

was then carried out. Dried gels were exposed to x-ray film and protein bands were quantitated.

CHAPTER 3: IDENTIFICATION OF TARGETING SIGNALS FOR CLC-3

INTRODUCTION

Newly synthesized proteins are delivered specifically to the cellular compartments that require them. This process is called sorting and relies on complex distribution systems in eukaryotic cells. Sorting of membrane proteins is mediated by signals present within the cytosolic domains of the proteins. These sequence motifs specifically bind to a series of adaptor proteins. Many diseases are caused by a failure of specific proteins to be sorted properly in the endocytic and secretory pathways. For example, cystic fibrosis is caused by a defective gene for the chloride channel protein, CFTR. The most common mutation in CFTR is a deletion of phenylalanine at position 508 (ΔF508-CFTR). This mutant impairs trafficking of the molecule to the cell surface, thus altering salt and fluid transport in epithelial cells. As a consequence, patients are susceptible to chronic infection and inflammation of the airways and this eventually leads to loss of lung function (69). In general, the sorting signals consist of short, linear arrays of amino acid residues, in which two or three are critical for function. Two of the best-described motifs which produce intracellular retention of proteins are the tyrosine-based tetra-peptide motif, and the dileucine motif. Both motifs can mediate internalization from plasma membrane, lysosomal targeting, basolateral targeting and TGN-to-endosome sorting (20, 30, 31, 70).

An examination of the structure of short form ClC-3 identifies distinct domains: a transmembrane channel core and N and C terminal cytosolic domains. Several putative signal motifs are included in the cytosolic domains. Within the N terminal domain of ClC-3, there are 2 potential tyrosine motifs and one dileucine cluster. Similarly, there are 2 potential tyrosine motifs and one dileucine motif at the C terminal of ClC-3 as well. Figure 3.1 shows potential targeting motifs of ClC-3 (Shimada K et al, 2000).

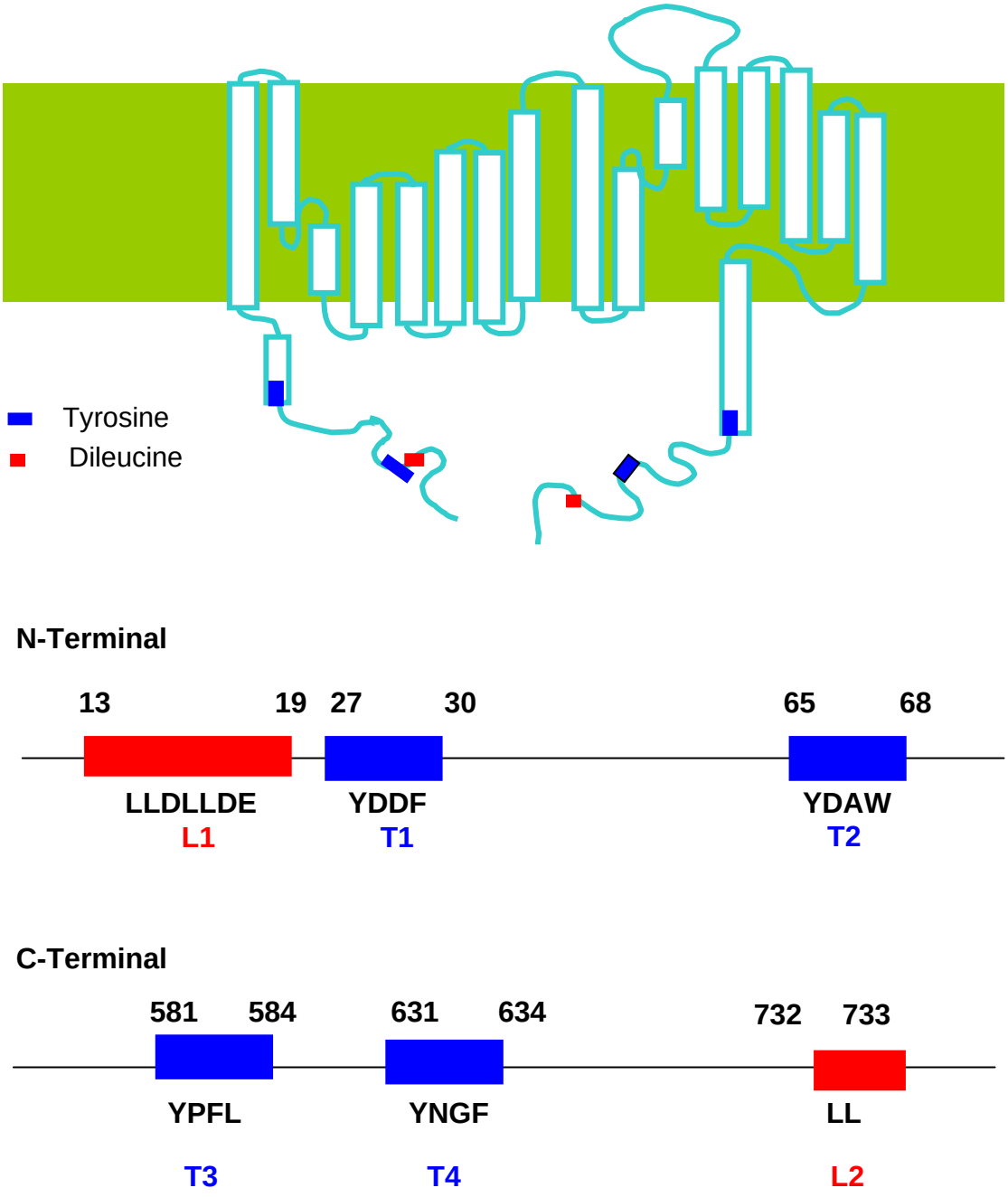

Fig 3.1 Putative targeting motifs present in the cytosolic domains of ClC-3. There are two tyrosine motifs and a dileucine signal present at both the N and C terminal domains of ClC-3.

Not every putative targeting motif will really function as a targeting signal in vivo because some of the signals are buried inside and may not be able to be exposed to the sorting machinery. Others may lack required accessory factors around their micro-environment. The aim of the experiments described in this chapter was to determine whether the potential targeting motifs of ClC-3 short form are really determinants for intracellular localization. The importance of this aim is to identify the targeting motifs that interact with the sorting machinery.

The approach we employed was to generate mutants of the potential targeting motifs, express full-length versions of these mutant ClC-3 molecules and assess the steady-state localization in single cells by fluorescent microscopy. Trafficking of mutants with altered distributions was then evaluated in more detail by biotinylation studies and following trafficking of external epitope labeled versions.

RESULTS

Screening of putative targeting signals at N and C terminal domains of ClC-3

Generation of mutants and screening with fluorescence microscopy

I first generated a series of mutant ClC-3/GFP fusion constructs that selectively abolished the putative targeting motifs at the cytosolic part of the molecule. I used fluorescent microscopy to screen these different constructs. Three different distribution patterns were observed (Fig. 3.2). One pattern is the formation of large vacuoles, just as occurred for the wild type ClC-3. A second group of mutants showed a reticular distribution pattern. The third type showed preferential plasma membrane localization.

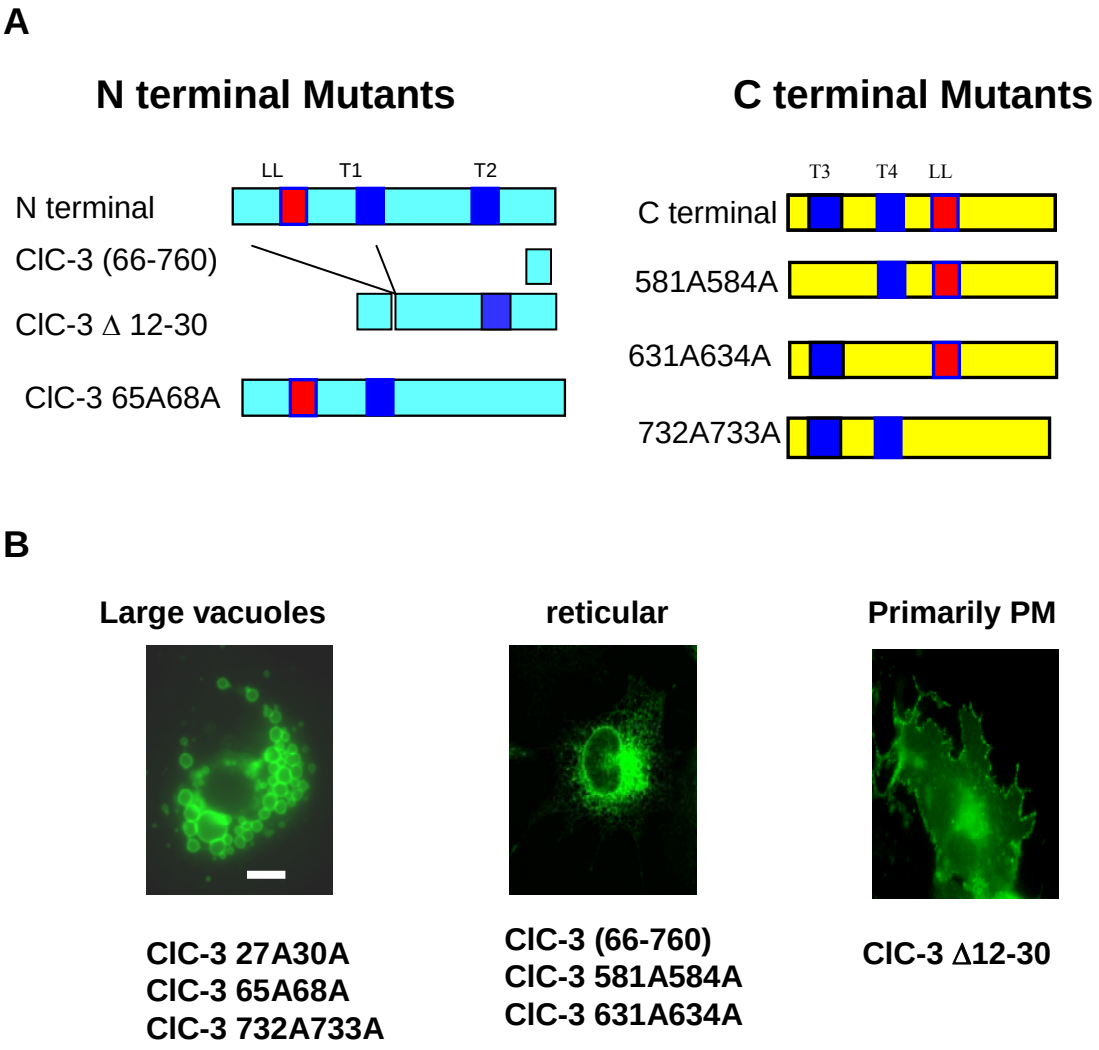

Fig 3.2 Different distribution patterns of mutant ClC-3 constructs. A. Topology of ClC-3 mutants. N terminal mutants: ClC-3 (66-760) deleted the whole N terminal of ClC-3; ClC-3 Δ 12-30 deleted the 1st tyrosine motif and the dileucine cluster at the N terminal; ClC-3 65A68A, replaced the indicated residues with alanine in the 2nd tyrosine motif at N terminal of ClC-3. C terminal mutants: ClC-3 581A584A, alanine substituted the 1st tyrosine motif at C terminal of ClC-3; ClC-3 631A634A, alanine substituted the 2nd tyrosine motif at C terminal of ClC-3; ClC-3 732A733A, alanine substituted the dileucine

motif at C terminal of ClC-3. **B.** Different distribution patterns of the mutant constructs. COS-7 cells were transfected with mutant ClC-3/GFP constructs, fixed, and observed by epi-fluorescent microscopy. Note that there are three patterns of distribution. Bar, 10 μm.

As a rough initial assessment, the mutants with the wild-type distribution pattern were presumed not to be likely to have trafficking defects. The reticular distribution pattern suggested that these constructs might have been retained in ER, perhaps due to the misfolding of the protein. Thus they might have little value in the study of post-ER sorting signals. The mutant that showed a plasma membrane distribution was likely to have a defect in post ER sorting. To further elaborate the trafficking pattern of these mutants we assessed whether they had indeed trafficked out of the ER by using glycosylation analysis and assessing the overlap with ER markers by immunofluorescent microscopy.

Glycosylation analysis

Asparagine-linked glycosylation (N-glycosylation) is the most ubiquitous protein co-translational modification in the eukaryotic cells. Oligosaccharyl transferase (OT), a multi-subunit enzyme, catalyzes the transfer of an oligosaccharyl moiety ($Glc_3Man_9GlcNAc_2$) from the dolichol-linked pyrophosphate donor to the side chain of Asn on the nascent polypeptides. The consensus sequence of this Asn site is Asn-*X*-Thr/Ser, where *X* can be any amino acid residue except for Pro. This modification is important in specific molecular recognition as well as protein folding and stability (71).

Endoglycosidase digestion is a tool to analyze the distribution of glycoprotein. PNGase F cleaves the entire N-linked carbohydrate, converting asparagine into aspartic acid. It is used to determine if a protein is N glycosylated or not. Endo H cleaves between the N-acetyl glucosamines of core carbohydrates. Endo H resistance is a marker for arrival of an N-linked glycosylated secretory protein at the cis-golgi compartment.

To learn more about the properties of the expressed ClC-3, I analyzed the state of glycosylation of the molecule by endoglycosidase digestion. We first used this analysis to examine wild-type ClC-3. In Figure 3.3, we show that the position of the ClC-3 band shifted obviously after the treatment of PNGase F. However, the band did not shift at all after the treatment of Endo H.

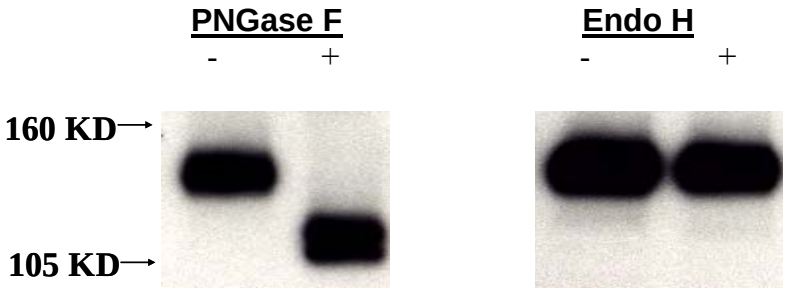

Fig 3.3 Endoglycosidase digestion of wtClC-3. COS-7 cells were transfected with ClC-3/GFP for 48h. Endo H (1 μl) was incubated per 25 μg of COS-7 lysate under standard assay conditions for 4h. Then the samples were subjected to SDS-polyacrylamide gel electrophoresis and western blot. ClC-3 was visualized with GFP antibody (1:2000). Wt ClC-3 is PNGase F sensitive and Endo H resistant. This indicates that the protein is localized in a post-golgi compartment. Note the high degree of glycosylation of wild type ClC-3 indicated by the dramatic shift of electrophoretic mobility after PNGase F treatment.

The first mutant generated for these studies was ClC3 (66-760)/GFP, in which the entire 65 amino acid at N terminal cytosolic domain was deleted. Unlike the wild type, this N-truncation mutant does not result in the formation of intracellular vesicles. Instead, the distribution is reticular and spread through the cell. Furthermore, the distribution of immunofluorescence was identical to that of an ER marker, PDI (Fig. 3.4). Further examination with endoglycosidase digestion revealed that the molecule was sensitive to

digestion with both PNGase F and Endo H, which means it has not trafficked beyond the cis-golgi compartment.

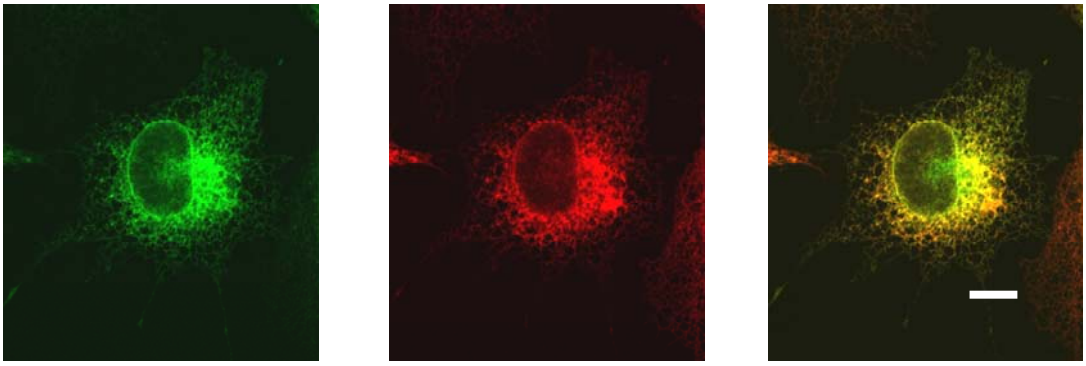

ClC-3 (66-760) **PDI** **Composite**

Fig 3.4 Distribution of ClC-3 (66-760). COS-7 cells were transiently transfected with ClC-3 (66-760)/GFP, fixed and dual stained for GFP epitope (green) and PDI (red). ClC-3 (66-760) colocalized with PDI, an ER marker as assessed by confocal microscopy. Bar, 10 μm.

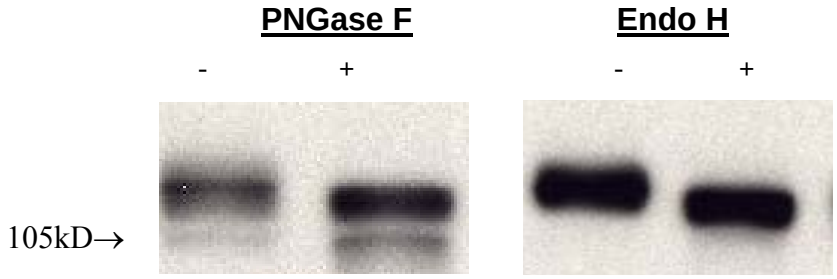

Fig 3.5 Endoglycosidase digestion of ClC-3 (66-760). COS-7 cells were transfected with ClC-3 (66-760)/GFP. The experiment was performed as described in Fig 3.3. This mutant was PNGase F and Endo H sensitive. This indicates it did not traffic out of the ER. Note that it had less PNGase F-induced shift in elctrophoretic mobility than wtClC-3 and thus is less heavily glycosylated.

In Table 3.1, we show the screening results of the different constructs. Constructs that fail to exit the ER have no value in evaluating the post-ER targeting signals and were not studied further. If the constructs showed wild type distribution patterns, it suggested that the specific mutation did not affect critical targeting signals that can regulate the trafficking of the molecule. The most interesting mutant is the one that exits the ER but then is found largely at the plasma membrane and not in the normal intracellular vesicles. This suggests that the mutant part of the molecule may contain the important targeting signal.

Table 3.1 Summary of the steady-state distribution of different mutants

Mutant	**Abolished Signal**	**Exit ER**	**Localization**
ClC-3 66-760	T1+T2+L1	No	ER
Δ 12-30	T1+L1	Yes	Primarily plasma membrane
27A30A	T1	Yes	Endosome/lysosome
65A68A	T2	Yes	Endosome/lysosome
581A584A	T4	No	ER
631A634A	T4	No	ER
732A733A	L4	Yes	Endosome/lysosome

Yeast two hybrid assessment of N terminal ClC-3 interaction with adaptor proteins

The majority of cellular phenomena are carried out by protein 'machines', and involve the interactions among proteins (72). One technique that can be used to study protein-protein interactions is the "yeast two hybrid" system. The yeast two-hybrid system uses two protein domains that have specific functions: a DNA-binding domain (BD), which is capable of binding to DNA, and an activation domain (AD), which is capable of activating transcription of the DNA. Both of these domains are required for transcription. However, the binding domain and the activation domain do not necessarily

have to be on the same protein. A protein with a DNA binding domain can activate transcription when simply bound to another protein containing an activation domain. In our experiments, we fused the N or C terminal of ClC-3 to the DNA binding domain and the μ subunits of AP proteins to the transcription activation domain and then selected for protein-protein interactions by assessing the ability of the cells to form colonies on appropriate nutritionally deficient media. The scheme is elaborated in the following figures:

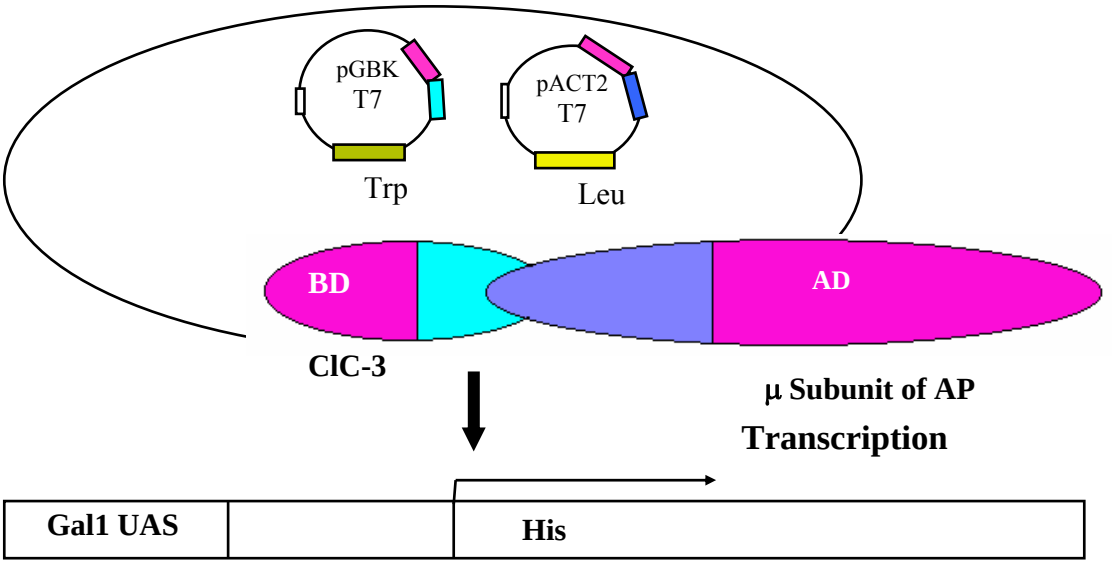

Fig 3.6 Yeast two hybrid assays to detect the interaction between ClC-3 and AP proteins. The N or C terminal of ClC-3 was fused to the DNA binding domain and the μ subunits of AP proteins were fused to the transcription activation domain. Protein-protein interactions were selected with His deficient media.

To evaluate the role of the cytosolic domains of ClC-3 in trafficking, we first performed yeast two hybrid assays to screen the interaction between the N or C terminal of ClC-3 and adaptor proteins. In these assays, the N terminal of ClC-3 interacted with μ subunits of AP-1 and AP-2 but not AP-3, while the C terminal did not interact with any

of the 3 tested proteins (Fig 3.7). When we deleted the 19 amino acids segment in the N terminal (Δ 12-30) that altered trafficking, the interaction with μ1 and μ2 was also abolished. This data provides further evidence that the N-terminal of ClC-3 is particularly important for the protein-protein interactions necessary for trafficking.

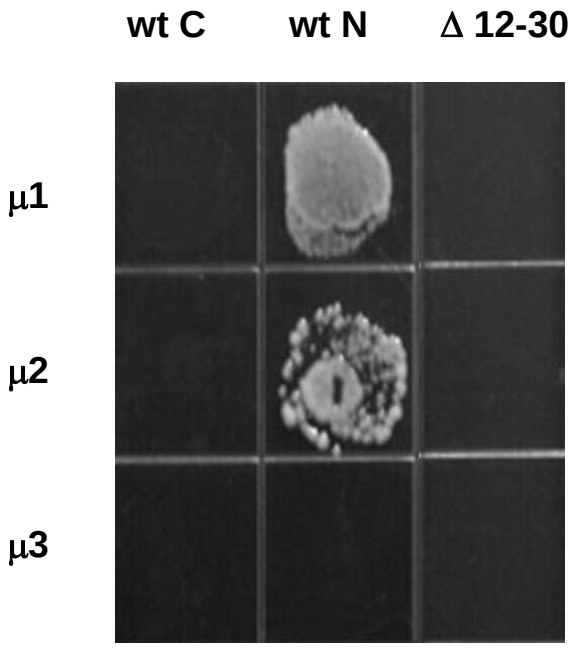

Fig 3.7 Yeast two hybrid assays demonstrate interaction between the N terminal of ClC-3 and the μ subunits of AP-1, AP-2 but not AP-3. N or C termini of ClC-3 were inserted into a yeast vector, pGBKT7 vector, which expresses GAL4 DNA binding domain. This vector contains the nutritional selectable mark TRP1 in yeast. The pACT2 vector was cloned in all AP genes μ subunits tested, which expresses GAL4 transcription activation domain (kindly gift from Dr. JS Bonifacino). This vector contains the nutritional selectable mark LEU2 in yeast. Protein-protein interactions were selected with His deficient media.

Detailed study of the targeting signals at N terminal of ClC-3

We performed further experiments using the deletion mutant, Δ 12-30, in which we abolished the dileucine cluster and the first tyrosine motif at the N terminal of ClC-3. As stated previously, the Δ12-30 construct displayed considerably greater steady-state surface expression than the wild type (Fig 3.2). To further assess the surface expression level and the endocytosis of this deletion mutant, we performed biotinylation experiments. We used the cleavage biotin method described in chapter 2 to test the surface expressed ClC-3 and look for evidence of internalization. Percent endocytosis was calculated from experiments in which cells were biotinylated, incubated at 37 °C for 15 min, and then exposed to the biotin cleavage reagent. Numerically it was represented as $100*(D_t-D_0)/S$ where D_t is the quantity of biotinylated ClC-3 remaining after cleavage at any given time, D_0 is the quantity of biotinylated ClC-3 after cleavage at time 0, and S is the total surface ClC-3 determined by biotinylation without cleavage at time 0. For wild type ClC-3, the percentage of endocytosis was 26% compared to only 6% for ClC-3 Δ 12-30 (Fig 3.10). This suggests that an important endocytosis signal is present between the amino acid 12 and 30.

We next separately tested the tyrosine motif and dileucine cluster in this segment. A mutant that specifically ablated the tyrosine motif showed a primarily intracellular distribution pattern, similar to the wild type ClC-3 (Fig 3.9). We thus focused on the dileucine cluster and generated a deletion mutant, Δ 13-19. This mutant displayed greater steady-state surface expression than the wild type (Fig.3.9). I then further evaluated this specific deletion mutant of the dileucine motif (ClC-3 Δ 13-19) by incorporating it into the variant of ClC-3 with an external HA epitope. Similar to wild-type, immediately after incubation of live cells with anti HA, staining was clearly defined at the plasma membrane. However, unlike wild-type, there was no internalization after chase at 37°C for 30 minutes and even 120 minutes (Fig 3.11). Therefore, an N-terminal sequence from 13-19 is necessary for endocytosis and lysosomal targeting.

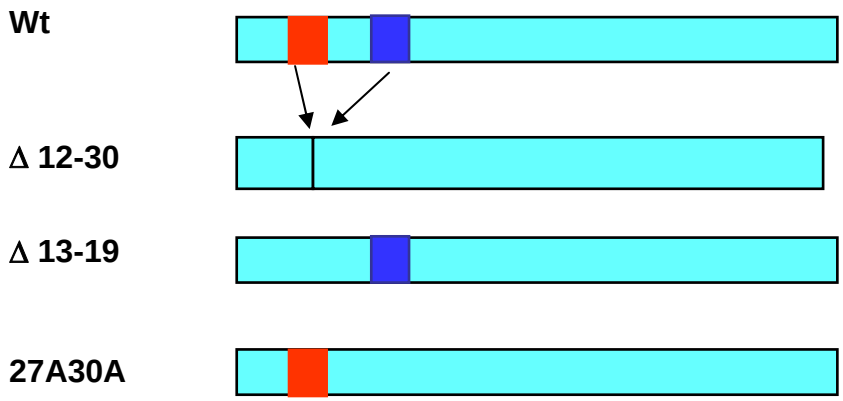

Fig 3.8 Topology of ClC-3 constructs. Δ 12-30, the dileucine cluster and the first tyrosine motif at N terminal of ClC-3 were deleted. **Δ 13-19,** the dileucine cluster at N terminal of ClC-3 was deleted. **27A30A,** first tyrosine motif at the N terminal of ClC-3 has been alanine substituted.

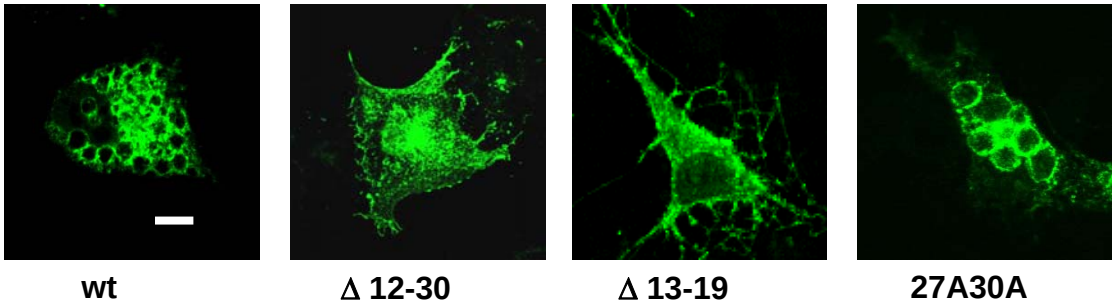

Fig 3.9 Steady-state distribution of ClC-3 and mutant constructs. COS-7 cells were transfected with ClC-3 constructs, fixed, and observed by confocal microscopy. ClC-3 fluorescence is represented in green. Confocal microscopy images demonstrated enhanced surface expression of ClC-3 Δ 12-30 and Δ 13-19 but primarily intracellular distribution of wt ClC-3 and ClC-3 27A30A. Bar, 10 μm.

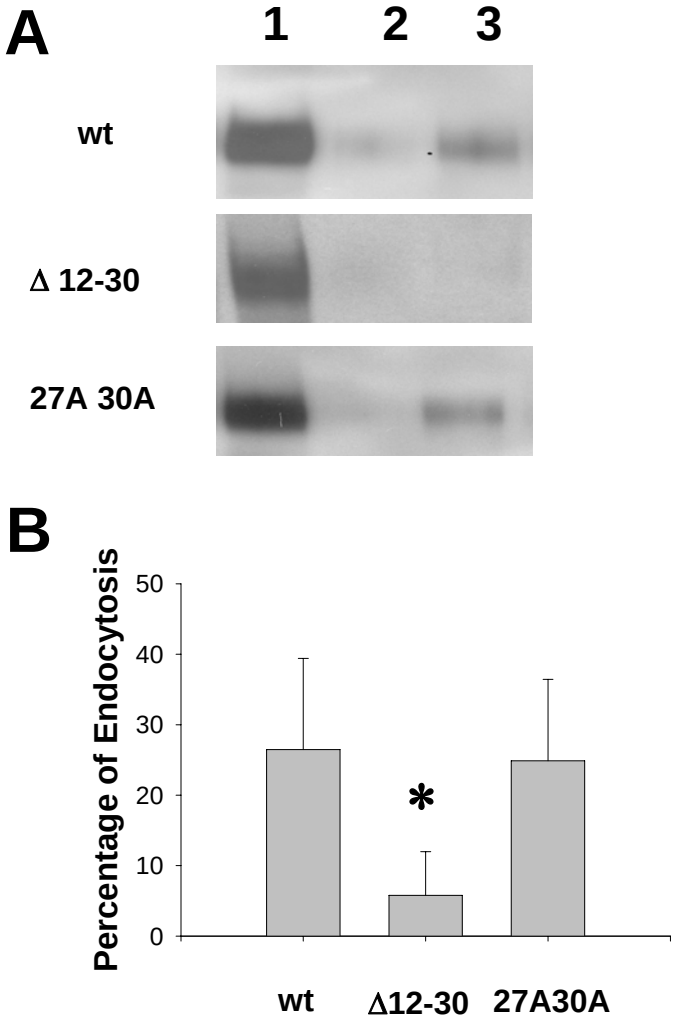

Fig 3.10 Deletion of the N-terminal amino acid 12-30 of ClC-3 impairs the endocytosis of the molecule. A. wt ClC-3/HA and ClC-3 mutants were transfected in COS-7 cells. The cells were then surface biotinylated with sulfo-NHS-SS-biotin, which was subsequently cleaved with MesNa, prior to streptavidin precipitation. Lane 1, streptavidin pellets before cleavage; lane 2, streptavidin pellets performed after immediate cleavage; lane 3, after biotinylation cells were first incubated for 15 min at 37°C followed by cleavage and streptavidin precipitation. B. Average percent protection

from cleavage determined by densitometry analysis of 4 experiments as shown in A. Data is presented as mean ± SE. % endocytosis=100×(Lane 3– Lane 2)/ Lane 2 ∗ P<0.05

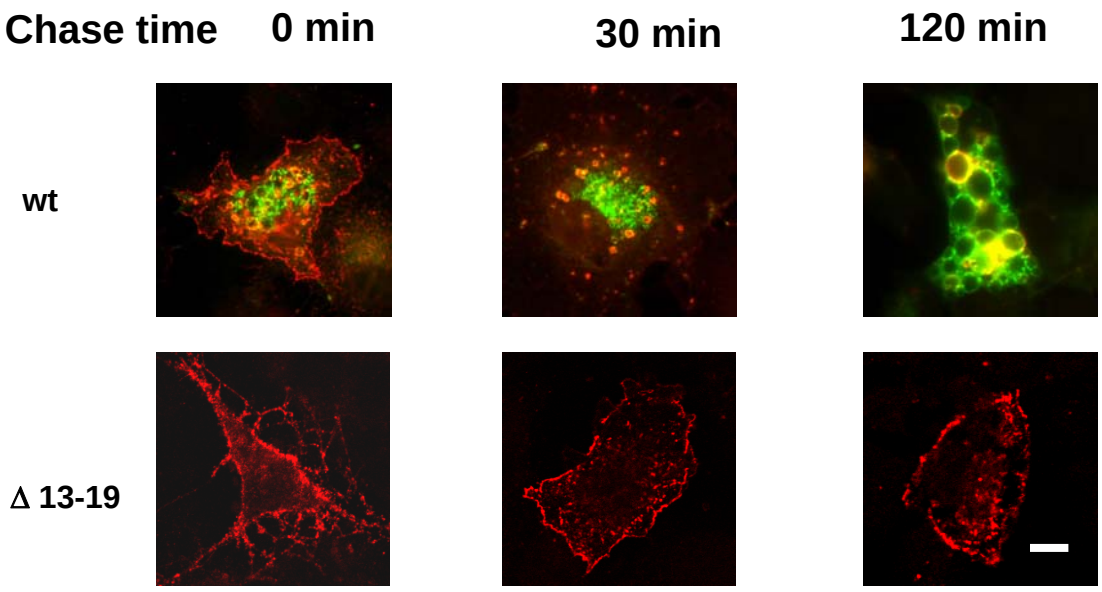

Fig. 3.11 ClC-3 Δ 13-19 Showed Impaired Endocytosis. COS-7 cells were transfected with wt ClC-3 or ClC-3 Δ 13-19 with external HA, incubated with HA antibody for 45min and chased at 37°C for 0 min, 30 min and 2 h. Anti-HA immunofluorescence is displayed in red and GFP fluorescence is in green. For wt ClC-3, after a 30 min chase, plasma membrane resident ClC-3 moved to small endocytic vesicles and by 2 h had accumulated into the large central vesicles that are the major site of total cellular ClC-3 at the steady state. For ClC-3 Δ 13-19, the epitope-tagged molecule stayed at the plasma membrane even after 37°C chasing for 2 hours. Bar, 10 μm.

DISCUSSION

In this chapter, our data clearly establish the importance of a specific N-terminal targeting motif to the overall distribution and trafficking of ClC-3. This conclusion was initially supported by yeast two hybrid assays to screen the interaction between N or C terminus and adaptor proteins. In these assays, the N termini of ClC-3 interacted with AP-1 and AP-2. When we abolished the putative 1st tyrosine motif and the dileucine acidic cluster (Δ 12-30), the interaction with μ1, μ2, and μ3 were all abolished. This result is consistent with the imaging studies. When we expressed ClC-3 Δ 12-30 in the cells, it primarily located at the plasma membrane while wild type localized primarily to intracellular sites. Furthermore, biotinylation studies showed that mutants with intracellular distribution were all readily endocytosed from the plasma membrane while the mutants with apparent plasma membrane localization displayed defective endocytosis.

Over-expression of several mutants (ClC-3 (66-760), ClC-3 581A584A, ClC-3 631A634A) showed reticular distribution patterns inside the cells (Fig 3.2). When we further evaluated them, they demonstrated Endo H sensitivity in glycosylation analysis. This means that these mutants never go beyond the cis-golgi compartment. Therefore, they have no value in evaluating the post-ER targeting signals, either for the direct pathway or for the indirect pathway.

The assembly of the oligosaccharide chains of N-linked glycoprotein occurred in both the endoplasmic reticulum and the Golgi complex. The trans Golgi compartment is where glycosylation is completed. Those mutants that never go beyond the cis-golgi compartment do not have the opportunity to complete the whole glycosylation process; therefore, they are less heavily glycosylated than wild type ClC-3. This is reflected by the band pattern after the PNGase F treatment. When we compared the molecular weight shift for wt ClC-3 and ClC-3 (66-760), we found that the wt ClC-3 showed a prominent molecular weight shift (Fig 3.3) while the mutant showed a minor shift (Fig. 3.5). This means that the mutant is less heavily glycosylated than the wild type ClC-3 protein.

One of the best described motifs which can mediate AP protein binding and trafficking is the tyrosine-based tetra-peptide motif, YXXϕ, where X can be any amino acid and ϕ is a hydrophobic amino acid (20, 29-31). Two tyrosine motifs are present in the ClC-3 N-terminus, but neither appears to be important for ClC-3 internalization since alanine substitution of the tyrosine at positions 27 or 65 and the ϕ at position 30 or 68 did not change ClC-3 distribution. However, one mutant (Δ 12-30) that abolished both the tyrosine motif and the dileucine cluster as well as the mutant (Δ 13-19) that abolished the dileucine cluster only displayed impaired endocytosis. These data demonstrate that the dileucine cluster at the N terminal of ClC-3 is required for endocytosis. It is important to note that the sequence LLDLLDE at position 13 to 19 is not the same as the canonical dileucine motif D/EXXXLL(I/V), but it is similar to a previously proposed clathrin binding sequence LLDLD (73). Furthermore, Kornfeld et al reported the identification of a new variant of the consensus clathrin box motif that resides within the hinge region of the γ subunit of human and mouse AP-1. This variant is LLDLL, which is able to bind the clathrin N-terminal domain (74). It is thus possible that the dileucine cluster interacts with clathrin. An additional hint comes from our yeast two hybrid experiment. We demonstrated the interaction between N terminal of ClC-3 and AP-1 as well as AP-2, the two adaptor proteins functioning in the clathrin coats. This also suggests an interaction between ClC-3 and clathrin may exist.

ClC-3 has a long C terminal segment. It contains the two carboxyl-terminal CBS domains that are present in all eukaryotic ClC-family chloride channels. The function of CBS domains remains obscure. A key question regarding CBS domains is whether they play important roles in Cl^- channel function or in sub-cellular trafficking. Carr et al reported a trafficking role for CBS domain 2 of mCLC-5 in CHO-K1 and IMCD-3 cells. They showed that three mutants in which the second CBS domain was disrupted were unable to traffic normally to acidic endosomes. These were retained in perinuclear compartments, colocalizing with the *Griffonia* Golgi marker (48). Other researchers have proposed that the CBS domains from ClC channels play a functional role in the common

gate (75). Still others propose that tandem pairs of CBS represent a newly identified class of binding domain for adenosine derivatives (76). Argument and investigation will be continued.

In contrast to the important observations made with the N-terminal mutants, the C terminal mutants we made did not provide much information about trafficking. When we abolished the two putative tyrosine motifs at the C terminal with alanine replacement, both mutants simply failed to exit the ER. When we abolished the dileucine motif at the C terminal, this construct behaved the same as wild type ClC-3. In addition, the Y2H studies suggested that the C-terminus was not involved in binding to AP proteins. The role of the C terminal in trafficking was thus not established in our study. These data may suggest that the C-terminus has a more complex folding pattern than the N-terminus and is both critical for normal folding of the rest of the molecule and requires the rest of the molecule for its own folding.

In summary, we identified seven amino acids at N terminal of ClC-3 is important for its internalization from the plasma membrane in this chapter. This opens the door to the further study of how this specific signal interacts with the endocytic machinery within the cells. I will report the data regarding to this aspect in the following chapter.

METHODS

Yeast two-hybrid screening

Two-hybrid screening was performed in the budding yeast, *Saccharomyces cerevisiae*, using the Matchmaker yeast two hybrid system (BD Biosciences, Mountain View, CA). N or C terminal of ClC-3 was inserted into a yeast vector, pGBKT7 vector, which expresses GAL4 DNA binding domain. This vector contains the nutritional selectable marker TRP1 in yeast. The pACT2 vector was cloned in all AP genes tested, which expresses GAL4 transcription activation domain (kindly gift from Dr. JS Bonifacino). This vector contains the nutritional selectable mark LEU2 in yeast. Protein-protein interactions were selected with His deficient media.

Constructs

ClC-3 Δ 12-30, ClC-3 Δ 13-19 and a series of alanine replacement mutants of ClC-3 were generated from the parent constructs using the QuikChange® site-directed mutagenesis kit (Stratagene). All constructs were confirmed by sequencing in the Protein Chemistry Laboratory of the University of Texas Medical Branch.

Endo H digestion

COS-7 cells were transfected with ClC-3 GFP for 48h. Cell lysates were collected as previously described. Endo H (1 µl, Roche Cat. No. 1 088) was incubated per with 25 µg of COS-7 lysate under standard assay conditions for 4h. The samples were then subjected to SDS-polyacrylamide gel electrophoresis and western blot. ClC-3 was visualized with GFP antibody (1:2000).

Immunostaining and microscopy: See chapter 2

Biotinylation experiments: See chapter 2

Trafficking of ClC-3 mutants: See chapter 2

CHAPTER 4: INTERACTION BETWEEN CLC-3 AND THE ENDOCYTSIS PROTEIN MACHINERY

INTRODUCTION

The previous chapters have defined the trafficking pattern of ClC-3 and identified a specific segment that is critical for trafficking. In this chapter, I will present data that attempts to define how this critical sequence interacts with other proteins to achieve the observed trafficking steps.

Newly synthesized proteins can access the endosomes either directly from the trans-golgi or indirectly after endocytosis from the plasma membrane. Internalization from the plasma membrane can be achieved by different mechanisms. There are two well-defined mechanisms, clathrin-mediated endocytosis, and caveolae-mediated endocytosis. A third category, clathrin- and caveolae-independent endocytosis is still under investigation (64). Caveolae-dependent endocytosis has been found to be involved in the uptake of some membrane components such as glycosphingolipids and integrins, as well as viruses, bacteria, and bacterial toxins. Accumulating evidence shows that endocytosis mediated by caveolae requires specific molecules such as caveolin-I and src kinase (77).

Several adaptor protein complexes direct clathrin assembly into curved lattices and couple it to cargo recruitment (37, 38). AP-1 and AP-2, two clathrin interacting adaptor proteins, participate in protein transport to the endosomal-lysosomal system from the trans-Golgi network (TGN) and the plasma membrane, respectively (78). Currently, very little is known about the mechanisms underlying ClC-3 trafficking and the adaptor proteins which play important roles in this process.

Sorting of transmembrane proteins in the cells is mediated by signals present within the cytosolic domains of the proteins. Most signals are composed of short, linear sequences of amino acid residues. As discussed previously, the tyrosine motif YXXΦ is a well defined sorting signal in cytosolic domains of membrane proteins. Tyrosine motifs are found in endocytic receptors such as the transferrin receptor, lysosomal membrane

proteins such as Lamp-1 and Lamp-2, and TGN proteins such as TGN38. They are also found in proteins localized to specialized endosomal-lysosomal organelles such as antigen-processing compartments (e.g., HLA-DM). In addition, they have been implicated in the targeting of transmembrane proteins to lysosomes and lysosome-related organelles as well as the sorting of some proteins to the basolateral plasma membrane of polarized epithelial cells. Since YXXΦ signals serve multiple roles in protein sorting, they may be recognized by different proteins and act at multiple sites such as the plasma membrane and TGN or endosomes. The YXXΦ sequence is common in the cytosolic domains of signaling receptors and in a number of cytosolic proteins as well. However, most of these sequences are not active as sorting signals because they are folded within the structure of the proteins and cannot interact with components of the sorting machinery (36).

Dileucine-containing motifs are important in trans-Golgi sorting, lysosomal targeting, and endocytosis from the plasma membrane. The dileucine-based signals contain [DE] XXXL [LI] or DXXLL consensus motifs. They are recognized specifically by the AP complexes and GGA (36, 70)**.**

A consensus sequence for clathrin binding has been identified by analysis of multiple different proteins. Fig 4.1, shows a sequence alignment illustrating the existence of a potential clathrin-binding motif within human β3A and β3B, β1, and β2; bovine arrestin3 and β-arrestin; human amphiphysins I and II as well as ClC-3. This motif consists of acidic and bulky hydrophobic residues and conforms to the consensus sequence L (L, I) (D, E, N) (L, F) (D, E). ClC-3 has a segment containing LLDLLDE, which is very similar to the consensus sequence of clathrin binding.

β3A	**817**	**S**	**L**	**L**	**D**	**L**	**D**	**D**	**F**	**N**	**825**
β3B	**806**	**S**	**L**	**L**	**D**	**L**	**E**	**D**	**F**	**T**	**814**
β1	**631**	**D**	**L**	**L**	**N**	**L**	**D**	**L**	**G**	**P**	**839**
β2	**630**	**D**	**L**	**L**	**N**	**L**	**D**	**L**	**G**	**P**	**638**
Arrestin3	**372**	**N**	**L**	**I**	**E**	**F**	**E**	**T**	**N**	**Y**	**380**
β-arrestin	**376**	**N**	**L**	**I**	**E**	**L**	**D**	**T**	**N**	**D**	**384**
Amphiphysin I	**350**	**T**	**L**	**L**	**D**	**L**	**D**	**F**	**D**	**P**	**358**
Amphiphysin II	**389**	**S**	**L**	**L**	**D**	**L**	**D**	**F**	**D**	**P**	**397**
ClC-3	**12**	**H**	**L**	**L**	**D**	**L**	**L**	**D**	**E**	**P**	**20**

Fig 4.1 Consensus Sequence for Clathrin Binding. ClC-3 contains LLDLLDE at its N terminal, which is very similar to the consensus clathrin binding sequence existing in other known clathrin-binding proteins.

In chapter 3, we have already established that amino acids 13-19 are important in the endocytosis of ClC-3. In this chapter, we will determine the general mechanism for ClC-3 internalization and whether the motif at amino acid 13-19 directly binds to proteins of the endocytosis machinery.

RESULTS

ClC-3 is endocytosed in association with clathrin

ClC-3 trafficks through clathrin containing small vesicles to non-clathrin containing big lysosomal vesicles

In this part of the work, we first tested the relationship between ClC-3 and clathrin during the process of endocytic internalization. We took advantage of the development of a ClC-3 construct with an extracellular HA epitope, which allowed us to label the ClC-3 molecule that appeared on the cell surface and then chase its trafficking. We used an HA antibody to label the extracellular HA epitope in live cells transfected with ClC-3/1217 HA. Live cells were incubated with anti-HA primary antibody, antibody

was washed away at time 0, and then cells were incubated at 37 °C for 2 h. Cells were then fixed, permeabilized, and treated with anti-clathrin antibody. The anti-HA that had prebound to ClC-3 and the anti-clathrin primary antibodies were identified with appropriate fluorophore-conjugated secondary antibodies. This method enabled us to assess the association of ClC-3 and clathrin during the process of endocytosis. Clathrin was detected as punctate labeling at the plasma membrane as well as being present in small intracellular vesicles (Fig. 4.2A, D). Immuno-labeling of the external epitope of ClC-3 (Fig. 4.2B, E) showed considerable co-localization with clathrin prior to the chase period (Fig. 4.2A-C). However, when large vesicles formed with longer chase time, ClC-3 moved to a more central area of the cell and dissociated from clathrin, leaving clathrin-containing vesicles primarily distributed near the plasma membrane (Fig 4.2D-F).

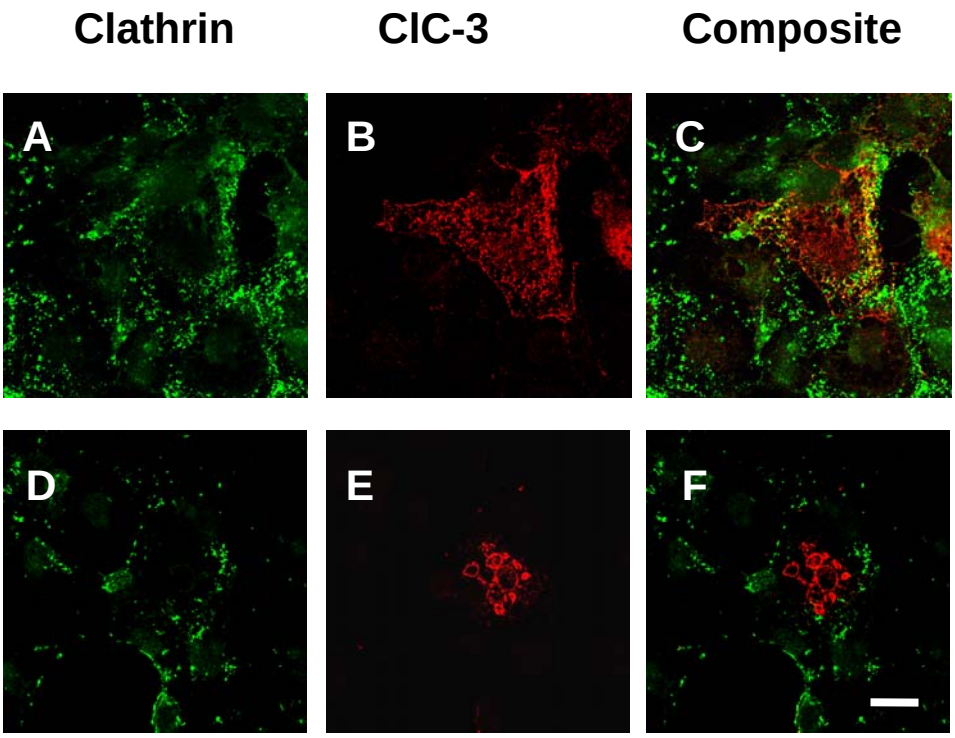

Fig 4.2 Association of ClC-3 with clathrin during endocytosis. COS-7 cells were transiently transfected with ClC-3 external HA. The fluorescent images of ClC-3 (red, *B*, *E*) or clathrin (green, *A, D)* are displayed along with the respective composite images (*C*, *F*). Areas of colocalization appear yellow in the composite images. Confocal microscopy images demonstrate that ClC-3 (B) colocalizes with clathrin (A) at the plasma membrane. However, ClC-3 (D) dissociated from clathrin (E) after the 2h chase. Bar, 10 μm.

Endocytosed ClC-3 colocalized with endocytosed transferrin

To further examine the association between endocytosis of ClC-3 and clathrin-dependent processes, we examined the colocalization of endocytosed ClC-3 with transferrin. Transferrin is internalized via clathrin coated pits (79) . After surface-labeling of ClC-3 for 45 minutes, we incubated the cells at 37°C for 15 minutes with transferrin-594 added to the medium. This condition allows endocytosis of both proteins and enables

us to chase the trafficking of the two. As shown in Fig 4.3., ClC-3 and transferrin were each endocytosed and frequently colocalized in the same population of endocytic vesicles.

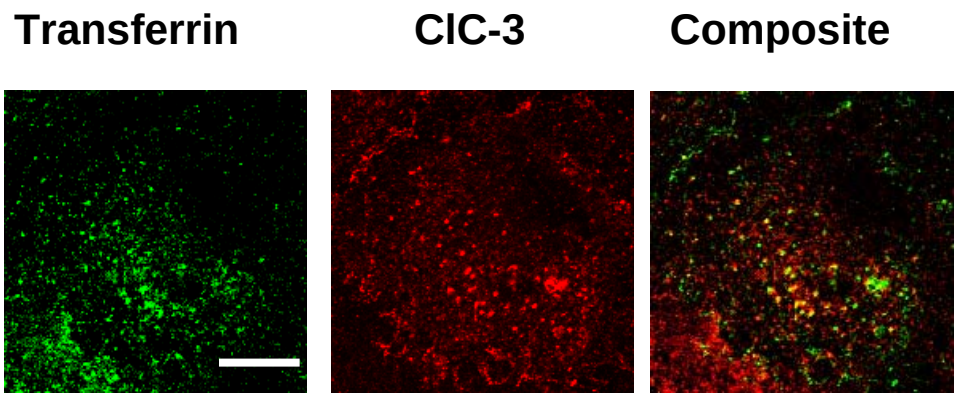

Fig 4.3 Endocytosed ClC-3 colocalizes with endocytosed transferrin. COS-7 cells were transfected with ClC-3/1217 HA, the wt ClC-3 construct with an extra-cellular HA epitope. After transfection for 48 h, living cells were incubated in PBS for 45 minutes with anti-HA antibody. Then the antibody was washed away and the cells were chased for 15 minutes with Alexa 594 conjugated transferrin ligand (5μg/ml) in DMEM at 37°C. The cells were then fixed, permeabilized and visualized with confocal microscopy. The composite image is shown in yellow. Bar, 10 μm.

High sucrose treatment inhibits ClC-3 internalization

We next employed a functional test to assess whether ClC-3 is internalized by the clathrin pathway. Clathrin-mediated endocytosis is known to be inhibited by hypertonic extracellular solutions (80). Hypertonic media is thought to inhibit the assembly of clathrin-coated pits, leading to cellular membranes that are devoid of endocytic sites (80). Exposing various cells to hypertonic medium removes the clathrin lattice and almost completely inhibits the uptake of TfnR (81). We performed cleavage biotinylation experiments with high sucrose treatment (0.45M) to determine if hypertonicity affected

ClC-3 internalization. We found internalization of ClC-3 channel decreased significantly after high sucrose treatment.

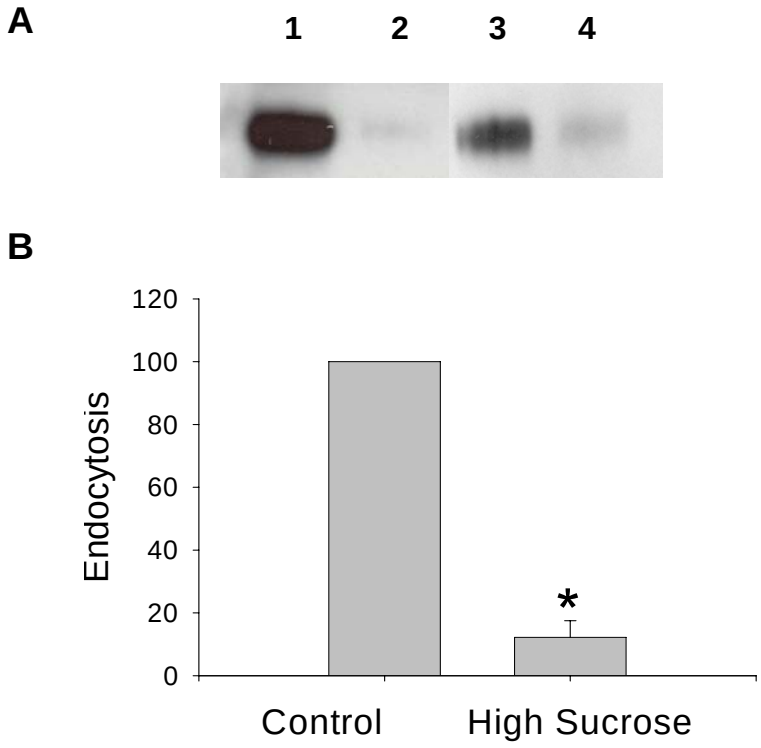

Fig 4.4 High sucrose inhibits ClC-3 endocytosis. A. ClC-3/HA transfected COS-7 cells were surface biotinylated with sulfo-NHS-SS-biotin, which was subsequently cleaved with MesNa, prior to streptavidin precipitation. Each lane shows the results of immunoblotting of streptavidin pellets for ClC-3. Lane 1, after biotinylation, before cleavage; lane 2, after immediate cleavage; lane 3, after biotinylated cells were first incubated for 15 min at 37 °C followed by cleavage and streptavidin precipitation; Lane 4, the same as lane 3, but with 0.45M sucrose treatment. **B.** Summary of densitometry analysis of 3 experiments as in A. Percent maximum endocytosis was calculated as described in the previous chapter. ∗ $P<0.05$

Clathrin siRNA experiments

Using siRNA for gene silencing is a rapidly developing tool in molecular biology. RNA interference (RNAi) is a ubiquitous mechanism in eukaryotic cells to inhibit the expression of genes that play roles in determining the fundamental cell fates of differentiation and survival. RNAi is generated from small double-stranded RNAs processed from long double-stranded RNAs or from transcripts that form stem-loops. The mechanisms of gene silencing consist of targeting mRNA for degradation, preventing mRNA translation or by establishing regions of silenced chromatin (82, 83). Small interfering RNA (siRNA) suppresses expression of a specific gene by mRNA degradation, with high efficiency and selectivity. Messenger RNA degradation occurs when the antisense strand of the short siRNA directs the RNA-induced silencing complex (RISC) that includes the RNA endonuclease Ago2 to cleave the target mRNA containing a complementary sequence (84). Because siRNA is an endogenous and ubiquitous pathway, the effectiveness of gene silencing achieved with RNAi is better than other techniques using small nucleic acids, such as antisense oligonucleotides or ribozymes (82, 83). In one direct comparison, siRNAs suppressed gene expression about 100–1000 fold more efficiently than antisense oligonucleotides (85). The reason may be due to the catalytic nature of siRNA and protection of the active component of the siRNA (the antisense or guide strand) from digestion by endogenous RNases through its incorporation into the RISC (84). Since previous studies have successfully used this technique to deplete clathrin and shown that clathrin depletion by siRNA inhibited the uptake of transferrin (86), I conducted a series of experiments designed to test the effect of clathrin siRNA on the endocytosis of ClC-3.

To inhibit the expression of the clathrin heavy chain, I used an siRNA duplex that targeted positions 3311-3333 of the heavy chain sequence (86). A negative control siRNA was also used in the experiment. Cell lysates were prepared after 72 h of siRNA transfection. An aliquot of lysates was subjected to electrophoresis and western blot.

Quantification of the results by densitometry and normalization relative to actin expression showed that the amount of the clathrin heavy chain had dropped to 15% on day 3 compared with control group.

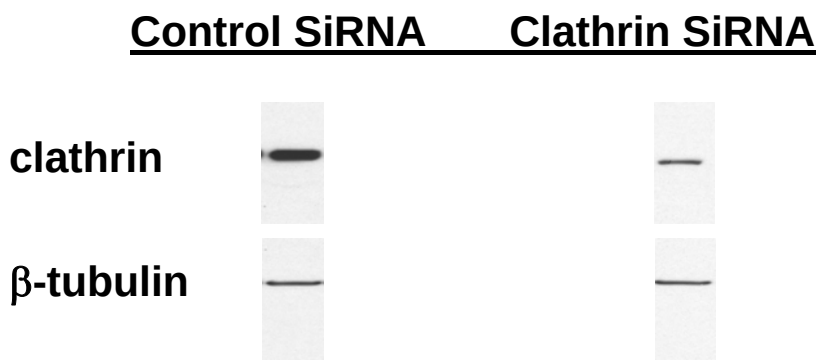

Fig 4.5 Clathrin HC depletion in HeLa cells by transfection with siRNA. siRNA duplex that targeted positions 3311-3333 of the heavy chain sequence (86) was used. For siRNA transfection studies, cells were seeded in the absence of penicillin and streptomycin. After 12 hours the cells were transfected with either clathrin or control siRNA (Santa Cruz), by using Oligofectamin (Invitrogen). Lysates were prepared 72 h after transfection. Lysates from control siRNA and clathrin siRNA-transfected cells were blotted with antibodies against clathrin heavy chain and β-tubulin.

Although lipid-based transfection reagents previously worked effectively for expression of ClC-3/HA in many different mammalian cell lines, the expression level of ClC-3 was reduced (to <5% of a typical transfection) when co-transfecting ClC-3/HA and clathrin siRNA (Fig 4.6). Therefore, we were not able to use this method to test whether clathrin knock down inhibited ClC-3 endocytosis.

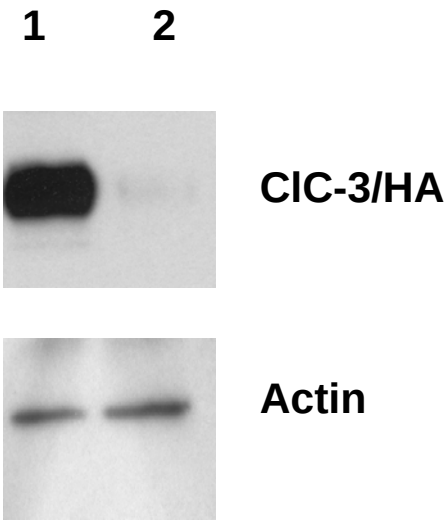

Fig 4.6 Co-transfection of ClC-3 and clathrin siRNA decreased the expression of ClC-3. The same siRNA was used as described in Fig 4.5. For the cotransfection of ClC-3 and siRNA, two transfections were performed. On day 1, clathrin siRNA was transfected as described. On day 2, the clathrin siRNA and ClC-3 plasmid were transfected simultaneously). Lysates were prepared 48 h after the 2nd transfection. Lysates from cells cotransfected with ClC-3 and control siRNA (Lane 1) or ClC-3 and clathrin siRNA (Lane 2) were blotted with HA epitope of ClC-3. An actin immunoblot here served as a loading control.

GST pulldown experiments demonstrated the interaction between the N terminal of ClC-3 and clathrin

Cellular proteins participate in extensive networks of protein-protein interactions which assemble and disassemble in response to ever-changing environmental cues. A preliminary step in understanding protein structure and function is to identify the protein-protein interactions, which will be essential to understand the relevant biological pathways. The pull-down technique has become a valuable tool for studying protein-protein interactions. In our study, we fused the N terminal of ClC-3 to GST, and used it to pull down binding partners from COS-7 lysates.

In chapter 3, I showed that at steady-state, two mutants of ClC-3, ClC-3 Δ12-30 and ClC-3 Δ13-19 are present preferentially at the plasma membrane and their internalization from the cell surface has been impaired. This was shown both with the cleavage biotin experiments and imaging studies. In order to explore the interactions between the N-terminal targeting segment and proteins involved in endocytosis, we performed GST-pull down assays. GST fusion constructs (ClC-3 N-terminal, ClC-3 N-terminal Δ12-30 or ClC-3 N terminal Δ13-19) were used to precipitate proteins derived from non-transfected COS-7 cell lysates. Pelleted proteins were blotted using antibodies against AP-2 β subunit, clathrin heavy chain, or caveolin I. As shown in Fig 4.7, the N-terminal of ClC-3 binds to both clathrin and AP-2β, but not caveolin I. ClC-3 N- terminal Δ 12-30 as well as ClC-3 N-terminal Δ 13-19 also bind to AP-2β, but not clathrin. These data demonstrate that the dileucine cluster at the N terminal of ClC-3 is required for clathrin binding (Table 4.1).

Amino acid sequence of N terminal ClC-3

MTNGGSINSST**H**LLDLLDE**PIPGVGT**YDDFHTIDWVREKCKDRERH
RRINSKKKESAWEMTKSLYDAW

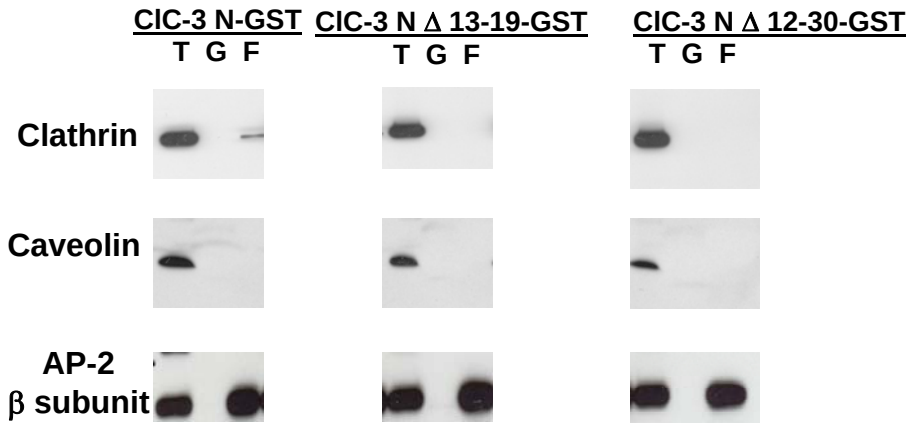

Fig 4.7 N terminal amino acids 13-19 interact with clathrin. A fusion protein of glutathione-S-transferase and the N-terminal of wt ClC-3 (ClC-3 N-GST) was used to pull down proteins from COS-7 cell lysates. Alternative fusion proteins were constructed similarly but using N-terminal ClC-3 segments with deletions encompassing amino acids 13-19 (ClC-3 N-Δ13-19 GST) or 12-30 (ClC-3 N-Δ12-30 GST). Beads were blotted using antibodies against β subunit of AP-2, clathrin heavy chain and caveolin I. T: Total lysate; G: GST only precipitation; F: ClC-3 N terminal construct fused with GST.

ClC-3 co-immunoprecipitated with clathrin

Our yeast two hybrid data (Fig 3.7) suggests that two clathrin adaptors, AP-1 and AP-2, could be involved in the interaction with the N terminal of ClC-3. The GST pull down assays also showed binding between the N segment of ClC-3 and clathrin (Fig 4.8). To further confirm the interaction between the intact clathrin and ClC-3 molecules in vivo, we performed the Co-immunoprecipitation experiments. Clathrin was first immunoprecipitated from total lysates. The immunoprecipitates were then probed for the presence of ClC-3. This protocol demonstrated immunoreactivity for ClC-3 (Fig 4.8 A). Immunoprecipitates of ClC-3 similarly demonstrated clathrin immunoreactivity (Fig 4.8 B). Importantly, the control IgG alone was not able to precipitate either ClC-3 or clathrin (Fig 4.8). The IgG control experiments demonstrated specificity of our co-immunoprecipitation procedure. Taken together, these results indicate that ClC-3 physically associated with clathrin in COS-7 cells.

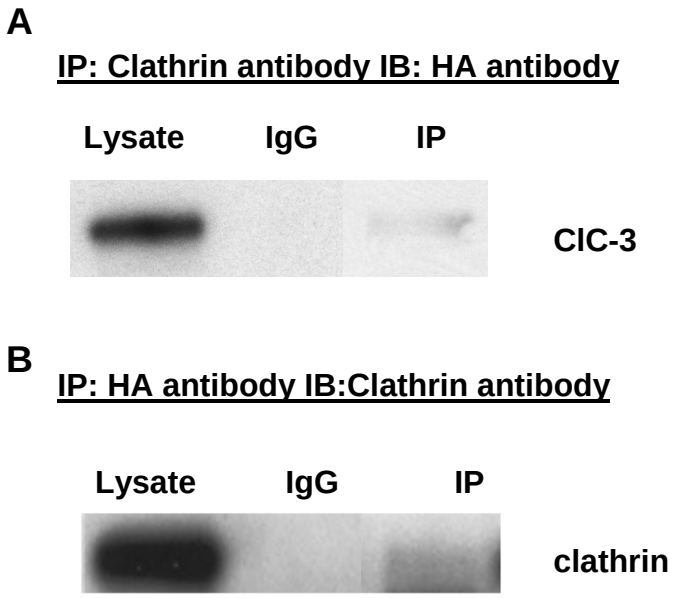

Fig 4.8 Co-immunoprecipitation of ClC-3/HA and clathrin. Whole cell lysates prepared from COS-7 cells transiently transfected with ClC-3/HA were used. Lysates

were immunoblotted with each antibody to demonstrate the presence of the respective proteins. **A.** ClC-3 co-IP with clathrin. Clathrin was immunoprecipitated from lysates and immunoblotting was performed with HA antibody. In order to evaluate the specificity of the ClC-3 interaction with clathrin, co-immunoprecipitation was also performed using mouse IgG, the same species as the clathrin antibody used for IP. **B**. Clathrin co-IP with ClC-3. Co-immunoprecipitation was also performed in the reciprocal manner. The IgG here is the rabbit IgG, the same species as HA antibody used for IP.

In table 4.1, I compare the different phenotype of wt ClC-3 and two important mutants: ClC-3 Δ 12-30 and ClC-3 Δ 13-19.

Table 4.1 Summary of phenotypes of ClC-3 constructs.

	Wt ClC-3	ClC-3 Δ 12-30	ClC-3 Δ 13-19
Steady-state distribution	Endosome/ lysosome	Plasma membrane	Plasma membrane
Endocytosis (Cleavage biotin)	Normal	Impaired	Not tested
Endocytosis (Trafficking image)	Normal	Impaired	Impaired
Clathrin binding (GST pulldown)	Yes	No	No

DISCUSSION

We used several experiments to investigate the interaction between ClC-3 and clathrin. First, our immunofluorescence results showed that endogenous clathrin and ClC-

3 partially colocalized in a punctate pattern at the plasma membrane. When we followed the movement of the internalized ClC-3, we found it ultimately dissociated from the clathrin-containing pits (Fig 4.2). This result is a good indication of the dynamic association between ClC-3 and clathrin. Since clathrin resides at different sorting stations and ClC-3 also travels along different compartments of the cell, it is reasonable that we cannot colocalize the two of them completely. Our result that endocytosed ClC-3 and transferrin colocalized in a population of endocytic vesicles is supported by results from Faundez et al. They showed that in PC-12 cells, ClC-3 was present in transferrin receptor-positive endosomes (55). Second, ClC-3 endocytosis is impaired by hypertonic media, a treatment which inhibits the assembly of clathrin-coated pits (80). However, high sucrose treatment is not an ideal way to affect the clathrin-mediated pathway specifically. Hypertonicity has pleiotropic effects inside the cells as it can affect the polymerization of actin. Third, GST pull down and co-immunoprecipitation experiments confirmed the physical interaction between ClC-3 and clathrin.

The selective recruitment of cargo proteins into clathrin coated pits occurs by binding of specific motifs in cytosolic domains of cargo proteins to adaptor proteins. Our fluorescence and biotinylation data showed that two constructs bearing a limited N terminal deletion, Δ12-30 and Δ13-19, showed an impairment of endocytosis and a failure to bind to clathrin in GST pulldown experiments. These data imply that the dileucine cluster at the N terminal of ClC-3 (positions 13-19) is required for both clathrin binding and endocytosis. Interestingly, this segment was not necessary for AP-2 binding. This is an unexpected finding since it has been generally assumed that AP-2 is the linker between clathrin and membrane cargo proteins. Our results suggests that in this case, the AP-2 interaction with the ClC-3 N terminal is not sufficient for optimal internalization and ClC-3 binds to clathrin via another mechanism, which could be either direct binding, or binding through another protein as an intermediary. Additional components may play important roles in the endocytosis of ClC-3 since sorting of membrane protein coated

pits is a complex process that can involve AP-2, other adaptor proteins which are linked to AP-2, or AP-2 independent mechanisms (87).

We attempted to use siRNA to determine the effect of clathrin depletion on ClC-3 trafficking. In our hands, clathrin siRNA can specifically inhibit the expression of clathrin. However, when we co-transfected clathrin siRNA and ClC-3, we found that the expression of ClC-3 was dramatically decreased. This unexpected result prohibited us from further studying the effect of clathrin siRNA on ClC-3 endocytosis. Whether this is a technical artifact, or whether clathrin is somehow responsible for the stability of ClC-3 protein in cells is not known. While the molecular details of the ClC-3 clathrin interaction have therefore not yet been defined, endocytosis of ClC-3 appears to be clathrin associated and a direct interaction between clathrin and the ClC-3 dileucine acidic cluster is an attractive hypothesis.

METHODS

Confocal microscopy-colocalization with endogenous clathrin and transferrin

Details of the internalization and immunofluorescence methods are described in Chapter 2. In the experiments designed to double-label endocytosed ClC-3 and clathrin, ClC-3 was visualized using Alexa Fluor 488-conjugated goat anti-mouse IgG (1:500) as a secondary antibody. Coverslips were then incubated with goat anti-clathrin antibody (1:100). Thereafter, cells were washed and incubated with Alexa Fluor® 594 chicken anti-goat IgG (H+L) for one hour at room temperature.

To visualize endocytosed ClC-3 and transferrin, live cells were incubated in PBS for 45 minutes with anti-HA antibody (Covance, MMS-101R). Then the coverslips were washed in PBS and chased for 15 minutes with Alexa 594 conjugated transferrin ligand (5μg/ml) in DMEM at 37°C. The cells were then fixed, permeabilized and visualized. Immunofluorescence was visualized with a Zeiss LSM 510 confocal microscope with a 63×oil (1.4 NA) immersion objective. Samples were visualized with the 480 nm and 543

nm laser lines and emission filter sets at 505-530 nm for GFP and Alexa 488 detection or 585-615 nm for Alexa 594 detection.

GST Pull-down Assays

GST and various GST fusion proteins were produced in *BL-21* bacterial cell lines using the glutathione *S*-transferase Gene Fusion System (Amersham Biosciences). GST or GST fusion proteins were incubated with glutathione-Sepharose 4B beads for 1h at room temperature followed by extensive washing in phosphate-buffered saline. The conjugated beads were then incubated with COS-7 cell lysates prepared as described in Chapter 2. After incubation overnight at 4 °C, the beads were washed three times with lysis buffer. Bound proteins were eluted by incubating the beads in SDS loading buffer containing β-mercaptoethanol at 95 °C for 5 min. Electrophoresis followed by Western blotting was subsequently performed.

Suppression of clathrin expression with siRNA

An siRNA duplex that targeted positions 3311-3333 of the heavy chain sequence (86) was used (Dharmacon custom siRNA) . For siRNA transfection studies, cells were seeded in the absence of penicillin and streptomycin. After 12 hours the cells were transfected with either clathrin or control siRNA (Santa Cruz), by using Oligofectamin (Invitrogen). 6 hours after transfection, FBS (10%), penicillin (100,000 U/L) and streptomycin (100,000 U/L) were added to the cells and the cells were further incubated 70 hours before they were used for experiments. To verify knockdown of clathrin, cells were harvested and the proteins were extracted for western blot analysis about 3 days after transfection. For the cotransfection of ClC-3 and siRNA, two transfections were performed. On day 1, clathrin siRNA was transfected as described. On day 2, the clathrin siRNA and ClC-3 plasmid were transfected simultaneously with Lipo2000 transfection reagent.

Co-immunoprecipitations and Immunoblotting

Whole cell lysates prepared from COS-7 cells transiently transfected with ClC-3/HA were used. Cells were grown in 100-mm plastic Petri dishes until confluent. Cells were washed twice with 2 ml of cold 1x PBS. Petri dishes were placed on ice-cold lysis buffer supplemented with a protease inhibitor mixture. Lysates were then spun at 10, 000 x *g* at 4 °C for 15 min. The supernatant was removed, and a protein assay (Biorad, cat# 500-0006) was performed to quantify the amount of total protein in the samples. First, supernatants were precleared of proteins with nonspecific binding. Protein A/G-agarose beads (100 µl of 50% slurry, Pierce, cat# 20421) were added to whole cell lysate (500 µg) for each immunoprecipitation reaction. After 6 h incubation at 4 °C, the beads were removed by centrifuged for 2 min at 3,000 x *g*. The beads were saved in 25 µl 2×sample buffer (Invitrogen, cat# LC2676). The precleared supernatant was subsequently incubated at 4 °C overnight on a rotator with the specific IP antibody (Sigma H6908 1:200, Santa Cruz sc-12734 1:100). Fresh protein A/G-agarose beads (100 µl of 50% slurry) were added and then incubated 6 h at 4 °C. After centrifugation at 3,000g for 2 min, the supernatant was aspirated. SDS-PAGE sample buffer was then added to the beads. The sample was heated and separated by SDS-PAGE with constant voltage at room temperature. Immunoblotting was subsequently performed as previously described.

CHAPTER 5 PERSPECTIVES AND FUTURE DIRECTIONS

ClC-3 and the other ClC family proteins have many characteristics demonstrating that they are highly important to cell function. Several of the family members are present in every mammalian cell, and while genetic knock-outs of a single ClC protein produces viable mice, double knock-outs tend to be lethal (Thomas Jentch, personal communication). In addition, ClC proteins are among the most highly conserved proteins throughout the evolution. The rat long form of ClC-3 identified by our group is 100% identical at the amino acid level to mouse ClC-3 and is 99.7% amino acid identical to human ClC-3. This level of evolutionary sequence conservation is extremely unusual. The short form of rat ClC-3 identified by our group bears a conservative valine to isoleucine substitution at amino acid 759 compared to the reported sequence by Sakamoto (88). Our sequence was identical to that of mouse, rabbit, and human ClC-3 at this position (50).

As critical as these molecules must be, it is remarkable how little is actually known about them. For the "intracellular" family of ClC proteins (ClC-3, 4, 5, 6, 7) the only functional consequence seen in single knock out models is the loss of acidification of a particular compartment.

In the present study, we have determined that ClC-3 is primarily an intracellular protein but it localizes to the plasma membrane as well. Plasma membrane ClC-3 is rapidly endocytosed and delivered to intracellular sites by a process that requires a dileucine cluster. This motif appears to be a specific clathrin-interacting sequence within the cytosolic N-terminal domain. Before I started this project, there was controversy over whether ClC-3 existed primarily at the plasma membrane or in intracellular compartments. After I finished my project, it's quite clear that ClC-3 is predominantly present intracellularly in the membrane of late endosomes/lysosomes. It takes both direct and indirect pathways to this final destination. Furthermore, I have identified an

important segment of ClC-3 which is necessary for interaction with clathrin.

FUTURE DIRECTIONS

Channel vs. Antiporter

An important recent finding is that some ClC molecules are Cl^--H^+ exchangers and not chloride channels. This contradicts the previously understood function of these proteins and suggests that their function and role in acidification may not have been understood correctly. A recent paper observed chloride/proton antiporter activity of the mammalian ClC proteins ClC-4 and ClC-5 (24). The high similarity between ClC-3 and these two family members suggests that ClC-3 may be an antiporter as well. Our previous work shows that ClC-3 has nearly identical chloride transport properties to ClC-4 and ClC-5. The short isoform of ClC-3 yields mediates outward rectifying currents with $Cl^- > I^-$ selectivity, and insensitivity to DIDS. These properties appear to be identical to those reported for ClC-4 and ClC-5. Because ClC-3 shares an overall 80% amino acid identity with ClC-5, most of the differences are in the cytosolic domains, and the two proteins have nearly identical channel pore regions, it is possible that they share similar biophysical properties and thus it is likely that ClC-3 is an antiporter as well.

This new understanding would explain a previous observation that has never been understood. The channel activity for ClC-3, 4, 5 that has been measured in whole cell patch clamp experiments always displays extreme outward rectification. This voltage dependence is so extreme that the channel is only open at voltages more positive than +30 mV. Since plasma membranes and vesicular membranes actually have negative voltages using this polarity convention, these channels would never be able to open at any conceivable cellular site. If they cannot be open, perhaps the observed "channel" activity, while true, is not the real biological function. The antiporter hypothesis thus explains this contradiction. Instead of being channels, these ClCs are actually antiporters. The channel function exists but only under artificial voltage conditions.

The unexpected finding that some ClC proteins are antiporters produces many new questions in the study of these proteins. The estimated stoichiometry of ClC-4/ClC-5 was similar to ClC-ec1, the bacterial chloride antiporter. This means that the transporter is highly electrogenic with 2 Cl^- ions exchanging for 1 H^+, and a net transfer of 3 elementary charges per transport cycle.

This stoichiometry has major implications for transport. It may initiate the acidification of the nascent endocytic vesicles from the plasma membrane. The 2:1 stoichiometry makes the transport cycle most sensitive to the Cl^- gradient. Therefore, the ClC antiporter might directly acidify endosomes shortly after they pinch off from the plasma membrane because Cl^- is present at a higher extracellular concentration than the cytosolic side. Therefore, H^+ in the cytoplasm may exchange for luminal Cl^-. To test this possibility, future experiments could use bafilomycin to inhibit the proton-ATPase and then measure the pH value of endocytic vesicles while manipulating the extracelllar Cl^- concentration. If alterations of vesicle pH are associated with the change of extracellular Cl^- concentration, this experiment would provide a direct proof that Cl^-/H^+ exchangers play important roles in initiating the pH change of endocytic vesicles.

The ClC antiporter may also play a greater role in volume regulation of the intracellular vesicles than could be accomplished by a simple channel. When the proton-ATPase pumps H^+ into the lumen of vesicles, anions are expected to follow and the volume of the vesicles would therefore increase. The ClC antiporter would be expected to amplify this effect. Coupled to the proton ATPase, the system functions to use some of the energy generated by the proton gradient to fill the lumen with osmotically active chloride ions. In a sense, this is analogous to the situation in both bacteria and mitochondria where the proton gradient is used to power other necessary transport functions. As a result, the net effect is both acidification and solute accumulation. This solute accumulation can serve to expand the vesicles.

This theory is supported by our previous work (16), although at the time of its publication, Cl^-/H^+ antiporter was not considered as an explanation. We observed that

manipulation of chloride gradients had profound and rapid effects on the size of ClC-3 containing vesicles. Reduction of intracellular Cl^- resulted in dramatic shrinkage of the vesicles and sudden increase in cytosolic Cl^- resulted in rapid expansion, sometimes to volumes more than 3 fold increased. These are unexpected findings for an ion conductance where solute movement is limited by the generation of an opposing diffusion potential, but not unexpected for a coupled transport process, the electrogenicity of which can be compensated by the activity of the proton ATPase.

A final implication of the antiporter hypothesis is that ClC transport proteins may play physiological roles not only in facilitating endosomal acidification, but also in regulating the Cl^- concentration in endosomal compartments. Unlike Cl^- channels, Cl^-/H^+ antiporter will directly couple Cl^- gradients to vesicular pH gradients. The energy consumed by the proton pump is thus used for the entry of Cl^- from the cytosol to the vesicle lumen. This suggests Cl^- concentration is important and there is proof that the vesicular Cl^- concentration might influence enzymatic activities (89). How the amount of Cl^- in the lumen of intracellular vesicles affects the components and function of cells still needs to be investigated.

The recent finding that ClC channels are antiporters thus has a major impact on our understanding of their function. We know that these molecules are necessary for both acidification and vesicle function. Further investigation will be required to determine how.

Direct vs. indirect pathway

In this dissertation, I have demonstrated that both direct and indirect pathways exist for the trafficking of ClC-3 molecules. Several lines of evidence support the existence of the indirect pathway. First, using a ClC-3 derivative with an externally accessible epitope, we have shown that plasma membrane ClC-3 is internalized and the endocytosed ClC-3 traffics to a distal compartment with the characteristics of late endosomes or lysosomes. Second, the biotinylation studies further confirmed the cell

surface location and the rapid endocytosis of ClC-3. Third, with pulse chase-labeling, we identified that about 25% of newly-synthesized wt ClC-3 reaches the plasma membrane. This result is consistent with the data from other lysosomal membrane proteins such as lgp-A and Lamp proteins (20, 90). Further indirect support was obtained by the finding of interaction between AP-2 and ClC-3 in both the yeast two hybrid and GST pull down assays. These data support the indirect trafficking pathway since it is known that AP-2 is involved in rapid internalization from the cell surface and delivery of MPRs and other membrane proteins to lysosomes through the indirect pathway (26).

However, evidence supporting the direct pathway also was obtained. This is primarily our finding in the pulse labeling experiments (Chapter 2). In these experiments I determined that the direct pathway to the lysosomes seems to be dominant for ClC-3 since the majority of newly synthesized ClC-3 (75%) did not reach the plasma membrane after 2 hours. Circumstantial supporting evidence for the direct pathway was also obtained. This is the interaction between AP-1 and ClC-3 seen with yeast two hybrid assays. This result also support the direct trafficking path since it is known that AP-1 mediates transport of lysosomal integral membrane proteins from the TGN to endosomes. The direct pathway is further supported by the work of Faundez and colleagues. They demonstrated that AP-3-dependent mechanisms control the targeting of ClC-3 in both neuronal and non-neuronal cells (55). AP-3 is also known to be involved in sorting of some lysosomal membrane proteins from TGN or endosomes and is important in the biogenesis of lysosome-related organelles (26).

Although only a small portion of ClC-3 (25%) takes the indirect pathway, this pathway is still important. In this dissertation, we have proven that steady-state plasma membrane ClC-3 accounts for approximately 6% of the total (Fig 2.8). However, we also demonstrate in Fig 2.15 that 25% of newly synthesized ClC-3 travels through the plasma membrane. This means that a significant portion of the ClC-3 protein that resides at the lysosomal membranes is retrieved through the endocytic pathway. Other lysosomal proteins have been shown to function at the plasma membrane as well. For example, in

activated platelets, the plasma membrane expression of Lamp-1 and Lamp-3 molecules is significant (90). Assuming that ClC-3 will function as an antiporter, similar to its relatives ClC-4 and ClC-5; it may also be functional at the plasma membrane to initiate the acidification of endocytic vesicles from the cell surface, as described.

It is reasonable to ask whether plasma membrane insertion of ClC-3 is an over expression artifact. The answer to this question is clearly no. In a recent paper, Nelson and colleagues verified that ClC-3 is expressed on the plasma membranes of neurons. These results, performed with biotinylation experiments and immuno-electron microscopy, show that native ClC-3 is expressed at the synaptic plasma membrane in hippocampal neurons (91). This shows that surface expression is not a unique phenomenon seen only in over-expression systems. However, in some over-expression systems, surface expression of lysosomal proteins may be amplified. It has been shown that the fraction of newly synthesized lgp-A reaching the cell surface was enhanced by increased expression levels of the total protein (20). Therefore we still need to evaluate the trafficking of ClC-3 in native cells with pulse-chase experiments in the future to obtain information of ClC-3 trafficking under physiological conditions.

Another unresolved question is to what extent heterodimer formation may be responsible for some of the trafficking events. We observed the colocalization of ClC-3/Flag and ClC-5/GFP in our imaging study (Fig 2.3). Hetero-oligomer formation was reported in cells co-transfected with pair-wise combinations of ClC-3, ClC-4, and ClC-5 channels (12). Hetero-oligomer formation may have physiological significance because variable ratios and assortments of channels in the cells may increase the functional diversity of intracellular transport proteins. Homo-dimers and hetero-dimers of ClC-3 molecules might function at different sites in the cells. A future direction is to study the different distribution pattern and trafficking paths of the homo-dimer and hetero-dimer ClC-3 molecules and test the different roles they play in the endocytic pathway.

Recycling

In our study, we demonstrated that, like transferrin receptors, plasma membrane ClC-3 is rapidly endocytosed and undergoes recycling. To further explore the significance of this recycling it will be necessary to confirm our recycling data with native cells like hippocampal neurons or acid-reabsorbing beta-intercalated cells of the collecting ducts in kidney, which have a high level of expression of ClC-3 (14, 92).

Recycling proteins are sorted in the early endosomes. After arrival at early endosomes, endocytosed membrane proteins either travel back to the plasma membrane or are transported to late endosomes and lysosomes. Another transport route leads to the *trans*-Golgi network (TGN). From the early endosome, recycling components can return directly to the plasma membrane through a 'fast' recycling route, or can take a 'slow' recycling pathway through perinuclear recycling endosomes (93).

Rab GTPases recruit specific effector proteins to the membranes on which they are localized, exerting a regulatory function in both the secretory and endocytic pathways. Roberts et al. showed that alpha (v) beta (3) and alpha (5) beta (1) integrins recycle through a Rab4-dependent and Akt-dependent pathway. Hsu et al have shown that the activity of the alpha (5) beta (1) integrin on cell surface was regulated by Rab11 and Arf6, two GTPases that are known to regulate membrane recycling. The common conclusion from these two groups is that integrin recycling is regulated by Rab-dependent trafficking events (94).

Rab5 recruits multiple effector proteins such as Rabaptin-5 and EEA1, organizing a membrane domain at the site of entry into early endosomes. Rab4 and Rab11 are involved in the fast and slow recycling pathway, respectively. They are localized to separate membrane domains on early endosomes that are distinct from those bearing Rab5. Therefore, there are three major endosomal populations; one containing mainly Rab5, a second containing both Rab5 and Rab4 (fast recycling), and a third containing mainly Rab4 and Rab11 (slow recycling). Recycling proteins internalized from the plasma membrane first enter the Rab5 domain, rapidly fill the adjacent Rab4 tubular

domain and then enter the Rab11 domain, where they are retained for long periods. Endocytosed transferrin moved sequentially through Rab5, Rab4 and Rab11 domains of the early endosomes before recycling back to the plasma membrane (93). In our biotinylation experiments, we demonstrated that ClC-3 behaved similarly to transferrin receptors. Stobrawa et al showed that ClC-3 was present in Rab 4 positive endosomes by Western blot of fractionated protein samples from liver (14). It is therefore reasonable to ask whether ClC-3 also recycles through these specific Rab-organized domains within the endosomes. Future studies can determine whether ClC-3 colocalizes with Rab4/5/11, and whether the recycling of ClC-3 will be altered by disturbing the specific Rab members.

Hrs is another protein important in endocytic sorting of ubiquitylated membrane proteins at the early endosome. There are two different clathrin coats on early endosomes, one that is involved in budding to form recycling vesicles, and a flat Hrs-containing coat that is involved in routing the cargo proteins for lysosomal degradation (40). Some of the ClC family members are known to be regulated by ubiquitylation. ClC-5 has a PY motif at its cytosolic COOH terminus. This motif is required for binding to WWP2, a Nedd4 type ubiquitin E3 ligase, and for the regulation of internalization and function of ClC-5 (95). ClC-K, a pair of renal specific ClC members, needs an associated transmembrane β-subunit, Barttin to be functional in vivo. There is a PY motif at C terminal of Barttin which may be regulated by Nedd4-2 (4, 96). ClC-3 does not contain a PY motif. However, considering the two pathways it takes, it could also be regulated by ubiquitylation. For example, it is possible that ubiquitylated ClC-3 molecules travel to late endosome/lysosome while non-ubiquitylated ClC-3 molecules recycle to the plasma membrane. Future studies can test whether ClC-3 colocalizes or interacts with Hrs. It can also be tested whether ClC-3 binds ubiquitin beads. We can also measure the K_D value between ClC-3 and ubiquitin with biophysical techniques such as surface plasmon resonance (40).

Is ClC-3 an accessory protein in the endocytic pathway?

This is a very speculative question. The fact that ClC-3 can interact with clathrin and AP-2 leads to the question of whether ClC-3 itself is an accessory molecule that is part of macromolecular complexes which regulate the internalization of other proteins at plasma membrane. A well-established function of adaptors is to recognize the sorting signals present in the cytosolic segment of cargo proteins that are recruited to coated pits. A recent paper reported that ClC-3 was co-immunoprecipitated from synaptosomal membrane preparations with PSD-95, NMDAR1, and NMDAR2B. This raises the issue of whether PSD-95, NMDAR1, and NMDAR2B are cargo molecules for ClC-3. To further investigate this broader function of ClC-3, we will have to identify the binding partners for ClC-3 in native cells. An unbiased proteomics approach may be the best way forward. We can isolate clathrin coated vesicles (CCVs) from hippocampal neurons from wt ClC-3 mice and ClC-3 knock out mice. Comparing the cargo content between these two will help to identify the bona fide components that can interact with ClC-3 (97). With this data, it will be possible to begin constructing a map of the binding interactions of the ClC molecule.

Why does ClC-3 overexpression result in enlarged vesicles?

An interesting question about ClC-3 is why its over-expression specifically produces unusual large intracellular vesicles. These vesicles have the characteristics of late endosome/lysosome. They may even contain different subpopulations. How do these vesicles form? Several possible explanations are proposed here.

One hypothesis is that ClC-3 is actually the mechanism by which vesicles expand. Over expression of ClC-3 results in size expansion of the compartments it normally occupies. In our previous work, we demonstrated Cl^--dependent volume changes of the ClC-3-associated vesicles. This provides direct proof that ClC-3 containing vesicles are expandable. We previously observed that expansion of ClC-3 containing vesicles requires that both the proton ATPase the ClC-3 molecule be active. This was supported by the

observation that inhibition of the V-type ATPase (V-ATPase) with bafilomycin A1, a highly specific inhibitor of vacuolar proton-ATPase, nearly abolished formation of enlarged vesicles in ClC-3 transfected cells. Similarly, when we over expressed ClC-3 E224A, a mutant that eliminated the H^+ coupling of anion currents, vesicles were also small as in the case of bafilomycin treatment (Li 2002). The phenotype of this mutant and bafilomycin A treatment suggests that expansion of these ClC-3-associated vesicles was dependent on normal ClC-3 Cl^--H^+ exchange.

A second possibility is that over-expression of ClC-3 may lead to sequestration of ClC-3 binding partners such as AP-1, AP-2 and clathrin and these proteins are responsible for the formation of big vesicles. At present, the specific mechanisms of the expansion effects are unknown. However, the fact that the E224A mutant failed to support expansion in spite of its having similar expression level to the wild type ClC-3, and the same cytosolic domains (both N and C terminal) as wild type ClC-3, suggests that it is the antiporter activity but not simple binding that are critical. Thus the result from the mutant argues against the clathrin sequestration possibility because E224A is likely to interact with clathrin in a same way as the wild type.

Another non-mutually exclusive possibility is that over-expression of ClC-3 primarily alters fusion events, resulting in either a greater number of incoming vesicles fusing with lysosomes or a decrease in the budding and removal of membrane component from lysosomes. With our extra-cellular HA construct, we are able to track the trafficking path of ClC-3 molecules. After a 30 min chase, plasma membrane resident ClC-3 moved to small endocytic vesicles and by 2 h accumulated into the large central vesicles that are the major site of total cellular ClC-3 at the steady state (Fig 2.13). The small vesicles originate from the cell surface and finally fuse with other vesicular structures, thus big vesicles come into being.

Rabs are known for their roles in regulation of the fusion of vesicles. Several components in the endocytic pathway have been shown to be involved in formation of the enlarged vesicles in cells. There is precedent in the literature for changes in Rab protein

expression causing vesicle expansion. For example, IL4 (a Th-2 cytokine)/PGE2 (prostaglandin E2) induced Rab5 and its effector proteins such as EEA1 and Rin1, thus promoting the formation of an enlarged early endocytic compartment. The enlargement is associated with a prominent induction of internalization of cargo protein such as mannose receptor (94). Over expressing a constitutively active Rab7 mutant caused enlarged lysosomes while dominant negative Rab7 mutant disperses lysosome. These results suggest that Rab7 is critical in endosome-lysosome fusion events (98). It is possible that ClC-3 promotes Rab function as well. To test this possibility, one could knock down ClC-3 and then look for changes in Rab function. One could also directly manipulate the Rab proteins themselves to determine if they play roles in the formation of the enlarged vesicles seen with ClC-3 over-expression. A future experiment is to manipulate the expression of specific Rabs with different strategies such as siRNA, dominant negative mutants, or specific blocking antibody, and observe whether these affect the formation of ClC-3 associated vesicles.

SNAREs reside on both vesicles and target membranes and promote the fusion events. If ClC-3 affects SNARE protein function, it could also cause vesicle enlargement. Therefore it is also worth examining the interactions between ClC-3 and SNAREs. Again, a proteomics approach would be a good choice for this purpose in the future.

Clinical implications of the trafficking of chloride channels: pH regulation and virus trafficking

Entry of viruses into cells occurs in several tightly controlled, consecutive steps. As the virus progresses in its entry process, changes occur that lead to events such as penetration, capsid destabilization, and uncoating of the genome. Many of these changes are triggered by receptor binding, exposure to low pH, re-entry into a reducing environment, and enzyme-induced covalent modifications. (99-101).

The majority of viruses require endocytic internalization for penetration and productive infection due to the following advantages. Viruses that are transported by

endocytic vesicles can move deep into the cytoplasm, bypassing obstacles associated with the membrane cortex and intracellular crowding (102), and use the sorting molecules that are normally recruited to endocytic vesicles (103). A dependence on low pH for penetration makes viruses able to escape to the cytoplasm at specific locations or before the viruses arrive at the hydrolytic lysosomes (104). Furthermore, an endocytic entry mechanism means that after entry no viral antigen is left on the plasma membrane to be detected by the host's immune defenses.

Viruses take endocytic pathways into cells by the clathrin-mediated endocytic route (Ebola virus, SARS coronavirus), the caveolae pathway (SV40, coxsackie B), as well as macropinocytosis (adenoviruses). ClC-3 is known to facilitate the acidification of synaptic vesicles and endosomal/lysosomal compartments (14, 16, 17). Therefore, ClC-3 may affect the virus penetration. In addition, the work presented in this dissertation has shown that ClC-3 can bind to AP-2 and clathrin separately. This suggests that in addition to pH regulation, ClC-3 may serve as an accessory protein itself and play fundamental roles in the endocytic mechanism. Future research will try to answer questions such as what the relation between ClC-3 and other cargo receptors is and whether or not ClC-3 contributes to virus entry.

TECHNICAL LIMITATIONS OF THE PRESENT WORK

Our work was carried out in cell culture systems over-expressing ClC-3. This limitation was a result of the absence of sufficiently sensitive and specific antibodies directed against the native protein. In spite of the limitations of over-expression, our system is useful in the identification of trafficking patterns, the role of specific motifs in trafficking, and the interaction with adaptor proteins. However, in the future, further efforts will need to be directed to the development of specific ClC-3 antibodies and performing trafficking studies on native cells.

SIGNIFICANCE

In summary, our studies demonstrate that ClC-3 is largely an intracellular protein, but it can traffic to lysosomes from an intracellular route or first be inserted into the plasma membrane from where it travels dynamically to different sites inside the cell. The protein associates with clathrin and both clathrin binding and endocytosis require the presence of a dileucine acidic cluster in the N-terminal of ClC-3. The presence of multiple binding motifs, multiple AP protein interactions, and the possibility that ClC channels form hetero-dimers with other family members and splice variants (105) suggests that these proteins may play a scaffolding role in addition to their functions in chloride and proton translocation.

The disruption of ClC-3 results in severe CNS degeneration (14). The full reasons are not known yet, but might result from intracellular trafficking defects. Our study provides a fundamental understanding of ClC-3 localization and trafficking. Study of ClC-3 and the specific sorting proteins should enhance our understanding of this particularly protein-protein interaction and give insight into how intracellular chloride channels are distributed and controlled. In addition, a further understanding of the functions of these proteins can lead to novel therapeutic approaches for diseases in which the endocytic and intracellular acidification systems are involved.

Reference

1. **Li X-H and Weinman SA**. Chloride channels and hepatocellular function. Prospects for molecular identification. *Ann Rev Physiol* 64: 13.1-13.25, 2002.

2. **Koch MC, Steinmeyer K, Lorenz C, Ricker K, Wolf F, Otto M, Zoll B, Lehmann-Horn F, Grzeschik KH and Jentsch TJ**. The skeletal muscle chloride channel in dominant and recessive human myotonia. *Science* 257: 797-800, 1992.

3. **Steinmeyer K, Lorenz C, Pusch M, Koch MC and Jentsch TJ**. Multimeric structure of ClC-1 chloride channel revealed by mutations in dominant myotonia congenita (Thomsen). *EMBO J* 13: 737-743, 1994.

4. **Estevez R, Boettger T, Stein V, Birkenhager R, Otto E, Hildebrandt F and Jentsch TJ**. Barttin is a Cl- channel beta-subunit crucial for renal Cl- reabsorption and inner ear K+ secretion. *Nature* 414: 558-561, 2001.

5. **Waldegger S and Jentsch TJ**. Functional and structural analysis of ClC-K chloride channels involved in renal disease. *J Biol Chem* 275: 24527-24533, 2000.

6. **Piwon N, Gunther W, Schwake M, Bosl MR and Jentsch TJ**. ClC-5 Cl^- -channel disruption impairs endocytosis in a mouse model for Dent's disease. *Nature* 408: 369-373, 2000.

7. **Kasper D, Planells-Cases R, Fuhrmann JC, Scheel O, Zeitz O, Ruether K, Schmitt A, Poet M, Steinfeld R, Schweizer M, Kornak U and Jentsch TJ**. Loss of the chloride channel ClC-7 leads to lysosomal storage disease and neurodegeneration. *EMBO J* 24: 1079-1091, 2005.

8. **Kornak U, Kasper D, Bosl MR, Kaiser E, Schweizer M, Schulz A, Friedrich W, Delling G and Jentsch TJ**. Loss of the ClC-7 chloride channel leads to osteopetrosis in mice and man. *Cell* 104: 205-215, 2001.

9. **Jentsch TJ, Poet M, Fuhrmann JC and Zdebik AA**. Physiological functions of CLC Cl- channels gleaned from human genetic disease and mouse models. *Annu Rev Physiol* 67: 779-807, 2005.

10. **Dutzler R, Campbell EB, Cadene M, Chait BT and MacKinnon R**. X-ray structure of a ClC chloride channel at 3.0 A reveals the molecular basis of anion selectivity. *Nature* 415: 287-294, 2002.

11. **Jentsch TJ, Friedrich T, Schriever A and Yamada H**. The CLC chloride channel family. *Pflugers Arch* 437: 783-795, 1999.

12. **Suzuki T, Rai T, Hayama A, Sohara E, Suda S, Itoh T, Sasaki S and Uchida S**. Intracellular localization of ClC chloride channels and their ability to form hetero-oligomers. *J Cell Physiol* 206: 792-798, 2006.

13. **Mohammad-Panah R, Harrison R, Dhani S, Ackerley C, Huan LJ, Wang Y and Bear CE**. The chloride channel ClC-4 contributes to endosomal acidification and trafficking. *J Biol Chem* 278: 29267-29277, 2003.

14. **Stobrawa SM, Breiderhoff T, Takamori S, Engel D, Schweizer M, Zdebik AA, Bosl MR, Ruether K, Jahn H, Draguhn A, Jahn R and Jentsch TJ**. Disruption of ClC-3, a chloride channel expressed on synaptic vesicles, leads to a loss of the hippocampus. *Neuron* 29: 185-196, 2001.

15. **Yoshikawa M, Uchida S, Ezaki J, Rai T, Hayama A, Kobayashi K, Kida Y, Noda M, Koike M, Uchiyama Y, Marumo F, Kominami E and Sasaki S**. CLC-3 deficiency leads to phenotypes similar to human neuronal ceroid lipofuscinosis. *Genes Cells* 7: 597-605, 2002.

16. **Li X, Wang T, Zhao Z and Weinman SA**. The ClC-3 chloride channel promotes acidification of lysosomes in CHO-K1 and Huh-7 cells. *Am J Physiol Cell Physiol* 282: C1483-C1491, 2002.

17. **Hara-Chikuma M, Yang B, Sonawane ND, Sasaki S, Uchida S and Verkman AS**. ClC-3 chloride channels facilitate endosomal acidification and chloride accumulation. *J Biol Chem* 280: 1241-1247, 2005.

18. **Poet M, Kornak U, Schweizer M, Zdebik AA, Scheel O, Hoelter S, Wurst W, Schmitt A, Fuhrmann JC, Planells-Cases R, Mole SE, Hubner CA and**

Jentsch TJ. Lysosomal storage disease upon disruption of the neuronal chloride transport protein ClC-6. *Proc Natl Acad Sci U S A* 103: 13854-13859, 2006.

19. **Kornfeld S and Mellman I**. The biogenesis of lysosomes. *Annu Rev Cell Biol* 5: 483-525, 1989.

20. **Harter C and Mellman I**. Transport of the lysosomal membrane glycoprotein lgp120 (lgp-A) to lysosomes does not require appearance on the plasma membrane. *J Cell Biol* 117: 311-325, 1992.

21. **Al-Awqati Q**. Chloride channels of intracellular organelles. *Curr Opin Cell Biol* 7: 504-508, 1995.

22. **Accardi A and Miller C**. Secondary active transport mediated by a prokaryotic homologue of ClC Cl- channels. *Nature* 427: 803-807, 2004.

23. **Scheel O, Zdebik AA, Lourdel S and Jentsch TJ**. Voltage-dependent electrogenic chloride/proton exchange by endosomal CLC proteins. *Nature* 436: 424-427, 2005.

24. **Picollo A and Pusch M**. Chloride/proton antiporter activity of mammalian CLC proteins ClC-4 and ClC-5. *Nature* 436: 420-423, 2005.

25. **Mullins C and Bonifacino JS**. The molecular machinery for lysosome biogenesis. *Bioessays* 23: 333-343, 2001.

26. **Mullins C and Bonifacino JS**. The molecular machinery for lysosome biogenesis. *Bioessays* 23: 333-343, 2001.

27. **Bonifacino JS**. The GGA proteins: adaptors on the move. *Nat Rev Mol Cell Biol* 5: 23-32, 2004.

28. **Bonifacino JS and Lippincott-Schwartz J**. Coat proteins: shaping membrane transport. *Nat Rev Mol Cell Biol* 4: 409-414, 2003.

29. **Canfield WM, Johnson KF, Ye RD, Gregory W and Kornfeld S**. Localization of the signal for rapid internalization of the bovine cation-independent mannose 6-phosphate/insulin-like growth factor-II receptor to amino acids 24-29 of the cytoplasmic tail. *J Biol Chem* 266: 5682-5688, 1991.

30. **Bonifacino JS and Dell'Angelica EC**. Molecular bases for the recognition of tyrosine-based sorting signals. *J Cell Biol* 145: 923-926, 1999.

31. **Rajasekaran AK, Humphrey JS, Wagner M, Miesenbock G, Le Bivic A, Bonifacino JS and Rodriguez-Boulan E**. TGN38 recycles basolaterally in polarized Madin-Darby canine kidney cells. *Mol Biol Cell* 5: 1093-1103, 1994.

32. **Heilker R, Spiess M and Crottet P**. Recognition of sorting signals by clathrin adaptors. *Bioessays* 21: 558-567, 1999.

33. **Bonifacino JS**. The GGA proteins: adaptors on the move. *Nat Rev Mol Cell Biol* 5: 23-32, 2004.

34. **Robinson MS and Bonifacino JS**. Adaptor-related proteins. *Curr Opin Cell Biol* 13: 444-453, 2001.

35. **Bonifacino JS and Lippincott-Schwartz J**. Coat proteins: shaping membrane transport. *Nat Rev Mol Cell Biol* 4: 409-414, 2003.

36. **Bonifacino JS and Traub LM**. Signals for sorting of transmembrane proteins to endosomes and lysosomes. *ARB* 72: 395-447, 2003.

37. **Brodsky FM, Chen CY, Knuehl C, Towler MC and Wakeham DE**. Biological basket weaving: formation and function of clathrin-coated vesicles. *Annu Rev Cell Dev Biol* 17: 517-568, 2001.

38. **Kirchhausen T**. Adaptors for clathrin-mediated traffic. *Annu Rev Cell Dev Biol* 15: 705-732, 1999.

39. **Warren RA, Green FA and Enns CA**. Saturation of the endocytic pathway for the transferrin receptor does not affect the endocytosis of the epidermal growth factor receptor. *J Biol Chem* 272: 2116-2121, 1997.

40. **Raiborg C and Stenmark H**. Hrs and endocytic sorting of ubiquitinated membrane proteins. *Cell Struct Funct* 27: 403-408, 2002.

41. **Jones MC, Caswell PT and Norman JC**. Endocytic recycling pathways: emerging regulators of cell migration. *Curr Opin Cell Biol* 18: 549-557, 2006.

42. **Simonsen A, Lippe R, Christoforidis S, Gaullier JM, Brech A, Callaghan J, Toh BH, Murphy C, Zerial M and Stenmark H**. EEA1 links PI(3)K function to Rab5 regulation of endosome fusion. *Nature* 394: 494-498, 1998.

43. **Zerial M and McBride H**. Rab proteins as membrane organizers. *Nat Rev Mol Cell Biol* 2: 107-117, 2001.

44. **Bertrand CA and Frizzell RA**. The role of regulated CFTR trafficking in epithelial secretion. *Am J Physiol Cell Physiol* 285: C1-18, 2003.

45. **Sharma M, Pampinella F, Nemes C, Benharouga M, So J, Du K, Bache KG, Papsin B, Zerangue N, Stenmark H and Lukacs GL**. Misfolding diverts CFTR from recycling to degradation: quality control at early endosomes. *J Cell Biol* 164: 923-933, 2004.

46. **Christensen EI, Devuyst O, Dom G, Nielsen R, Van der SP, Verroust P, Leruth M, Guggino WB and Courtoy PJ**. Loss of chloride channel ClC-5 impairs endocytosis by defective trafficking of megalin and cubilin in kidney proximal tubules. *Proc Natl Acad Sci U S A* 100: 8472-8477, 2003.

47. **Schwake M, Friedrich T and Jentsch TJ**. An internalization signal in ClC-5, an endosomal Cl-channel mutated in dent's disease. *J Biol Chem* 276: 12049-12054, 2001.

48. **Carr G, Simmons N and Sayer J**. A role for CBS domain 2 in trafficking of chloride channel CLC-5. *Biochem Biophys Res Commun* 310: 600-605, 2003.

49. **Ludwig M, Doroszewicz J, Seyberth HW, Bokenkamp A, Balluch B, Nuutinen M, Utsch B and Waldegger S**. Functional evaluation of Dent's disease-causing mutations: implications for ClC-5 channel trafficking and internalization. *Hum Genet* 117: 228-237, 2005.

50. **Shimada K, Li X, Xu G, Nowak DE, Showalter LA and Weinman SA**. Expression and canalicular localization of two isoforms of the ClC-3 chloride channel from rat hepatocytes. *Am J Physiol Gastrointest Liver Physiol* 279: G268-G276, 2000.

51. **Ogura T, Furukawa T, Toyozaki T, Yamada K, Zheng YJ, Katayama Y, Nakaya H and Inagaki N**. ClC-3B, a novel ClC-3 splicing variant that interacts with EBP50 and facilitates expression of CFTR-regulated ORCC. *FASEB J* 16: 863-865, 2002.

52. **Vessey JP, Shi C, Jollimore CA, Stevens KT, Coca-Prados M, Barnes S and Kelly ME**. Hyposmotic activation of ICl,swell in rabbit nonpigmented ciliary epithelial cells involves increased ClC-3 trafficking to the plasma membrane. *Biochem Cell Biol* 82: 708-718, 2004.

53. **Huang P, Liu J, Di A, Robinson NC, Musch MW, Kaetzel MA and Nelson DJ**. Regulation of human CLC-3 channels by multifunctional Ca2+/calmodulin-dependent protein kinase. *J Biol Chem* 276: 20093-20100, 2001.

54. **Weylandt KH, Valverde MA, Nobles M, Raguz S, Amey JS, Diaz M, Nastrucci C, Higgins CF and Sardini A**. Human ClC-3 is not the swelling-activated chloride channel involved in cell volume regulation. *J Biol Chem* 276: 17461-17467, 2001.

55. **Salazar G, Love R, Styers ML, Werner E, Peden A, Rodriguez S, Gearing M, Wainer BH and Faundez V**. AP-3-dependent mechanisms control the targeting of a chloride channel (ClC-3) in neuronal and non-neuronal cells. *J Biol Chem* 279: 25430-25439, 2004.

56. **Duan D, Zhong J, Hermoso M, Satterwhite CM, Rossow CF, Hatton WJ, Yamboliev I, Horowitz B and Hume JR**. Functional inhibition of native volume-sensitive outwardly rectifying anion channels in muscle cells and Xenopus oocytes by anti-ClC-3 antibody. *J Physiol* 531: 437-444, 2001.

57. **Loder MK and Melikian HE**. The dopamine transporter constitutively internalizes and recycles in a protein kinase C-regulated manner in stably transfected PC12 cell lines. *J Biol Chem* 278: 22168-22174, 2003.

58. **Fournier KM, Gonzalez MI and Robinson MB**. Rapid trafficking of the neuronal glutamate transporter, EAAC1: evidence for distinct trafficking pathways differentially regulated by protein kinase C and platelet-derived growth factor. *J Biol Chem* 279: 34505-34513, 2004.

59. **Li X, Shimada K, Showalter LA and Weinman SA**. Biophysical properties of ClC-3 differentiate it from swelling-activated chloride channels in CHO-K1 cells. *J Biol Chem* 275: 35994-35998, 2000.

60. **Lin HJ, Herman P, Kang JS and Lakowicz JR**. Fluorescence lifetime characterization of novel low-ph probes. *Anal Biochem* 294: 118-125, 2001.

61. Shimada, K., Li, X., Xu, G, Showalter, L. A., and Weinman, S. A. Expression and properties of the ClC-3 chloride channel from rat hepatocytes. Hepatology . 1999. Ref Type: Abstract

62. **Yan S, Sanders JM, Xu J, Zhu Y, Contractor A and Swanson GT**. A C-terminal determinant of GluR6 kainate receptor trafficking. *J Neurosci* 24: 679-691, 2004.

63. **Hammond DE, Carter S, McCullough J, Urbe S, Vande WG and Clague MJ**. Endosomal dynamics of Met determine signaling output. *Mol Biol Cell* 14: 1346-1354, 2003.

64. **Conner SD and Schmid SL**. Regulated portals of entry into the cell. *Nature* 422: 37-44, 2003.

65. **Wang T and Weinman SA**. Involvement of chloride channels in hepatic copper metabolism: ClC-4 promotes copper incorporation into ceruloplasmin. *Gastroenterology* 126: 1157-1166, 2004.

66. **Rossow CF, Duan D, Hatton WJ, Britton F, Hume JR and Horowitz B**. Functional role of amino terminus in ClC-3 chloride channel regulation by phosphorylation and cell volume. *Acta Physiol (Oxf)* 187: 5-19, 2006.

67. **Xia W, Zhang J, Ostaszewski BL, Kimberly WT, Seubert P, Koo EH, Shen J and Selkoe DJ**. Presenilin 1 regulates the processing of beta-amyloid precursor protein C-terminal fragments and the generation of amyloid beta-protein in endoplasmic reticulum and Golgi. *B* 37: 16465-16471, 1998.

68. **Ding W, Albrecht B, Luo R, Zhang W, Stanley JR, Newbound GC and Lairmore MD**. Endoplasmic reticulum and cis-Golgi localization of human T-lymphotropic virus type 1 p12(I): association with calreticulin and calnexin. *J Virol* 75: 7672-7682, 2001.

69. **Van GF, Straley KS, Cao D, Gonzalez J, Hadida S, Hazlewood A, Joubran J, Knapp T, Makings LR, Miller M, Neuberger T, Olson E, Panchenko V, Rader J, Singh A, Stack JH, Tung R, Grootenhuis PD and Negulescu P**. Rescue of DeltaF508-CFTR trafficking and gating in human cystic fibrosis airway primary cultures by small molecules. *Am J Physiol Lung Cell Mol Physiol* 290: L1117-L1130, 2006.

70. **Haft CR, De La Luz SM, Hamer I, Carpentier JL and Taylor SI**. Analysis of the juxtamembrane dileucine motif in the insulin receptor. *Endocrinology* 139: 1618-1629, 1998.

71. **Yan A and Lennarz WJ**. Unraveling the mechanism of protein N-glycosylation. *J Biol Chem* 280: 3121-3124, 2005.

72. **Alberts B**. The cell as a collection of protein machines: preparing the next generation of molecular biologists. *Cell* 92: 291-294, 1998.

73. **Slepnev VI, Ochoa GC, Butler MH and De Camilli P**. Tandem arrangement of the clathrin and AP-2 binding domains in amphiphysin 1 and disruption of clathrin coat function by amphiphysin fragments comprising these sites. *J Biol Chem* 275: 17583-17589, 2000.

74. **Doray B and Kornfeld S**. Gamma subunit of the AP-1 adaptor complex binds clathrin: implications for cooperative binding in coated vesicle assembly. *Mol Biol Cell* 12: 1925-1935, 2001.

75. **Estevez R, Pusch M, Ferrer-Costa C, Orozco M and Jentsch TJ**. Functional and structural conservation of CBS domains from CLC chloride channels. *J Physiol* 557: 363-378, 2004.

76. **Scott JW, Hawley SA, Green KA, Anis M, Stewart G, Scullion GA, Norman DG and Hardie DG**. CBS domains form energy-sensing modules whose binding of adenosine ligands is disrupted by disease mutations. *J Clin Invest* 113: 274-284, 2004.

77. **Cheng ZJ, Singh RD, Marks DL and Pagano RE**. Membrane microdomains, caveolae, and caveolar endocytosis of sphingolipids. *Mol Membr Biol* 23: 101-110, 2006.

78. **Dell'Angelica EC, Mullins C, Caplan S and Bonifacino JS**. Lysosome-related organelles. *FASEB J* 14: 1265-1278, 2000.

79. **Minana R, Duran JM, Tomas M, Renau-Piqueras J and Guerri C**. Neural cell adhesion molecule is endocytosed via a clathrin-dependent pathway. *Eur J Neurosci* 13: 749-756, 2001.

80. **Hulet SW, Heyliger SO, Powers S and Connor JR**. Oligodendrocyte progenitor cells internalize ferritin via clathrin-dependent receptor mediated endocytosis. *J Neurosci Res* 61: 52-60, 2000.

81. **Watts C and Marsh M**. Endocytosis: what goes in and how? *J Cell Sci* 103 (Pt 1): 1-8, 1992.

82. **Dykxhoorn DM, Novina CD and Sharp PA**. Killing the messenger: short RNAs that silence gene expression. *Nat Rev Mol Cell Biol* 4: 457-467, 2003.

83. **Dykxhoorn DM and Lieberman J**. The silent revolution: RNA interference as basic biology, research tool, and therapeutic. *Annu Rev Med* 56: 401-423, 2005.

84. **Dykxhoorn DM, Palliser D and Lieberman J**. The silent treatment: siRNAs as small molecule drugs. *Gene Ther* 13: 541-552, 2006.

85. **Bertrand JR, Pottier M, Vekris A, Opolon P, Maksimenko A and Malvy C**. Comparison of antisense oligonucleotides and siRNAs in cell culture and in vivo. *Biochem Biophys Res Commun* 296: 1000-1004, 2002.

86. **Hinrichsen L, Harborth J, Andrees L, Weber K and Ungewickell EJ**. Effect of clathrin heavy chain- and alpha-adaptin-specific small inhibitory RNAs on endocytic accessory proteins and receptor trafficking in HeLa cells. *J Biol Chem* 278: 45160-45170, 2003.

87. **Sorkin A**. Cargo recognition during clathrin-mediated endocytosis: a team effort. *Curr Opin Cell Biol* 16: 392-399, 2004.

88. **Sakamoto H, Kawasaki M, Uchida S, Sasaki S and Marumo F**. Identification of a new outwardly rectifying Cl^- channel that belongs to a subfamily of the ClC Cl^- channels. *J Biol Chem* 271: 10210-10216, 1996.

89. **Davis-Kaplan SR, Askwith CC, Bengtzen AC, Radisky D and Kaplan J**. Chloride is an allosteric effector of copper assembly for the yeast multicopper oxidase Fet3p: an unexpected role for intracellular chloride channels. *Proc Natl Acad Sci U S A* 95: 13641-13645, 1998.

90. **Fukuda M**. Lysosomal membrane glycoproteins. Structure, biosynthesis, and intracellular trafficking. *J Biol Chem* 266: 21327-21330, 1991.

91. **Wang XQ, Deriy LV, Foss S, Huang P, Lamb FS, Kaetzel MA, Bindokas V, Marks JD and Nelson DJ**. CLC-3 channels modulate excitatory synaptic transmission in hippocampal neurons. *Neuron* 52: 321-333, 2006.

92. **Obermuller N, Gretz N, Kriz W, Reilly RF and Witzgall R**. The swelling-activated chloride channel ClC-2, the chloride channel ClC-3, and ClC-5, a chloride channel mutated in kidney stone disease, are expressed in distinct subpopulations of renal epithelial cells. *J Clin Invest* 101: 635-642, 1998.

93. **de RS, Sonnichsen B and Zerial M**. Divalent Rab effectors regulate the sub-compartmental organization and sorting of early endosomes. *Nat Cell Biol* 4: 124-133, 2002.

94. **Wainszelbaum MJ, Proctor BM, Pontow SE, Stahl PD and Barbieri MA**. IL4/PGE2 induction of an enlarged early endosomal compartment in mouse macrophages is Rab5-dependent. *Exp Cell Res* 312: 2238-2251, 2006.

95. **Hryciw DH, Ekberg J, Lee A, Lensink IL, Kumar S, Guggino WB, Cook DI, Pollock CA and Poronnik P**. Nedd4-2 functionally interacts with ClC-5: involvement in constitutive albumin endocytosis in proximal tubule cells. *J Biol Chem* 279: 54996-55007, 2004.

96. **Embark HM, Bohmer C, Palmada M, Rajamanickam J, Wyatt AW, Wallisch S, Capasso G, Waldegger P, Seyberth HW, Waldegger S and Lang F**. Regulation of CLC-Ka/barttin by the ubiquitin ligase Nedd4-2 and the serum- and glucocorticoid-dependent kinases. *Kidney Int* 66: 1918-1925, 2004.

97. **Hirst J, Miller SE, Taylor MJ, von Mollard GF and Robinson MS**. EpsinR is an adaptor for the SNARE protein Vti1b. *Mol Biol Cell* 15: 5593-5602, 2004.

98. **Bucci C, Thomsen P, Nicoziani P, McCarthy J and van DB**. Rab7: a key to lysosome biogenesis. *Mol Biol Cell* 11: 467-480, 2000.

99. **Harrison SC**. Mechanism of membrane fusion by viral envelope proteins. *Adv Virus Res* 64: 231-261, 2005.

100. **Smith AE and Helenius A**. How viruses enter animal cells. *Science* 304: 237-242, 2004.

101. **Earp LJ, Delos SE, Park HE and White JM**. The many mechanisms of viral membrane fusion proteins. *Curr Top Microbiol Immunol* 285: 25-66, 2005.

102. **Marsh M and Bron R**. SFV infection in CHO cells: cell-type specific restrictions to productive virus entry at the cell surface. *J Cell Sci* 110 (Pt 1): 95-103, 1997.

103. **Dohner K and Sodeik B**. The role of the cytoskeleton during viral infection. *Curr Top Microbiol Immunol* 285: 67-108, 2005.

104. **Helenius A, Kartenbeck J, Simons K and Fries E**. On the entry of Semliki forest virus into BHK-21 cells. *J Cell Biol* 84: 404-420, 1980.

105. **Suzuki T, Rai T, Hayama A, Sohara E, Suda S, Itoh T, Sasaki S and Uchida S**. Intracellular localization of ClC chloride channels and their ability to form hetero-oligomers. *J Cell Physiol* 206: 792-798, 2006.

VITA

Zhifang Zhao was born to parents Huawen Li and Shuyun Zhao in Shanghai, P. R. China on May 18, 1971. She graduated from Tongji Medical University in 1994, receiving her Bachelor Degree of Medicine. She then worked as an Assistant Teacher in the Department of Pharmacology in the same institution, conducting teaching and research work. From 1997 to 2000, she attended graduate school and received her Master Degree of Medicine in Pharmacology. During this time she realized she should go abroad to learn advanced sciences and technologies. She was accepted in the Ph.D. program in biomedical sciences at University of Texas Medical Branch. She joined Dr. Steven A. Weinman's lab to help establish a new project exploring the distribution and trafficking of ClC-3 chloride protein.

Zhifang possessed a unique combination of knowledge and training experiences to conduct biomedical research. As an MD who graduated from a prestigious medical university in China, she practiced in a comprehensive hospital and obtained first-hand knowledge of human diseases. During her Masters training in China, she was involved in the development of Lotusine, an alkaloid extracted from the seeds of the lotus plant, into a new drug for the treatment of heart failure. Her professional training has spanned the subjects of clinical medicine, pharmacology, electrophysiology, molecular biology and cell biology. She also obtained considerable teaching experience. From 1994 to 1997, she was an assistant teacher in Dept. of pharmacology, Tongji Medical University. Her work is to teach pharmacology experiment and theory classes for undergraduates in the medical university. While in Dr. Steven Weinman's lab, she also helped to supervise a technician and gained valuable experience in manuscript preparation and fellowship application.

Education

M.S. September 1997	Tongji Medical University, Wuhan, P.R. China
M.D. September 1989	Tongji Medical University, Wuhan, P. R. Chia

Publications

1. ***Zhao, Z.***; Li, X.H.; Hao, J.F.; Weinman, S.A. ClC-3 traffics from plasma membrane via interaction of its N-terminal dileucine cluster with the clathrin (manuscript)

2. Li, X.H.; Wang, T.; ***Zhao, Z.***; Weinman, S.A. The ClC-3 chloride channel promotes acidification of lysosomes in CHO-K1 and Huh-7 cells" (Am J Physiol Cell Physiol, 282(6):C1483-C1491; 2002

3. ***Zhao, Z.***; Zhang, Y.L.; Yu, X.; Feng, X.L.; Wang, J.L. Effects of Lotusine on the cyclic nucleotides content and the contraction of myocardium and corpus spongiosum. Chinese Journal of Pharmacology and Toxicology Jun; 16 (3):202-205;2002

4. ***Zhao, Z.***; Wang, J.L. Ceramide: an intracellular Mediator of Multiple biological Effects" Review, Foreign Medical Sciences 21 (4): 229-232; 1999

5. Wang, J.L.; ***Zhao, Z.***; Cao, Q.; Yu, J.; Feng, X.L. Effects of Lotusine on contractions of Blood Vessels and Platelet Cyclic Nucleotides" Pharmacology and clinics of Chinese Materia Medica 15(4): 14-17; 1999

6. Wang, J.L.; ***Zhao, Z.***; Yao, W.X.; Jiang, M.X. Effects of Lotusine on the action potentials in myocardium and slow inward current in cardiac purkinje fibers" Chinese Pharmacological Bulletin 15 (6): 524-527; 1999

7. Wang, J.L.; ***Zhao, Z.***; Li, M. Positive Inotropic Effect of Lotusine on Isolated Myocardium and its Mechanism Acta Univ. Med, Tongji 28 (5):385-388; 1999

Abstracts

1. ***Zhao, Z.***; Weinman, S.A. Clathrin Dependent Endocytic Trafficking of the ClC-3 Chloride Channel, Cell Biology Meeting 2005:San Francisco

2. ***Zhao, Z.***; Li, X..; Weinman, S.A. Involvement of the N-terminal of the ClC-3 Chloride Channel in Plasma Membrane Internalization and Trafficking, Cell Biology Meeting 2004:Washington D.C.

3. ***Zhao, Z.***; Li, X.; Weinman, S.A. Role of N and C terminal cytosolic domains in intracellular targeting of the ClC-3 chloride channel, Experimental Biology Meeting 2003: San Diego